RETURN TO 1998 ROD AR INDEX

#60153
NEW BEDFORD
11.12.2

Circulation and Pollutant Transport Model of New Bedford Harbor

Submitted to:

Ropes and Gray
225 Franklin Street
Boston, Massachusetts 02110
Attn: Mr. Paul Galvani

Submitted by:

Applied Science Associates, Inc.
70 Dean Knauss Drive
Narragansett, Rhode Island 02882

3 July 1986

ASA 86-18

Attachment VII 71

SDMS DocID 60153

List of Figures

		PAGE
Figure 1.1	New Bedford Harbor Acushnet River study area.	2
Figure 2.1	Acushnet River watershed.	4
Figure 2.2	Bathymetry of the dredged channels in outer New Bedford Harbor (Corps of Engineers, 1970).	5
Figure 2.3	Sea surface elevation for the 1938, 1944, and 1954 hurricanes in New Bedford Harbor (Corps of Engineers, 1970).	16
Figure 2.4	Percent chance of tidal flooding per year in New Bedford Harbor.	21
Figure 2.5	Summary of tidal current measurements collected in the upper Acushnet River estuary (north of Coggeshall Street Bridge) (Cortell, 1982).	22
Figure 2.6	Variations in water properties and current velocities in surface and bottom waters for two stations (H4 and H5) through one complete tidal cycle June 8 and 9, 1976 (Summerhayes et al, 1976).	25
Figure 2.7	Time series of tidal height and current speed at the hurricane barrier and cross sectionally averaged speed at the I-195 bridge causeway, 20 June 1986.	26
Figure 3.1	Comparison of Acushnet River sediment erosion thresholds based on laboratory data (ASA, 1983) with the Shields criterion (Raudkivi, 1967).	39
Figure 3.2	Simplified model study area, upper Acushnet River estuary.	45
Figure 3.3A	Model predicted particle deposition sites for a flow rate of 30 ft^3/s (0.85 m^3/s) and a sediment particle size of 15.6 microns (ϕ=6).	48
Figure 3.3B	Model predicted particle deposition sites for a flow rate of 30 ft^3/s (0.85 m^3/s) and a sediment particle size of 3.906 microns (ϕ=8).	49
Figure 3.3C	Model predicted particle deposition sites for a flow rate of 30 ft^3/s (0.85 m^3/s) and a sediment particle size of 1.95 microns (ϕ=9).	50
Figure 3.3D	Model predicted particle deposition sites for a flow rate of 650 ft^3/s (18.4 m^3/s) and a sediment particle size of 15.6 microns (ϕ=6).	51
Figure 3.3E	Model predicted particle deposition sites for a flow rate of 650 ft^3/s (18.4 m^3/s) and a sediment particle size of 3.906 microns (ϕ=8).	52

Figure 3.3F	Model predicted particle deposition sites for a flow rate of 650 ft^3/s (18.4 m^3/s) and a sediment particle size of 1.95 microns (ϕ=9).	53
Figure 5.1	Model triangular finite element grid system.	61
Figure 5.2	Model predicted tidal currents at maximum flood approximately 3 hours after high water at the hurricane barrier.	63
Figure 5.3	Model predicted tidal currents at maximum ebb approximately 9 hours after high water at the hurricane barrier.	66
Figure 5.4	River induced flow for the mean annual flow rate (0.85 m^3/s).	71
Figure 5.5	Time series plot of surface elevation and tidal currents at the Coggeshall Street Bridge causeway.	72
Figure 5.6	Longitudinally averaged tidal height and currents as a function of distance along the upper Acushnet River estuary. The reference is at the head of the estuary. Plots are shown at selected times over a complete tidal cycle.	73
Figure 5.7A	Finite element model predicted particle deposition sites for a flow rate of 30 ft^3/s (0.85 m^3/s) and a sediment particle size of 15.6 microns (ϕ=6).	75
Figure 5.7B	Finite element model predicted particle deposition sites for a flow rate of 30 ft^3/s (0.85 m^3/s) and a sediment particle size of 3.906 microns (ϕ=8).	76
Figure 5.7C	Finite element model predicted particle deposition sites for a flow rate of 30 ft^3/s (0.85 m^3/s) and a sediment particle size of 1.95 microns (ϕ=9).	77
Figure 5.7D	Finite element model predicted particle deposition sites for a flow rate of 650 ft^3/s (18.4 m^3/s) and a sediment particle size of 15.6 microns (ϕ=6).	78
Figure 5.7E	Finite element model predicted particle deposition sites for a flow rate of 650 ft^3/s (18.4 m^3/s) and a sediment particle size of 3.906 microns (ϕ=8).	79
Figure 5.7F	Finite element model predicted particle deposition sites for a flow rate of 650 ft^3/s (18.4 m^3/s) and a sediment particle size of 1.95 microns (ϕ=9).	81
Figure 5.8	Location of Battelle PCB water column sampling stations.	86
Figure 5.9A	Filtrate PCB concentrations (ng/l) vs. longitudinal distance (km) for Battelle Cruise #1, Sept-Oct. 1984.	90

Figure 5.9B	Particulate PCB concentrations (ng/l) vs. longitudinal distance (km) for Battelle Cruise #1, Sept-Oct. 1984.	91
Figure 5.9C	Total PCB concentrations (ng/l) vs. longitudinal distance (km) for Battelle Cruise #1, Sept-Oct. 1984.	9.
Figure 5.10A	Filtrate PCB concentrations (ng/l) vs. longitudinal distance (km) for Battelle Cruise #2, November 1984.	91
Figure 5.10B	Particulate PCB concentrations (ng/l) vs. longitudinal distance (km) for Battelle Cruise #2, November 1984.	94
Figure 5.10C	Total PCB concentrations (ng/l) vs. longitudinal distance (km) for Battelle Cruise #2, November 1984.	95
Figure 5.11A	Filtrate PCB concentrations (ng/l) vs. longitudinal distance (km) for Battelle Cruise #3, June-July 1985.	96
Figure 5.11B	Particulate PCB concentrations (ng/l) vs. longitudinal distance (km) for Battelle Cruise #3, June-July 1985.	97
Figure 5.11C	Total PCB concentrations (ng/l) vs. longitudinal distance (km) for Battelle Cruise #3, June-July 1985.	98
Figure 5.12A	Filtrate PCB concentrations (ng/l) vs. longitudinal distance (km) for Battelle, summary of cruises 1, 2 and 3.	99
Figure 5.12B	Particulate PCB concentrations (ng/l) vs. longitudinal distance (km) for Battelle, summary of cruises 1, 2 and 3.	10
Figure 5.12C	Total PCB concentrations (ng/l) vs. longitudinal distance (km) for Battelle, summary of cruises 1, 2 and 3.	10
Figure 5.13	Comparison of (conservative) model predicted and observed total PCB concentrations (ng/l) vs. longitudinal distance (km).	10
Figure 6.1	Spill trajectories for the winter.	10
Figure 6.2	Spill trajectories for the spring.	11
Figure 6.3	Spill trajectories for the summer.	11
Figure 6.4	Spill trajectories for the fall.	11

List of Tables

		PAGE
Table 2.1	River drainage area and runoff rate estimates for the Acushnet River estuary.	7
Table 2.2	Extreme river runoff estimates for the Acushnet River estuary.	8
Table 2.3	Summary of precipitation and temperature data for New Bedford, Massachusetts (Corp of Engineers, 1961).	10
Table 2.4	Summary of meteorological data for Green Airport, Warwick, R.I.	13
Table 2.5	Maximum tide elevations for New Bedford, Massachusetts (Corps of Engineers, 1961).	17
Table 3.1	Sediment grain size data from Huidobro et al (1983) for samples nearest to the Aerovox facility.	36
Table 3.2a	Measured particle size distribution in sediments in the Acushnet River.	38
Table 3.2b	Sediment particle size data normalized as a percentage of particles between ϕ=4 and ϕ=9.	38
Table 5.1	Comparison of model predicted maximum ebb/flood tidal currents to observed values for selected sites in the Acushnet River estuary.	70
Table 5.2	Percent of ϕ=9 size particles passing south of Coggeshall Street Bridge as a function of river flow rate.	84
Table 6.1	Mean, standard deviation, minimum, and maximum time for spill trajectory to reach shore. Release point near the Aerovox facility.	113
Table 6.2	Maximum, minimum, mean and standard deviation of trajectory lengths for each season of the year. Also included are the directional distributions of trajectory lengths in percent.	114

1. INTRODUCTION

Applied Science Associates, Inc. (ASA) has been retained by Ropes and Gray, Boston, Massachusetts to investigate the circulation and pollutant transport dynamics in the Acushnet River estuary and New Bedford Harbor (Figure 1.1). The primary focus of the study is to determine the transport of PCBs in the harbor. Mechanisms of primary interest include: adsorption of PCBs on fine grained sediment and the subsequent transport of the sediment by advection and dispersion, transport by advection and dispersion of PCBs dissolved in the water column and movement of PCB contaminated oil in the form of surface slicks. These three mechanisms were studied because of their importance in determining how PCBs are redistributed in the receiving water after their initial disposal (NUS, 1984; Battelle, 1984). A series of models that incorporate the key physical/chemical features of the processes and have been verified with available field and laboratory observations are employed to quantify the transport dynamics and their associated rates.

Section 2 of the report provides a review of the circulation and pollutant transport dynamics of the New Bedford Harbor study area. This review includes the physical setting, hydrology, climate, hurricanes, circulation, and sediment transport dynamics. A simplified analysis of the transport and deposition of suspended particulate matter is given in Section 3. More complex finite element hydrodynamic and pollutant transport (sediment and dissolved constituents) models are described in Section 4. The application and results of the complex model simulations are presented in Section 5. Simulations of oil spill releases in the upper estuary are given in Section 6 with particular emphasis on the location of shoreline impacts. Section 7 summarizes the key findings of the study.

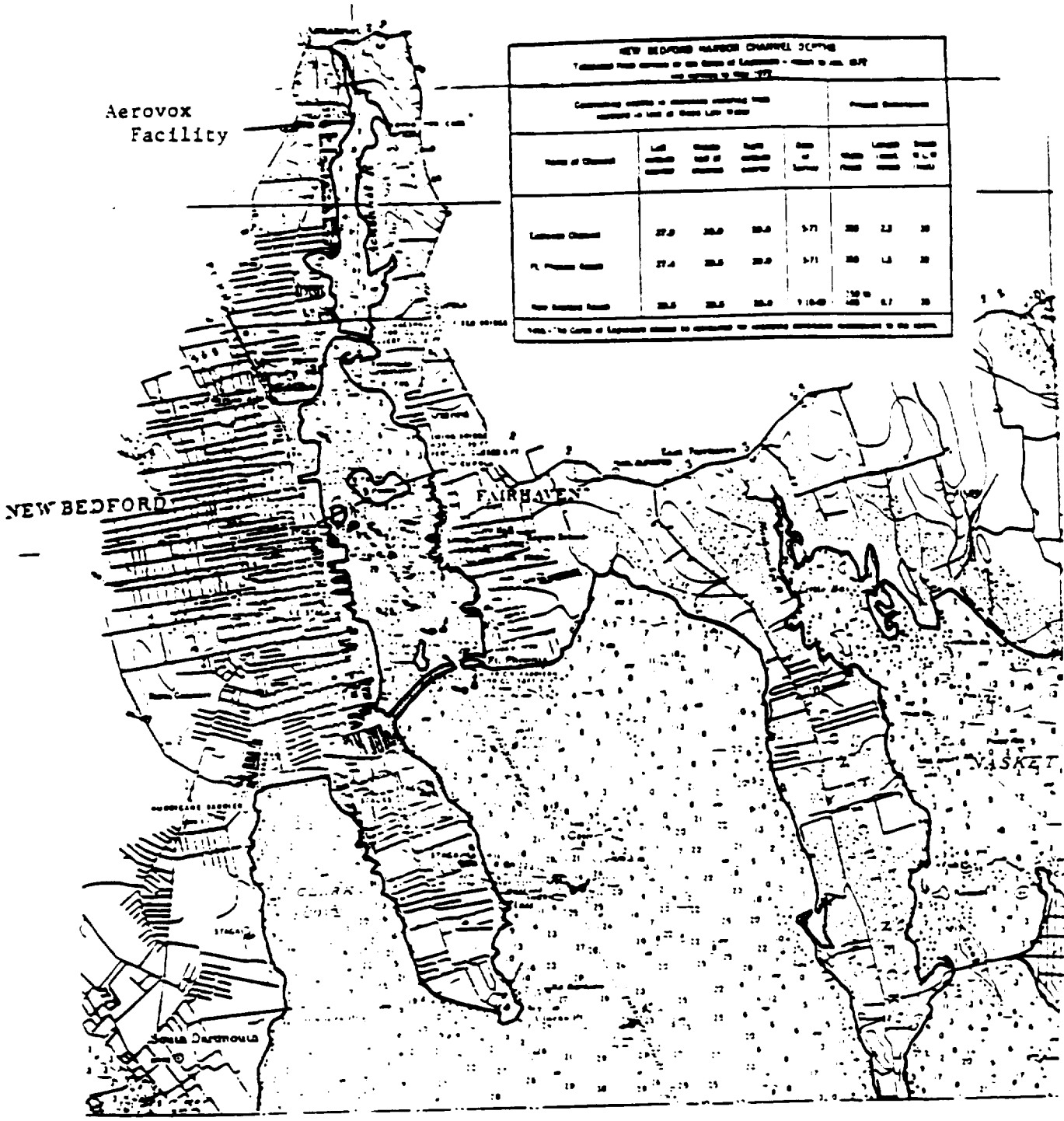

Figure 1.1 New Bedford Harbor; Acushnet River study area.

2. CIRCULATION AND SEDIMENT TRANSPORT DYNAMICS IN STUDY AREA

2.1 Physical Setting

The information reviewed here concerns the New Bedford - Fairhaven Harbor of Bristol County on the southeast shore of Massachusetts. Specifically, we will refer to the inner harbor as that portion of the Acushnet River Estuary which is north of the hurricane barrier (Figure 2.1). The outer harbor is defined as the area south of the barrier but north of the line connecting Wilbur and Clarks Pts.

2.1.1 Topography

The Acushnet River bed is a smooth-floored drowned valley with steep-sided, relatively low-lying ridges of New Bedford (<180 ft. (54.9 m) above sea level) on the west and Fairhaven (<50 ft. (15.2 m) above sea level) on the east.

2.1.2 Bathymetry

Several natural 30 ft. (9.1 m) channels and one dredged 30 ft. (9.1 m) channel in otherwise shallow water characterize the bathymetry of the outer harbor. The hurricane barrier, completed in 1966, restricts the basin to a width of 150 ft. (45.7 m) and a depth of 39 ft (11.9 m) near Palmer Island and Fort Pheonix (Figure 2.2). Inside the barrier the harbor is approximately 1.5 miles (2.4 km) in length (up to Popes Island) and 3/4 mile in width (1.2 km). The 300 ft. (9.1 m) wide channel depth decreases north of Popes Island to 23 ft. (7 m) and then gradually to 15 ft. (4.6 m) near the Coggeshall Street Bridge. North of the Coggeshall Street Bridge the river becomes a non-navigable stream. An Army Corps of Engineers 1985 depth survey in this

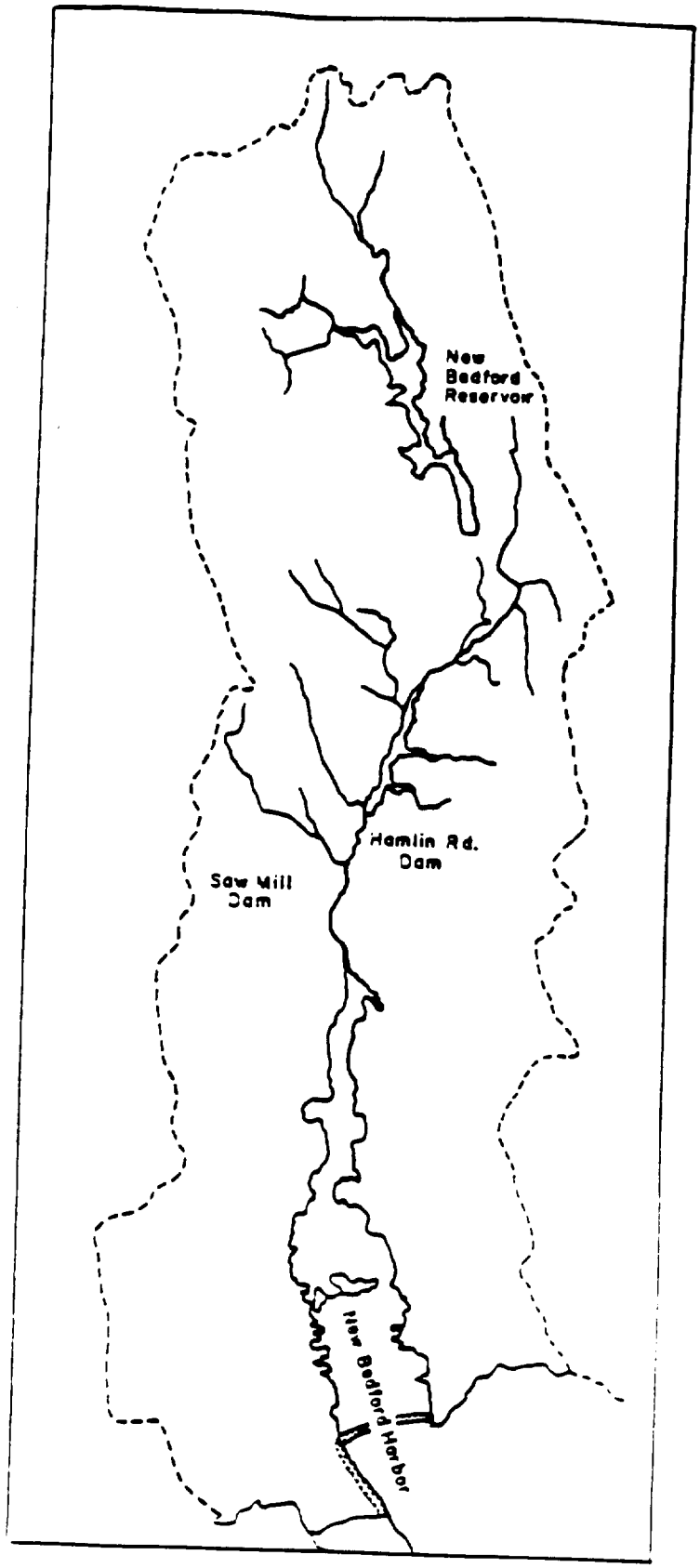

Figure 2.1 Acushnet River watershed.

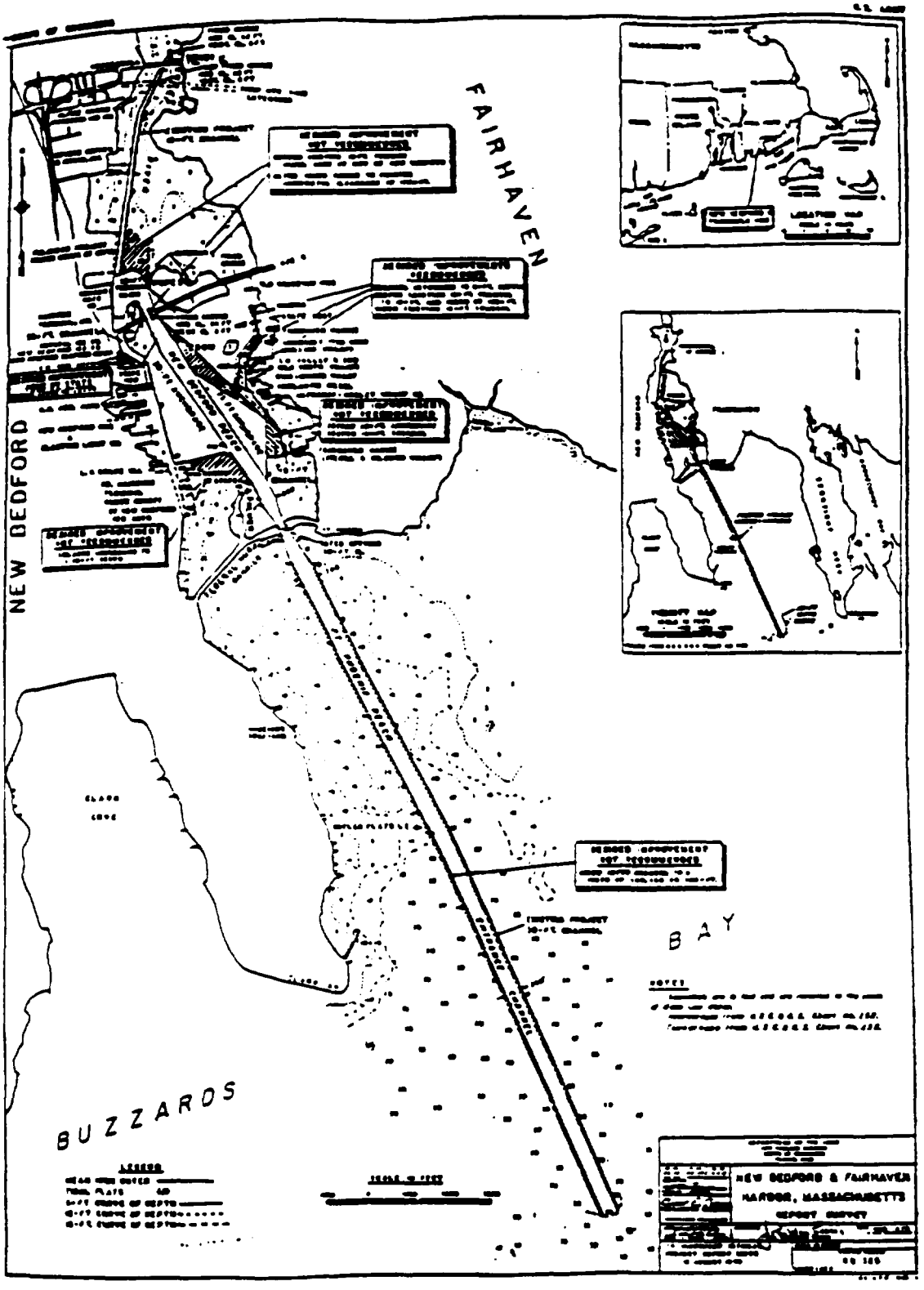

Figure 2.2 Bathymetry of the dredged channels in outer New Bedford Harbor (Corps of Engineers, 1970).

area found depths typically less than 1 ft. (0.33 m) below mean low water (MLW) near the Wood St. Bridge (north of the Aerovox facility). The Army Corp of Engineers (1982) describe the river as being eleven miles (17.6 km) long, eight miles (12.8 km) of which are above the head of the tide.

2.1.3 River Drainage Area and Runoff Rates

As there is no long term stream gauge data available for the Acushnet River (the only tributary to drain into the New Bedford Harbor), estimates of freshwater input are variable (Table 2.1). The USGS measured river runoff at selected times over a two year period a few miles upstream of the Coggeshall Street Bridge near the Leonard Street Bridge. They estimated flow rates ranging from 0.008 to .025 m^3/s for the annual minimum 7-day mean low flow with a 2-year recurrence interval (USGS, 1984). Cortell (1982) estimates the drainage basin of the Acushnet River above the tidal limit as approximately 18.4 $mile^2$ (47.6 km^2). Cortell notes that most rivers in New England produce a mean annual discharge (in cubic feet per second) equal to approximately 1.6 to 1.7 times their drainage basin area in square miles. They use this formula to estimate a mean annual freshwater discharge of 30 ft^3/s (0.85 m^3/s). Signell (1986) used the ratio of runoff to drainage area for Westport River (.05 $m^3/s\text{-}mile^2$), to estimate the runoff in the Acushnet. Assuming the Acushnet has a 16.4 $mile^2$ (42.5 km^2) drainage area (Signell, 1986), he estimates an average runoff rate of 28 ft^3/s (0.8 m^3/s). From these various estimates the mean annual flow rate is approximately 30 ft^3/s (0.85 m^3/s).

NUS (1984) has provided estimates of the river runoff for the 10, 25, 50 and 100 year storm events. These estimates are included in Table 2.2. It is unknown from the NUS report whether these represent peak values during the storm or if they are average flow rates over the rainfall event. The Corps of

TABLE 2.1

River drainage area and runoff rate estimates

Watershed	Drainage area mile^2	Runoff rate	Definition of runoff rate	Source
Acushnet River above Leonard St. Bridge	7.5	0.03 m^3/s	annual minimum 7 day mean low for 2-yr. recurrence interval	USGS (1984)
Acushnet River Leonard St. Bridge	-	.74 to .02 m^3/s	maximum and minimum values in 2 yr. period	Malcolm Pirnie (1981)
Entire Acushnet River drainage	16.4	.8 m^3/s	interpolated from runoff/drainage ratio of area Westport river	Signell (1986)
Acushnet River ubanized drainage area	3.6	-	-	Summerhayes et al(1976) Malcolm Pirnie (1981)
Acushnet River drainage above tidal limit	18.4	.85 m^3/s	1.6 times (in cfs) the drainage are in square miles	Cortell (1982)
Entire Acushnet River	18.6	-	-	U.S. Army Corps of Engineers (1982)

TABLE 2.2

Extreme river runoff estimates for the Acushnet River estuary

Event	NUS (1984)** Estimates
100 yr. Storm	38.2 m^3/s
50 yr. Storm	22.7 m^3/s
25 yr. Storm	20.5 m^3/s
10 yr. Storm	17.0 m^3/s

** These are peak values whereas the Corps of Engineers (1961) estimate is an average over a 5 hour storm and gives 18.4 m^3/s for the 100 year storm.

Engineers estimates 2780 acre-feet of water storage for a 5 hour gate closure during the 100 year storm (Corps of Engineers, 1961) which gives an average flow rate of 650 ft^3/s (18.4 m^3/s). Since this value is less than the NUS estimate it seems probable that the NUS value represents a peak.

2.2 Hydrology

The average annual precipitation based on 151 years of record is 45 inches (114 cm), or about 4 inches (10 cm) per month, distributed approximately uniformly throughout the year, (Corps of Engineers, 1982) as shown in Table 2.3. The maximum monthly rainfall at New Bedford totaled 18.7 inches (47.5 cm) in August 1826. The minimum monthly rainfall was 0.01 inch (0.025 cm) in June 1949.

Snowfall based on 65 years of record at New Bedford averages about 34 inches (86.4 cm) over the winter season. A maximum of 97 inches (246 cm) was recorded during the winter of 1904 and a minimum of 10 inches (25.4 cm) during the winter of 1919. Snow cover usually reaches a maximum depth about 15 February. Spring freshets resulting from snowmelt occur frequently, but this factor alone rarely causes serious flooding.

Thunderstorms are responsible for much of the rainfall from May through August. They usually produce heavy, and sometimes even excessive amounts of rainfall; but since the duration is relatively short, damage is ordinarily light. The thunderstorms of summer are frequently accompanied by extremely gusty winds which may result in some damage to property, especially to small pleasure and fishing craft (Corps of Engineers, 1972).

The first measurable snowfall of winter usually arrives at the end of November, whereas the last in spring is about the middle of March. Because of the temperature effects of the ocean, it is unusual for the ground to remain well covered with snow for any long period of time.

Climatological Data - New Bedford, Massachusetts

Elevation 63 Ft., M.S.L.

Item & Description	Years of Record	JAN	FEB	MAR	APR	MAY	JUN	JUL	AUG	SEP	OCT	NOV	DEC	ANNUAL
TEMPERATURE (°F)														
Average	72	30.1	29.6	37.1	46.5	56.6	65.4	71.2	69.8	63.6	53.8	43.8	33.2	50.1
Average Maximum	72	39.6	37.5	44.8	53.2	64.2	73.2	78.0	76.0	70.2	61.4	50.4	41.2	57.5
Average Minimum	72	21.6	20.6	29.0	37.6	48.4	57.0	63.4	61.6	55.4	44.4	35.2	25.1	41.6
Absolute Maximum	59	64	58	77	85	95	102	101	96	92	90	76	63	102
Year of Absolute Maximum	-	1916	1913	1910	1957	1919	1923	1919	1949	1953	1946	1956	1951	1923
Absolute Minimum	59	-9	-12	6	20	32	42	51	44	30	22	10	-11	-12
Year of Absolute Minimum	-	1904	1934	1916	1908	1903	1904	1909	1912	1904	1904	9104	1933	1934
PRECIPITATION (in)														
Average	146	3.92	3.67	4.14	3.85	3.67	3.04	3.06	4.17	3.37	3.67	4.05	3.96	44.57
% of Average Annual	-	8.8	8.3	9.3	8.6	8.2	6.8	6.8	9.4	7.6	8.3	9.0	8.9	100.0
Maximum	146	10.75	8.30	9.77	9.64	9.80	9.31	12.00	18.72	12.06	10.09	9.74	10.05	65.41
Year of Maximum	-	1915	1814	1890	1958	1948	1938	1830	1826	1850	1890	1897	1901	1829
Minimum	146	0.77	0.91	0.09	0.91	0.57	0.01	0.02	0.24	0.21	0.15	0.35	0.45	25.82
Year of Minimum		1839	1816	1915	1942	1923	1949	1952	1854	1930	1924	1917	1928	1957
Average Snowfall Unmelted	60	8.8	10.3	6.3	1.4	-	-	-	-	-	-	0.8	6.6	34.1
Year of Maximum Snowfall	1904	-	-	-	-	-	-	-	-	-	-	-	-	96.6
Year of Minimum Snowfall	1919	-	-	-	-	-	-	-	-	-	-	-	-	10.8

Table 2.3 Summary of precipitation and temperature data for New Bedford Massachusetts (Corp of Engineers, 1961).

In early fall, severe coastal storms of tropical origin sometimes bring destructive winds to the area. Also, at other times of the year, it is usually coastal storms which produce the most severe kind of weather, such as the typical "Nor'easter" of late winter. Coastal storms may occur in any month of the year, but generally occur from the late fall through to spring. The hurricane season is from June to November. (See Section 2.4).

The biggest storms of the present century that have struck the New Bedford area occurred on 30 November 1944, 6-7 November 1953, 30 November 1963, 9 January 1978. The Corps of Engineers, (1982) presents a brief description of these four events.

Although wind and tide surges from these storms are not as great as hurricanes, they do pose a more frequent threat to the New Bedford-Fairhaven area. During storms it has been observed that winds predominantly come from the south, with gusts reaching up to 70 mph (31.3 m/s); tides of 1 to 3 feet (0.3 to 0.91 m) above normal and an average of 0.5 inch (1.3 cm) rainfall.

2.3 Climate

The New Bedford-Fairhaven area has a variable temperature climate characterized by frequent but generally short periods of heavy precipitation. The area lies in the path of the "prevailing westerlies" and is exposed to cyclonic disturbances that cross the country from west or southwest towards the east or northeast. Coastal storms that travel up the Atlantic coast in the form of hurricanes also harass the area with heavy rainfall and abnormally high tides. In winter, the temperatures are modified considerably, and many major storms drop their precipitation in the form of rain rather than snow. In summer, many days that would otherwise be uncomfortably warm are cooled by sea breezes. At other times of the year, sea fog may be advected over the

area by onshore winds; however, the number of such days is relatively few, averaging two or three days per month.

2.3.1 Winds

The New Bedford airport has routinely collected wind data since 1947. For the vast majority of the time, wind observations are only available 12 to 18 hours per day during daylight hours. It is difficult to derive an accurate description of the wind from this limited data set.

Otis Air Force Weather Station located about 32 km to the north west of the harbor has 27 years of continuous records while Green Airport in Warwick, R.I. located 45 km to the west northwest has a record since 1947. The Green Airport data is reasonably representative of the wind conditions in the general area and a summary is presented in Table 2.4. Also summarized in the table are other climatic data such as temperatures, precipitation and relative humidity.

The average wind has a speed of 4.8 m/s coming predominantly from the northwest in winter and from the southwest in summer. The mean winds are about 15% stronger in the winter/spring than the average and 15% lower than the average in the summer. The peak values are in March and April and the minimum in August. The fastest mile winds occur in August, associated with hurricanes, and reach 90 mph (40.3 m/s). Typical values for the rest of the year are 50 mph (22.3 m/s).

Summerhayes et al (1976) have observed that the highest winds usually come from the WNW or NNW. Variations in the wind speed have two characteristic periodicities: one to several days due to migration of weather cells across the area; and a daily cycle due to sea breeze.

Normals, Means, And Extremes

Station: PROVIDENCE, RHODE ISLAND 0 10700 — THEO FRANCIS GREEN STATE AP — Standard time used: EASTERN — Latitude [illegible] — Longitude [illegible] — Elevation (ground): [illegible] feet

	Temperature °F: Normal			Temperature °F: Extremes				Normal Degree days Base 65 °F		Precipitation in inches: Water equivalent								Precipitation in inches: Snow, ice pellets				Relative humidity pct				Wind					Percent possible sunshine	Mean sky cover tenths	Mean number of days											Average station pressure mb
	Daily max.	Daily min.	Mean	Highest	Year	Lowest	Year	Heating	Cooling	Mean	Greatest monthly	Year	Least monthly	Year	Greatest in 24 hrs.	Year	Mean	Greatest monthly	Year	Greatest in 24 hrs.	Year	Hour 01	Hour 07	Hour 13	Hour 19	Prevailing direction	Mean speed mph	Fastest mile direction	Fastest mile speed	Year			Clear	Partly cloudy	Cloudy	Precipitation .01 inch or more	Snow, ice pellets 1.0 inch or more	Thunderstorms	Heavy fog visibility 1/4 mile or less	Temperature °F Max. 90 and higher	Temperature °F Max. 32 and lower	Temperature °F Min. 32 and lower	Temperature °F Min. 0 and lower	Elev. [illegible] feet msl
(a)				24		2					24		2		2			24			24	17	17	17	17		23	23	23	23		23	23	23	23	23	23	23	23	23	23	23	23	0
1	36.4	20.6	28.5	64	1955	-5	1934	1135	0	3.53	11.60	1955	0.50	1934	3.15	1962	24.7	104.7	1967	24.7	1967	63	73	57	65	33.5	NW	55	20	1972	53	1.7	10	9	12	11	3	0	2	0	17	29	1	1013.0
2	32.4	23.2	29.5	63	1950	-2	1934	900	0	3.53	5.63	1965	1.34	1960	3.15	1934	38.5	176.2	1978	27.5	1978	63	71	55	61	33.2	NNW	55	15	1972	54	1.6	9	7	13	12	2	1	2	0	7	20	0	1013.0
3	36.2	26.8	36.5	70	1955	8	1964	620	0	3.53	6.18	1960	1.72	1965	4.15	1960	31.6	155.5	1960	16.5	1960	63	71	55	61	32.2	SW	55	20	1955	54	1.6	9	7	15	12	2	1	2	0	2	7	0	1013.0
4	53.2	35.6	43.5	90	1960	19	1955	333	0	3.32	3.37	1960	1.96	1965	2.0	1970	3.2	1955	3.2	1955	66	67	52	58	30.9	S	57	20	1955	57	1.5	8	10	15	11	3	1	2	1	0	1	0	1012.0
5	66.4	46.4	56.5	90	1965	29	1950	25	0	3.53	5.57	1972	0.72	1965	3.34	1962	3.6	1973	3.6	1973	71	67	57	63	30.0	SW	50	20	1955	59	1.5	8	13	13	11	3	0	2	2	0	0	0	1013.5
6	76.7	56.5	66.5	96	1964	41	1964	3	3	3.53	6.05	1972	0.17	1957	2.0	1972	0.0			0.0		72	72	57	63						59	1.5	9	17	13	11	3	0	2	2	0	0	0	1013.5
7	81.5	61.0	72.5	100	1966	51	1957		28	3.53	9.00	1971	1.04	1957	5.0	1976	0.0			0.0		73	73	57	63	9.5	SW	55	30	1965	61	1.5	9	17	13	9	3	0	0	0	0	0	0	1012.0
8	80.4	61.4	70.5	100	1975	50	1965	15	13	3.53	11.12	1955	0.75	1955	3.15	1955	0.0			0.0		73	73	57	63	9.3	SSW	60	33	1975	59	1.7	9	11	12	10	3	0	2	3	0	0	0	1015.0
9	73.4	53.4	63.5	93	1960	35	1966	93	0	3.53	3.93	1966	0.73	1955	2.0	1955	0.0			0.0		73	73	57	63	9.5	SW	50	30	1960	60	1.5	9	9	12	9	3	0	2	1	0	0	0	1015.5
10	63.4	43.4	53.5	84	1974	24	1974	372	0	3.53	11.00	1962	1.67	1965	6.0	1962	7.5	17.0	1977	7.5	1977	73	73	57	63	9.2	NW	53	35	1955	57	1.5	11	8	12	9	3	1	3	0	0	0	0	1015.5
11	52.4	34.4	43.5	79	1975	15	1977	630	0	3.53	6.57	1977	0.93	1958	3.1	1955	9.1	19.0	1958	9.1	1958	73	73	57	63	10.5	SW	52	30	1955	59	1.5	9	8	13	11	3	1	2	0	1	0	0	1015.0
12	39.4	23.4	31.5	64	1950	-17	1950	1035	0	3.53	10.27	1967	0.50	1957	3.0	1960	19.4	36.5	1960	11.7	1960	73	73	57	63	11.0	WNW	60	35	1950	53	1.5	9	8	13	12	3	0	2	0	6	25	0	1014.0
					2000		2000					1967		1957		1960			1960		1960									2000													
(a)	55.0	40.0	48.0	104	1959	-17	1934	5072	532	42.37	11.60	1967	0.50	1957	6.15	1960	31.6	155.5	1960	27.5	1978	73	73	57	63	10.3	SW	50	35	1955	57	1.7	101	101	157	124	18	20	24	9	29	123	1	1013.0

Means and extremes above are from existing and comparable exposures. Annual extremes have been recorded at other sites in the locality as follows: lowest temperature -17 in February 1934; maximum monthly precipitation 12.24 in August 1948; minimum monthly precipitation .06 in June 1949; maximum monthly snowfall 31.9 in January 1948; fastest mile wind 95 SW in September 1938.

(a) Length of record, years, through the current year unless otherwise noted, based on January data.
(b) 90° and above at Alaskan stations.
* Less than one half.
T Trace.

NORMALS - Based on record for the 1941-1970 period.
DATE OF AN EXTREME - The most recent in case of multiple occurrences.
PREVAILING WIND DIRECTION - Record through 1965.
WIND DIRECTION - Numerals indicate tens of degrees, clockwise from true north. 00 indicates calm.
FASTEST MILE WIND - Speed is fastest observed 1 minute value when the direction is in tens of degrees.

Table 2.4. Summary of meteorological data for Green Airport, Warwick, R.I.

2.3.2 Temperature

The mean annual temperature based on 77 years of record at New Bedford, Massachusetts is approximately 50° F (10° C). The average monthly temperature varies from 71°F (22° C) in July to 30°F (-1° C) in January.

Freezing temperatures occur on the average about 120 days and cease to be common near the end of March. Sub-zero weather seldom occurs, averaging less than one day for December and only one day for each of the months of January and February. Seventy degree temperatures become a common daily occurrence near the end of May, and cease to be common the latter part of September. During this period, there may be several days with 90°F (32° C) and over, averaging six days per year. Air temperatures of 100°F (38° C) and over do not occur very often, and have been confined to the months of June, July and August (Corps of Engineers, 1961).

2.4 Hurricanes

Descriptions of hurricanes affecting the southeast New England coast have been found in the literature as far back as the time of William Bradford and the Plymouth Plantation. Much of this information was gathered by the Army Corps of Engineers and other agencies in the design of the hurricane barrier built in the mid-sixties (1964-66).

A hurricane is defined as an intense tropical cyclone originating and sustained over a warm tropical ocean, north of the equator, with a counter-clockwise circulation (Corps of Engineers, 1982). It extends outward from a relatively calm "eye" to approximately 50 miles and is characterized by winds above 74 mph (33 m/s). These strong winds on the fringes of the hurricanes spiral upwards releasing rain at a rate of 1 to 2 inches (0.4-0.8 cm) per hour. Large waves and storm tide surges cause shoreline damages 5

to 25 feet (1.5 to 7.6 m) above stillwater.

Although there have been several high intensity hurricanes in the past few centuries (Aug. 1635, Aug. 1638, Oct. 1723, Oct. 1761, Sept. 1815, Sept. 1869), only those of the present century (Sept. 1938, Sept. 1944, Aug. 1954) have been monitored and described in detail. The 1938 hurricane was particularly destructive due to the wind induced storm surge (9.8 feet, 3 m) occurring simultaneously with the normal high tide (2.7 feet, 0.82 m). The total surge was 12.5 feet (3.8 m) above the National Geodetic Vertical Datum (NGVD). Peak wind velocities of 186 mph (83 m/s) were recorded in Milton, Massachusetts and minimum barometric pressures of 28.9 mb Hg were recorded in Providence, R.I. The storm passed over Long Island Sound at a speed of 63 mph (28.1 m/s). Parts of southern New England received as much as 17 inches (43 cm) of rain in four hours. The water level in New Bedford harbor remained above mean high water for six hours. Sea surface elevation data for the 1938, 1944 and 1954 hurricane is plotted in Figure 2.3. Maximum tidal surge information for these and other twentieth-century hurricanes is listed in Table 2.5. River runoff estimates for storm events are found in Section 2.1.3.

2.5 Circulation

Data indicate that tides are the strongest driving force for the circulation in New Bedford Harbor, however the circulation may be significantly altered by the wind. There is a clearly stratified density structure in the outer harbor and Buzzards Bay which may affect circulation in the harbor. Freshwater input into the harbor has little effect on circulation, while other mechanisms such as seiches and internal waves may have some influence on the harbor.

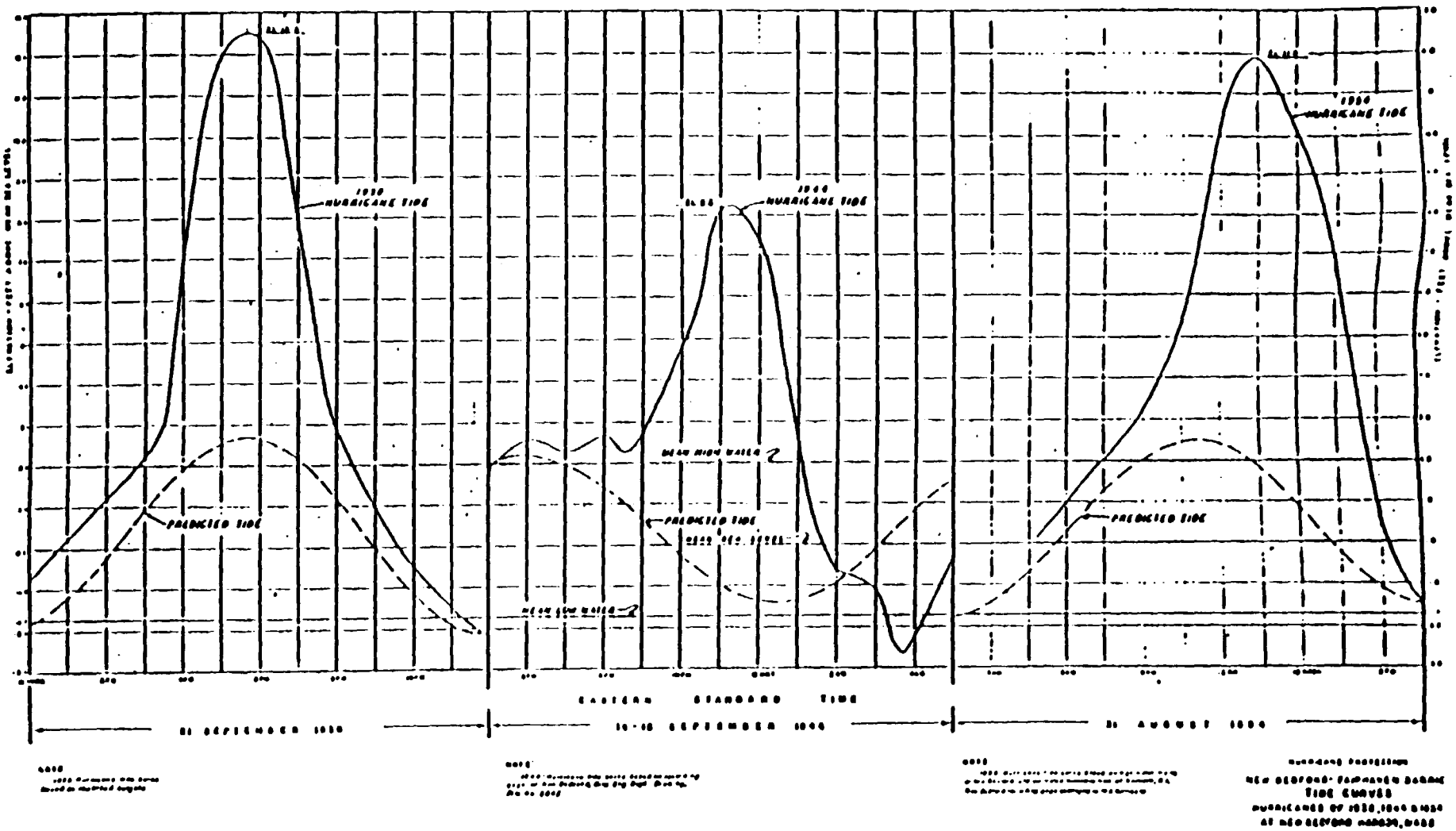

Figure 2.3 Sea surface elevation for the 1938, 1944, and 1954 hurricanes in New Bedford Harbor (Corps of Engineers, 1970).

TABLE 2.5

Maximum tide elevations
New Bedford, Massachusetts (EPA, 1983)

Date	Stillwater Elevation Relative to NGVD (ft)/(m)
21 Sept 1938 Hurricane	12.5/3.81
31 Aug 1954 Hurricane "Carol"	11.9/3.63
23 Sept 1815 Hurricane	11.5+/3.51+(est)
14 Sept 1944 Hurricane	8.1/2.57
30 Nov 1944	6.8/2.04
12 Sept 1960 Hurricane "Donna"	6.3/1.92
9 Jan 1978	6.3/1.92
7 Nov 1953	6.2/1.9
30 Nov 1963	6.1/1.86
30 July 1960 Tropical Storm "Brenda"	6.1/1.86
19 Feb 1960	6.1/1.86
10 June 1960	6.1/1.86
20 Nov 1972	6.1/1.86
29 Dec 1966	6.0/1.83
29 Dec 1959	5.8/1.77
2 Dec 1974	5.7/1.74

2.5.1. Tides

The tides in New Bedford harbor are primarily semi-diurnal with two high and low waters occurring each lunar day. The mean range of the tide is 3.7 ft (1.13 m) with a maximum diurnal inequality of 1.2 ft (0.36 m). The mean high water is 2.4 ft. (0.73 m) above the National Geodetic Vertical Datum (NGVD), i.e. mean sea level (MSL), while mean low water (MLW) is 1.3 ft (0.4 m) below MSL. The mean spring tide range is 4.6 ft. (1.4 m) with a maximum range of 6.7 ft. (2 m). A maximum probable spring high water reach 4.2 ft (1.3 m) above MSL, while a minimum probable spring low water falls 2.5 ft (0.76 m) below MSL. The time interval for a complete tidal cycle is predominated by the M2 tide with an average period of 12 hours and 25 minutes. This tidal data is summarized below:

SUMMARY OF ASTRONOMIC TIDES
NEW BEDFORD, MASSACHUSETTS

	Amplitude (Feet)	Amplitude (m)
Mean Tide Range	3.7	1.13
Mean High Water (above NGVD)	2.4	0.73
Mean Low Water (below NGVD)	1.3	0.4
Mean Spring Tide Range	4.6	1.4
Mean Spring High Water (above NGVD)	2.9	0.88
Maximum Probable Spring High Water (above NGVD)	4.2	1.3
Minimum Probable Spring Low Water (below NGVD)	2.5	0.76

Tidal constituents with amplitudes greater than 0.03 m for New Bedford are given below based on an analysis of a 369 day time series.

NOAA/NOS tidal constituents for New Bedford Harbor,
New Bedford, Massachusetts

Constituent	Period (hr)	Amplitude (m)	Modified Epoch (K') Degrees
M2	12.42	0.5356	218.6
N2	12.66	0.137	206.4
S2	12.00	0.130	234.6
M4	6.21	0.078	107.7
K1	23.93	0.062	095.2
SA	365.25*	0.054	156.5
O1	25.82	0.049	128.8
K2	11.96	0.040	234.4
μ2	12.87	0.031	205.5

*Period in days

The tabulated values show that the M2 constituent dominates tidal fluctuations, accounting for about 85 percent of the energy in the tidal band. The N2 and S2 are also significant semi-diurnal constituents. Their interaction with the M2 produces a neap-spring variation which modulates the amplitude of the semi-diurnal fluctuations at 14 and 28 day periods. The O1 and K1 diurnal constituents interact with the semi-diurnal constituents to produce a small diurnal inequality.

The M4 constituent is also significant. Its contribution to the characteristic tidal wave is to produce an inflection in the slope of the semi-diurnal tidal elevation during the flood tide (Signell, 1982). As a result, the slope of the flood tide is less than that of the ebb tide. This effect becomes most pronounced during neap conditions.

2.5.2. Maximum Tides

A tidal gauge was in operation at the New Bedford-Fairhaven Bridge from 1922 to 1965, and at the Hurricane Barrier from 1966 to present. All tides in excess of 5.5 feet (1.7 m) above MSL are listed in Table 2.5.

The frequency of tidal flooding in New Bedford harbor due to storms is shown in Figure 2.4. The frequency of tidal heights reaching 10 feet (3 m) or more is every 40 years, while tidal heights above 6 feet (1.83 m) occur every 5 years. With the hurricane barrier in operation the tidal heights in the harbor reach only 5 feet (1.5 m), compared to 16 feet (4.9 m) without the barrier (Corps of Engineers, 1982).

2.5.3 Tidal Currents

Figure 2.5 shows the average and maximum velocities during ebb and flood tides for 9 locations in the upper harbor (Cortell, 1982). The data was taken from two surveys consisting of hourly current measurements over two different tidal cycles on November 13, 1981 and December 11, 1981. Because tidal flow is confined to the opening beneath the Coggeshall Street Bridge, flood and ebb velocities throughout the upper basin vary widely. The narrow bridge underpass results in flood flows being directed up the main channel of the basin, where they are dominant. Conversely, ebb flow is relatively uniform throughout the basin directed toward the Coggeshall underpass and dominant in the shallows to either side of the main channel (Cortell, 1982). This is evidenced by the fact that ebb currents dominate at stations 1 and 4, while flood currents dominated the mid-channel stations 2 and 3. Also, the variation between maximum ebb flow velocities for all stations was only .08 ft/s (2.4 cm/s) while this value rose to 0.51 ft/s (15.5 cm/s) for flood currents (Cortell, 1982).

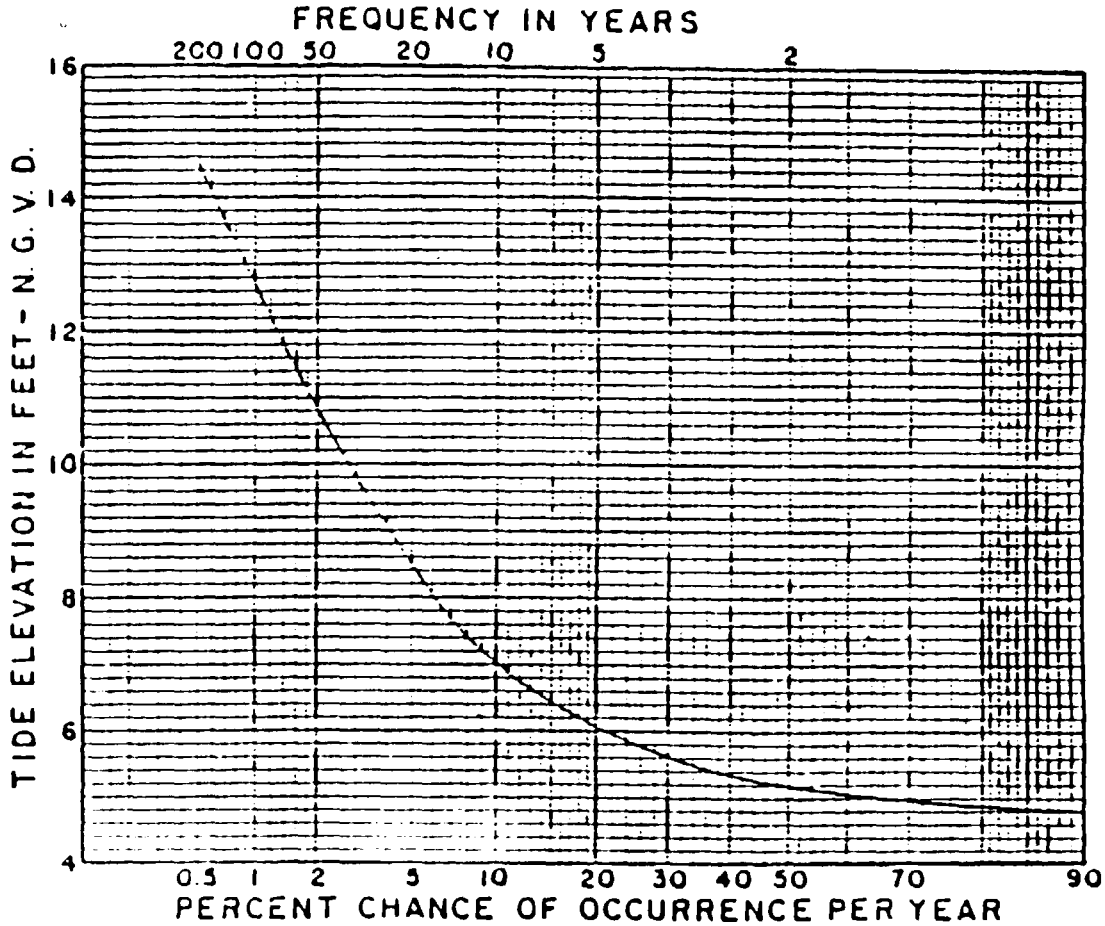

Figure 2.4 Percent chance of tidal flooding per year in New Bedford Harbor.

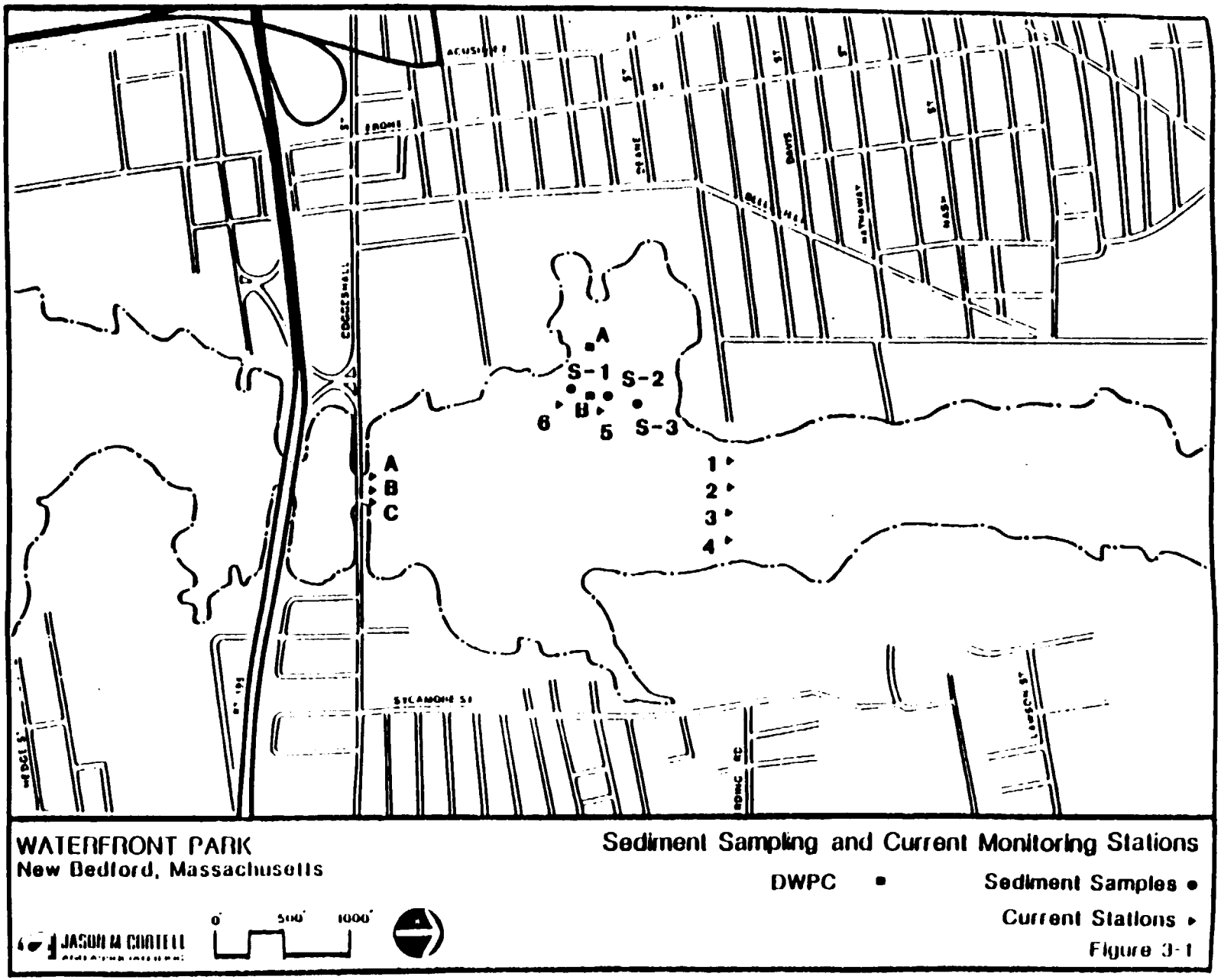

Figure 2.5 Summary of tidal current measurements collected in the upper Acushnet River estuary (north of Coggeshall Street Bridge) (Cortell, 1982).

In addition to influencing the direction and magnitude of tidal currents within the basin, the Coggeshall Street Bridge also affects the tidal duration. The bridge acts as a partial dam, limiting flow between the harbor to the south and the basin to the north. During the survey of November 13, 1981, flood flow beneath the eastern side of the bridge underpass was recorded concurrent to ebb flow on the western side for 1 hour and 29 minutes. This overlap of ebb and flood flow is directly related to the narrow width [approximately 150 ft (45.7 m)] of the channel through which the tidal prism must flow (Cortell, 1982).

A current meter located in center of the span on the south side of Coggeshall Street Bridge and five feet (1.5 m) off the bottom, indicates the mean tidal current during flood tide was .66 knots (33.8 cm/s), while during the ebb tide the mean current was 1.0 knots (51.5 cm/s) for two days during January 1983. The maximum current velocities were estimated at 1.68 knots (86.5 cm/s) during flood tide and 3.64 knots (187.5 cm/s) during ebb tide (EPA, 1983). The ebb tide maximum value however appears to be a single observation (2 minute sampling interval) and hence is likely not representative.

The brief EPA (1983) study on flow under the Coggeshall Street Bridge performed on 11 and 12 January 1983 indicate that reversals in flow direction frequently occur, predominantly during flood tide with a duration of 2 to 26 minutes. Short duration current reversals (2 to 6 minutes) mainly seen at the bottom of the water column may be due to strong eddy currents at the bottom of the channel which form as the incoming tide rushes through the constricted channel at the bridge. The longer current reversals (6 to 25 minutes) involved the entire water column and had significant current velocities (up to 1.3 knots, 67 cm/s) occurring in the opposite direction of the flood tide.

These current reversals may be due to the numerous constrictions placed on the water mass such as the hurricane barrier, Route I-195 Bridge and the Coggeshall Street Bridge (EPA, 1983). They also may have been caused by storm induced seiching in the harbor (Section 2.5.7).

Other than these periods of current reversal, measurements taken at all depths by a series of point measurements across the bridge transect show that the current speed and direction are comparable to measurements taken by the stationary meter located five feet off the bottom at the center of the bridge. These measurements indicate a uniform, turbulent flow in the constricted area beneath the Coggeshall Street Bridge.

During the present study, current measurements were made at three locations across the I-195 Bridge transect and at two meter intervals in the vertical on 20 June 1986 using an Endeco Model 110 impeller current meter. Maximum flood velocities reached 80 cm/s while the peak ebb currents were 60 cm/s. Figure 2.7 shows the cross sectionally average current versus time over one tidal cycle. The currents were relatively uniform across the cross section. A description of the experiment and the data set are included as Appendix A.

Summerhayes et al (1976) made continuous current measurements at two locations in the lower harbor (one near Popes Island and the second just inside the hurricane barrier) throughout one tidal cycle on June 8 and 9, 1976 (Figure 2.6). They reported values of 0.3 (15.5 cm/s) to 0.46 knots (23.7 cm/s) during flood tide and about 0.15 knots (7.7 cm/s) or less at other times. Current meters positioned at two levels within the water column, surface and subsurface, recorded current in the same directions during both flood and ebb tide.

The Corps of Engineers design memorandum (Corps of Engineers, 1961)

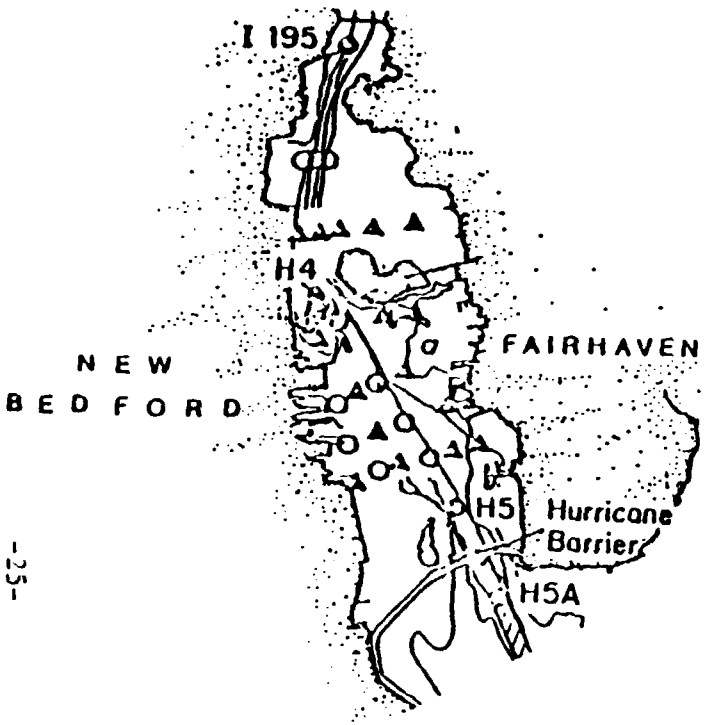

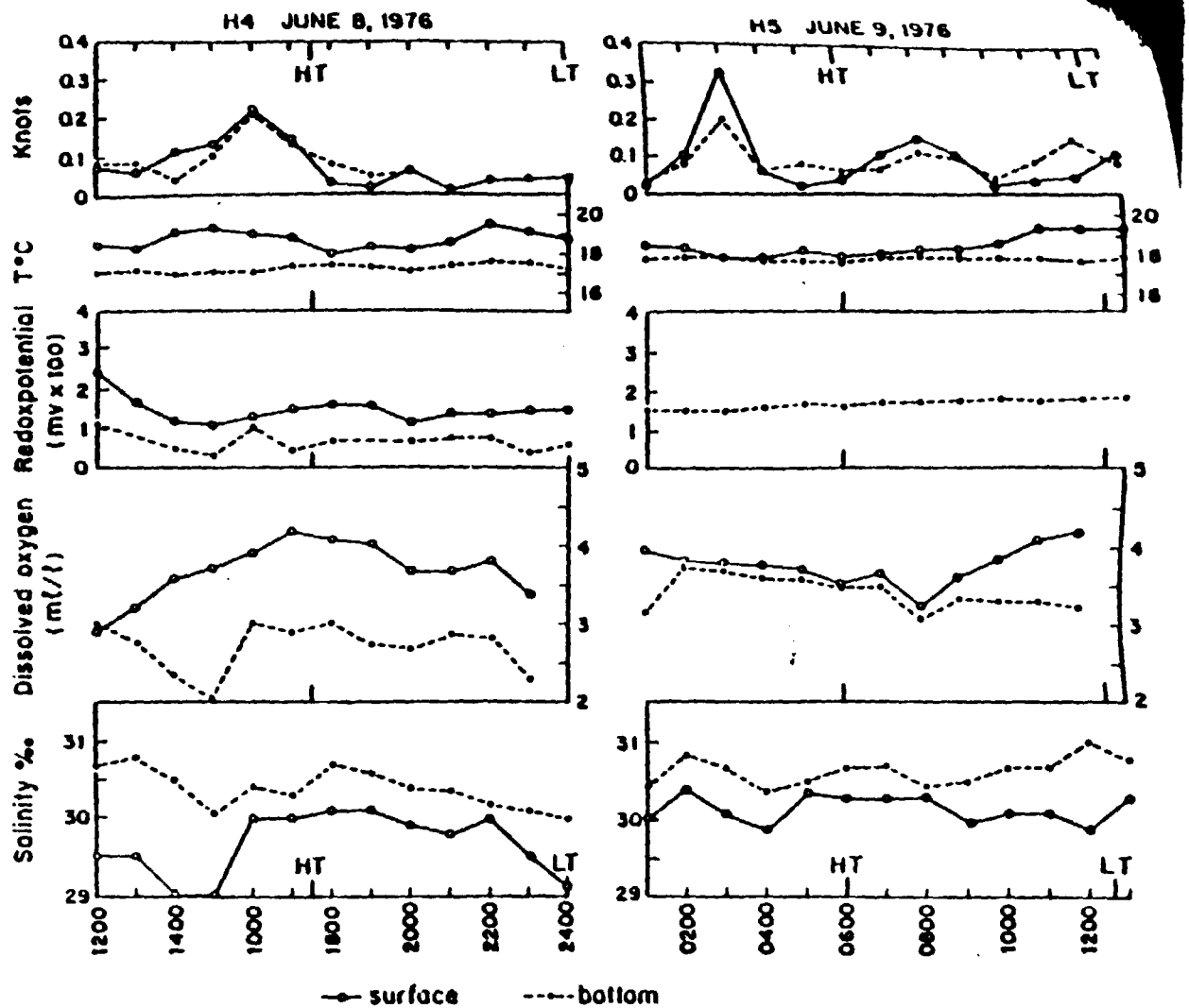

Figure 2.6 Variations in water properties and current velocities in surface and bottom waters for two stations (H4 and H5) through one complete tidal cycle (Summerhayes et al, 1976).

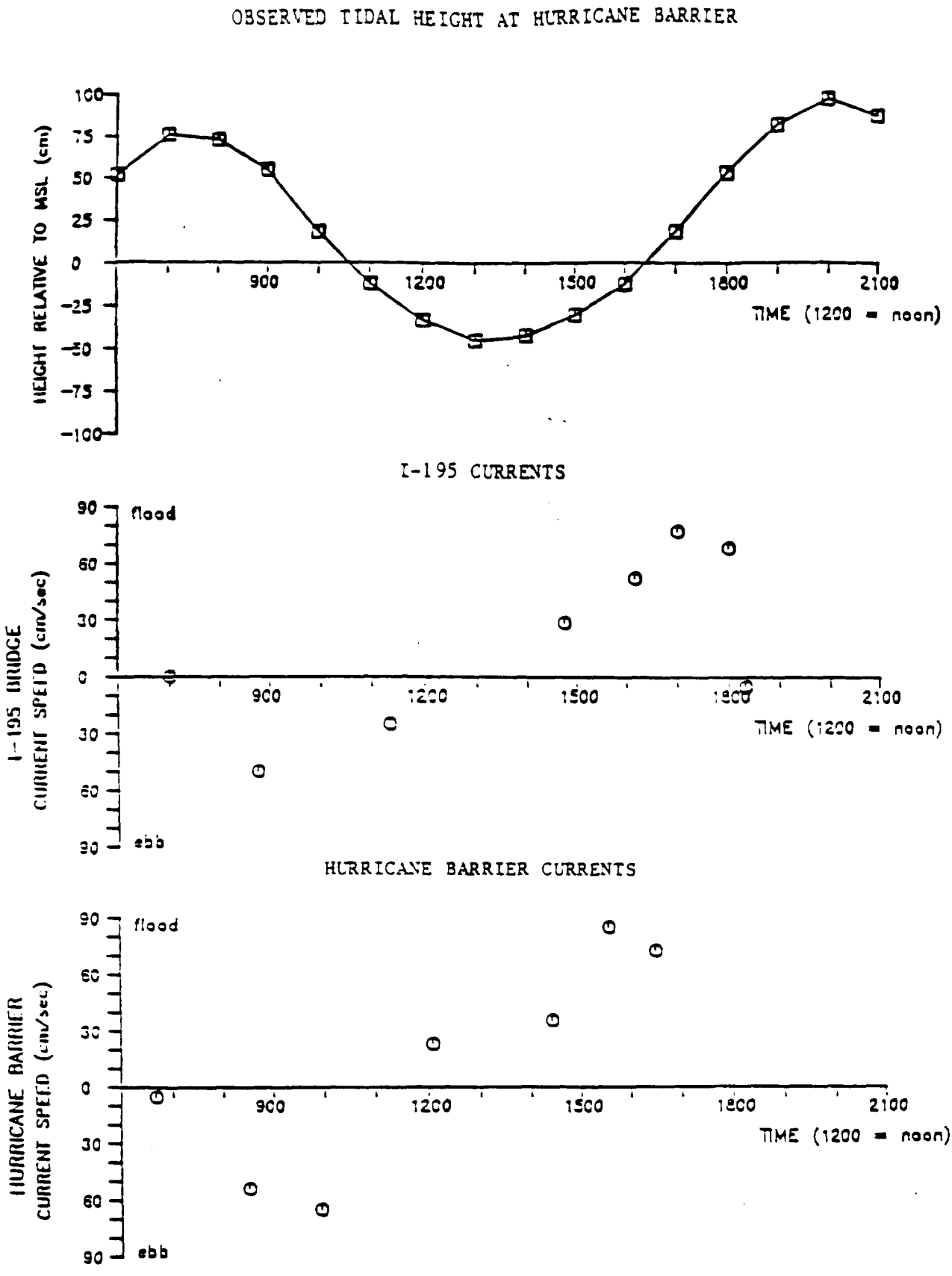

Figure 2.7 Time series of tidal height and current speed at the hurricane barrier and cross sectionally averaged speed at the I-195 bridge causeway, 20 June 1986.

estimates that the average maximum velocities through the hurricane barrier range from 2.1 ft/s (64 cm/s) during the normal tidal cycle to 3.2 ft/s (98 cm/s) during spring tide. This gives a flow rate of 12,500 ft^3/s (354 m^3/s) for the normal tide and 18,200 ft^3/s (515 m^3/s) during a spring tide. These calculations show an extremely small phase difference between the ocean and harbor tide and a 90° phase shift between the velocity and surface elevation, with the velocity leading the surface elevation. In a detailed small navigation project report (Corp of Engineers, 1970) the maximum velocities through the barrier opening area are given as 2.4 kts. (122 cm/s). The origin of this value is unknown but it is assumed that is based on actual measurements made after the barrier construction was completed.

Current measurements were also made in the hurricane barrier as part of this study on 20 June 1986 (Figure 2.7). These measurements were limited due to the extensive shipping traffic through the area. It was extremely difficult to make accurate measurements with the current meter deployed from a small craft and hence the measurements should be viewed with caution. Maximum ebb and flood currents were 75 cm/s and 85 cm/s, respectively. Current measurements were made in the center of the channel and at 2 m intervals in the vertical. There was little discernible vertical structure. The tidal height data shown in Figure 2.7 was obtained from the hurricane barrier control office. The data are given in Appendix A.

On 20 June 1986 current measurements were also made in the center of the channel directly opposite the Aerovox facility in the upper harbor. Measurements were made in water depths generally of 1 m. The maximum tidal currents were 3-5 cm/s and show low currents in the area near the head of the estuary. It should be noted that these currents are approximately at the lower limit of sensitivity for the instrument.

In the vast majority of circulation observations made in the area there was no recording of surface elevations. In the one case where both currents and sea level were recorded simultaneously [at Coggeshall Street Bridge by EPA (1983)]. The data show that the currents lead the surface elevation by approximately 90°. Maximum flood currents occur roughly 3 hrs. before high tide while maximum ebb currents occur 3 hrs. before low tide. The hurricane barrier measurements made as part of this study (Figure 2.7) also show the same basic pattern. This behavior is characteristic of a standing wave system (Officer, 1976).

In summary, there is a very limited amount of current meter data available for New Bedford Harbor. From records that do exist for a small number of tidal cycles at a few geographic points, the mean flood and ebb tide velocities range from 10 to 20 cm/s. The currents are much stronger (60-120 cm/s) in the narrow passages such as the hurricane barrier and the I-195 and Coggeshall Street Bridge causeways. It is not certain whether the flood or the ebb tide is stronger although some evidence suggests that flood dominates. When available the phase relationship between the currents and surface elevation show a classic standing wave pattern.

2.5.4 Tidal Prism Flushing

The tidal prism flushing times were calculated for the area north of the Coggeshall Street Bridge and for the entire harbor north of the hurricane barrier. The calculations give the following, assuming a mean tidal range of 1.13 m:

	New Bedford Harbor (north of hurricane barrier)	Coggeshall St. Bridge
Mean Low Water (MLW) Volume	1.16×10^7 m³	7.20×10^5 m³

MLW Surface Area	3.86×10^6 m^2	7.8×10^5 m^3
Average Depth	3.01 m	0.92 m
Tidal Prism	4.35×10^6 m^3	8.8×10^5 m^3
Flushing Time	45.5 hours 3.6 tidal cycles	22.5 hours 1.8 tidal cycles

The tidal flushing times are on the order of 2 to 4 cycles. The flushing time is defined as the time required to replace the existing freshwater in an estuary at a rate equal to the river discharge. The flushing time for the entire system is only twice that for the upper estuary. This is because the increase in surface area for the entire system compared to that in the upper estuary is partially compensated for by a three fold increase in the mean depth. For the entire estuary the tidal prism is 37.5% of the mean low water volume while a similar measure for the upper estuary is 122%. The tidal prism is defined as the volume of water contained in the estuary between mean high water and mean low water.

Actual flushing times are likely longer than this since this represents an optimum or fastest rate. Dr. Wayne Geyer (Woods Hole Oceanographic Institution, personal communication) has suggested rates of 9-30 days depending on the winds. He suggests that storm periods with strong winds would decrease the flushing time while calm periods would result in longer times.

2.5.5 Water Property Changes

Figure 2.6 shows the changes of five water properties through one complete tidal cycle for two locations in the harbor. The northern location (H4) shows maximum current speeds (12.4 cm/s) 1 1/2 hours before high tide, while at the southern location (H5) current speed reaches a maximum (18 cm/s) 3 hours before high tide or half way between high and low tide. There is

also a rise in current velocity 2-2 1/2 hours after high tide, though it is much more pronounced at the southern location.

At both locations the salinity drops to a minimum 2 hours before high tide for both the surface and bottom waters. However, the salinity rapidly rises to a maximum during the next hour, indicating the rapid flux of Buzzards Bay sea water into the harbor. At low tide, water at H4 is extremely fresh, while the salinity is still high at H5.

Salinity profiles along north-south transects of the harbor are shown in EPA (1983) for four consecutive tidal cycles between January 10-12, 1983. For the first two cycles the excursion of saline water up the harbor during the flood stage is seen. These cycles show the harbor to be well to partially mixed.

For the second two cycles, the circulation was altered by a storm that occurred on 11 January 1983 [0.5 inches (1.3 cm) of rain during the storm]. Two important consequences occur due to the storm. First the surface salinities drop dramatically from values at the Coggeshall Street Bridge station of 29.8% before the storm to 12.3% after the storm. Second, the harbor becomes stratified as evidenced from the final two transects. The fresh water overlays the saline water with very little mixing. This appears to occur over the length of the harbor.

2.5.6 Wind and Density Induced Circulation

While tides are the dominant mechanism driving circulation in New Bedford Harbor, other mechanisms can influence the circulation such as surface winds, storms and river runoff. The average annual wind speed in New Bedford harbor is 4.8 m/s. The seasonal averages range from a high of 5.4 m/s during winter to a low of 4.2 m/s during summer. The average wind

direction comes from the northwest during winter, and from the southwest in summer. Variations in wind speed have characteristic periodicities: one to several days due to migration of weather cells across the area and a daily cycle due to sea breeze (Signell, 1982).

Typical winds in New Bedford Harbor only influence the surface waters, and even they are only affected slightly. Typical bottom flow in the harbor is very weak, usually less than 10 cm/s. Wind generated wave induced currents do reach the bottom during storm events. It is only during storms that winds significantly affect circulation in the harbor.

As shown in the salinity transects of EPA (1983) river runoff can affect the circulation, especially after a storm. However on an average day, using a mean annual freshwater discharge of 30 cfs (0.8 m^3/s) from the Acushnet River, the average freshwater input to the harbor is 3.57×10^4 m^3. During this same cycle, the tidal flow in or out of the basin (above the Coggeshall Street Bridge) is 8.8×10^5 m^3. Therefore the freshwater input to the basin is only 4 percent of the average tidal input.

CTD profiles around the outer harbor (Signell, 1982) show stratification and virtually linear increases of density with depth. However CTD profiles taken at 1/2 hour intervals from the head of Buzzards Bay show a gradual evolution of the water column from well stratified in the afternoon to well mixed at night (Signell, 1982).

A series of cruises around Buzzards Bay were repeated every 3 months for 1 year (Rosenfeld, 1984). Temperature, salinity and density profiles were made for each season. The temperature and density profiles show a seasonal thermocline developing during the summer, while the water column shows no stratification during the fall and winter months. The salinity profiles show the influence of freshwater input as the profile for spring, when river runoff

is high, has lower salinities throughout the water column. The influence of this offshore density structure on the circulation in the harbor is unknown.

2.5.7 Other Circulation Mechanisms

Analysis of the energy spectrum of current fluctuations in the lower harbor (Signell, 1982), shows that a large amount of energy in the lower harbor is present between the M2 tidal period of 12.42 hours and the surface wave period. Two possible mechanisms of supplying energy at these frequencies are seiches and internal waves.

Seiches are movements of water in a basin resonating with the basin's natural frequency. Assuming a rectangular constant depth basin with one open side the seiching period for Buzzards Bay is 1.8 hrs. Since a peak occurs on the spectrum near 1.8 hours, it is possible that seiching of Buzzards Bay is contributing a significant amount of energy to the area. The seiching period for the harbor itself is 12-15 minutes and corresponds well to the observed fluctuations in the EPA (1983) current measurements at the Coggeshall Street Bridge.

The energy between the surface waves and tides could also be accounted for by internal waves. LTD profiles show vertical density gradients and hence a pynocline along which an internal wave could propagate. Calculating the Brunt-Vaisala frequency, for a typical density profile, yields a period of three minutes. Therefore any internal wave between this buoyant frequency and the inertial frequency is possible and could account for some of the spectral energy (Signell, 1982).

2.6 Sediment Dynamics

Summerhayes et al (1976) and Grant and Hannan (1984) are the two major

scientific studies related to the sediment dynamics of New Bedford Harbor. (Their papers will be referred to as "S76" and "GH84" respectively from this point on.) The S76 paper pertains to the distribution and dispersal of polluted sediments. It is an analysis of over a hundred sediment samples taken throughout the harbor. The GH77 paper focuses on the physical and biological resuspension of the sediment layer at a site outside the hurricane barrier.

2.6.1 Composition

It is generally agreed that the deeper portions of the harbor, especially the 30 ft (9.1 m) dredged channel, contain a higher proportion of mud to sand. The size and composition of the sediments is particularly important since the pollutants have been found to attach themselves to selective fine particles.

S76 suggest that the order of metal enrichment may be an agent in determining the source of the pollutants. They find that the heavily contaminated cores have a different enrichment order (Cu>Cr>Pb>Zn) than the less contaminated cores from outside the inner harbor (Pb>Cu>Zn>Cr). They also find a fractionization of clay along the axis of the harbor. While the inner harbor mud contains 20% clay, that of the outer harbor contains 40% clay.

2.6.2 Distribution

There is potentially a rapid removal of metals from the water column and an episodic selective resuspension of surface mud that redistributes the sediment outside the harbor (GH84). The relatively low values of copper (the dominant metal) found near the hurricane barrier are probably due to the

regular tidal current scouring of the shoaling bottoms.

The Massachusetts Division of Public Works (1975) reported highest concentration of metals in the sediment at the Coggeshall Street Bridge area. Core transects across the harbor sampled highest metal concentrations on the western shore. The distribution of metals down the bay may be inferred from copper concentrations (S76). Except for isolated areas of dredged mud deposit sites and sewage outflow sites, the concentrations of metals in the sediment was found to decrease exponentially towards the bay (S76). Summerhayes et al (1976) suggest that there seems to be a seaward transportation of metals by lateral mixing through eddy diffusion despite the predominantly landward bottom flow. The bottom boundary layer is 2-3 meters thick with 10-35 mg/l of suspended matter especially heavy shortly after flood tides (S76).

3. A SIMPLE MODEL STUDY OF RESUSPENSION AND DEPOSITION OF SEDIMENT PARTICLES IN THE ACUSHNET RIVER NEAR AEROVOX

One proposed mechanism for the transport of PCBs in the harbor is that fine grained sediment particles located in the upper estuary near the Aerovox facility and contaminated with PCBs are suspended during storm events and subsequently transported down estuary. To investigate this possibility the present study uses a simplified modeling approach to look at resuspension criteria, sediment grain sizes and fall velocities, tidal and river flow rates, and the behavior and fate of sediment particles possibly resuspended into the Acushnet River near Aerovox Corp [6600 ft: (2012 m) north of the Coggeshall Street Bridge].

Based upon all available data on flow and sediment properties in the Acushnet River near Aerovox, a simple one-dimensional unsteady flow model was implemented numerically on a computer and used to predict the deposition of particles in the range ϕ = 6 to 9 (diameters of 15.6 to 1.9 microns) when resuspended near Aerovox and carried into the river by tides and river flow. Two river flows are studied: normal average flow of 30 ft^3/s (0.85 m^3/s) and the 100-year predicted flood rate of 650 ft^3/s (18.4 m^3/s).

3.1 Sediment Grain Sizes

An extensive study of sediment grain sizes in the Acushnet River and New Bedford Harbor was reported by Huidobro et al (1983). The samples taken closest to Aerovox were three stations across the river at latitude 41° 39.97', which is 3000 ft (915 m) south of Aerovox. A rough guide to sediment sizes for these three stations is given in Table 3.1. Note the strong differences: station 1 (near the deep channel) contains mostly gravel and sand, station 2 mostly silt and clay, and station 3 mostly sand and silt. Thus

Table 3.1

Sediment-size Data from Huldobro et al., "New Bedford Environmental Investigation: Hydrodynamic Grain Size Measurements of Selected Harbor Sediments", May 1983, Vol. 2, page 24.

Results of Hydraulic Equivalent Grain Size Analysis

Station No.	GCA Control No.	Hydraulic equivalent grain size (percent)			
		Gravel (>2 mm)	Sand (62 μm 2 mm)	Silt (3.9 μm 62 μm)	Clay (< 3.9 μm)
1	24155	3.04	93.24	3.72	0.00
2	24157	0.00	10.49	57.12	32.39
3	24160	0.00	36.80	56.56	6.64
AVERAGE FREQUENCY:		1%	47%	39%	13%

NOTE: These are the three sediment-sampling stations nearest to the Aerovox Plant. They are at latitude 41° 39.97', or 3000 feet south of the plant in the Acushnet River, 3600 feet north of the Coggeshall Bridge.

it is difficult to characterize the properties of "average sediment" in the Acushnet River.

Since the particles most likely to carry contaminants from the sediments are in the silt and clay size ranges (Metcalf and Eddy, 1983), we concentrate our study on the ϕ = 4 to 10 range. In Table 3.2 we abstract the particle size frequency distribution from Huidobro et al (1983) for these three samples at 41° 39.97'. We see in Table 3.2a that the smallest size measured was ϕ = 9, or 1.95 microns. Just as in Table 3.1, the frequencies vary considerably among the three samples. Therefore we compute an 'average' frequency in Table 3.2a for computation purposes.

The total of these average frequencies for ϕ = 4 to 9 shows that 53.55% of all the Acushnet River sediments are in this size range of silt and clay. Table 3.2b restates this data to show the sizes as a percentage of the silt and clay range. We see that ϕ = 6, 8, and 9 account for 84% of all particles in this range. Therefore the numerical model in this study will concentrate on the erosion and deposition of particles whose sizes are ϕ = 6, 8, and 9.

3.2 Erodibility of Sediment

The erodibility of Acushnet River sediment was studied experimentally by Heavers [Appendix A, ASA (1983)] using sediment samples taken 3 December 1982 about 300 ft (91 m) upstream of the Aerovox plant. The water channel erosion test of these sediments were reported by Heavers as follows:

a) No erosion at U = 20 cm/s.
b) Significant erosion (0.267 $\mu g/cm^3/s$) at U = 30 cm/s.

where U is the centerline velocity in the water channel. We may compare these results with the classical Shields criterion for sediment motion, as described e.g. in the text by Raudkivi (1967), pages 20-24. The results are shown in Figure 3.1 and show that Heavers' data are in good agreement with

Table 3.2-A.

Measured particle size distribution*
in sediments in the Acushnet River

ϕ Size	d - μm	Sample* #21455	Sample* #24157	Sample* #24160	Average
4	62.5	0.01%	1.01%	2.49%	1.17%
5	31.25	3.72%	1.12%	2.51%	2.45%
6	15.63	0.0%	36.61%	4.42%	13.68%
7	7.81	0.0%	11.20%	3.79%	5.00%
8	3.91	0.0%	9.12%	45.82%	18.31%
9	1.95	0.0%	32.39%	6.44%	12.94%
10	0.96	----------NO DATA GIVEN----------			
				TOTAL:	53.55% of all particles

Table 3.2-B.

Data normalized as a percentage
of particles between ϕ=4 and ϕ=9

ϕ	Particle Frequency
4	2.2%
5	4.6%
6	25.5%
7	9.3%
8	34.2%
9	24.2%
TOTAL	100.0%

ϕ = 6, 8, and 9 account for 84% of all particles in this range.

*Data from Huidobro et al (1983).

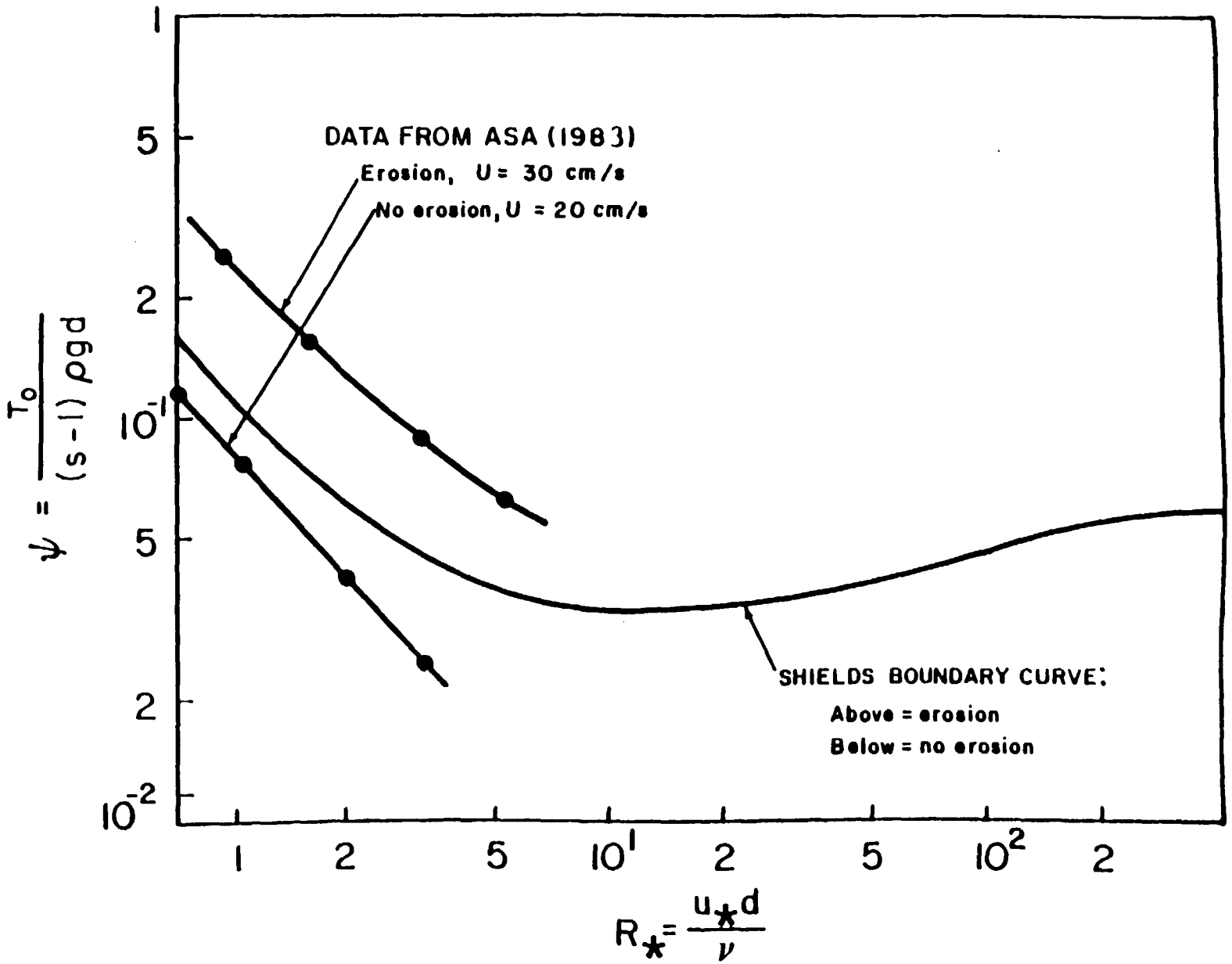

Figure 3.1 Comparison of Acushnet River sediment erosion laboratory data (ASA, 1982) with the Shields criterion (Raukivi, 1967).

the Shields criterion. We conclude that Acushnet River sediments are well described by the Shields boundary curve.

To convert Heavers' water channel experiment into field conditions for the Acushnet River, we assume that the Shields 'boundary curve' in Figure 3.1 is valid and determine what bottom shear stress and flow velocity are needed to cause sediment erosion in the river.

The bottom stress τ_o in a river flowing with average velocity U and average depth h may be predicted by either the Moody friction formula or by the formula recommended by Ippen (1966), page 570:

$$\frac{\tau_o}{1/2\rho U^2} \doteq 0.043\ (Uh/\nu)^{-1/4} \qquad (3.1)$$

If Eq. 3.1 is combined with the Shields curve in Figure 3.1, we predict the erosion shear stress and river velocity near Aerovox:

Average Depth, ft.	Sediment Size, μm	τ_o, pascals	U, ft/s
3.0	15.63	0.157	0.932
3.0	3.91	0.154	0.925
3.0	1.95	0.151	0.919

These are substantial erosion velocities, about 28 cm/s. Based on the hydrographic data of Cortell (1982) and the present observations, it is estimated that the maximum tidal velocity near Aerovox is 0.15 ft/s or 5 cm/s. The maximum river-flow velocity, at the 100-year flood level flow of 650 ft^3/s or 18.4 m^3/s is about 0.35 ft/s or 11 cm/s. The combined total of tidal and river flow velocities is about 16 cm/s, or well below the erosion threshold velocity of 28 cm/s predicted by the Shield criterion. Therefore it seems that

sediment erosion near the Aeroyox plant is an unusual occurrence except perhaps during very favorable conditions of neap tides, river flood levels, and strong wind and wave stresses.

3.3 Wave Environment and Wave Induced Bottom Currents

An analysis was undertaken to estimate the wave conditions and maximum wave-induced bottom currents generated by the passage of a severe (worst case) storm. The storm has a maximum average one-hour wind velocity of 35.76 m/sec (80 mph). This storm constitutes the design hurricane used in designing protective structures for the New Bedford-Fairhaven area (Corps of Engineers, 1957). The wave estimation methodology follows the approach described in the Shore Protection Manual (CERC, 1984).

The area under consideration reaches from Wood Street Bridge in the north to Coggeshall Street Bridge in the south. This gives a fetch length of 2540 m for winds blowing along the channel axis, oriented in a north-south direction. Predominant winds are from the west throughout the year, coming from the northwest in the winter and from the southwest in the summer. Winds from these directions do not have sufficient fetch to generate significant waves. The wind here is assumed either out of the north or south to approximate worst case conditions.

Wave conditions and bottom currents were calculated for three scenarios: storm passage at low tide, high tide and with a maximum storm surge. The mean water depth in the study area is estimated to be 1.0 m at MLW (NOS Chart 13229, 1982). For a tidal range of 1.13 m the mean water depth at high tide is 2.13 m. The maximum storm surge was based on the 1938 hurricane which produced water depths 3.81 m above mean sea level (Section 2.5.2) the highest recorded to date, and give a total water depth of 4.81 m. Under these conditions, the wave characteristics and bottom currents are shown

below. Bottom currents are calculated using Stokes 2nd order wave theory at 10 cm above the sea bed.

Wave Conditions and Wave-Induced Bottom Currents for Design Storm (Wind speed = 35.76 m/s, Fetch = 2540 m).

Scenario	Water Depth(m)	Wave Height(m)	Wave Period (s)	Wave Length (m)	Bottom Current (cm/s)
Low Tide	1.0	0.63	2.74	7.80	103.03
High Tide	2.13	0.98	2.95	11.24	74.67
Storm Surge	4.81	1.28	3.09	14.45	32.74

Bottom currents of 28 cm/s (Section 3.2) are required to resuspend bottom sediments. Clearly, resuspension is achieved for the three scenarios presented above.

Using the methodology employed for the previous calculations, the minimum wind velocity necessary to initiate resuspension was determined for low and high tide scenarios. At low tide a wind speed of 12.96 m/s (29 mph) is sufficient; at high tide a wind speed of 19.22 m/s (43 mph) is required. In each case, winds must blow along the channel axis (i.e. from the south) in order to have sufficient fetch to develop these bottom currents in the vicinity of the Aerovox plant. Using the available wind data and assuming a value of 16 m/s for wind speed out of the south is needed to achieve resuspension calculations show that this event occurs approximately once every 1.25 years with a duration of approximately 1 hour. Resuspension of bottom sediments is anticipated at this frequency although the amount is limited by the short duration.

3.4 Particle Settling Rates

The usual method for estimating particle settling rates, w, is the classical formula of Stokes:

$$w = (\rho_p - \rho_f)\, gD^2/18\mu \qquad (3.2)$$

where ρ_p is particle density, ρ_f is fluid density, g is gravity, D is particle diameter and μ is the viscosity of water. Certainly the Reynolds numbers of particles of sizes ϕ = 4 to 9 are less than unity. However, Hawley (1982) studied experimental settling rates for marine aggregate particles and found that they fell <u>faster</u> in some cases than predicted by Stokes' formula. Hawley recommended the following formula for settling of a typical marine-particle aggregate of diameter D:

$$w\ (\text{mm/s}) = 13.02\ D(\text{mm})^{0.937} \qquad (3.3)$$

Data are available for settling velocities of Acushnet River sediments near Aerovox (ERCO, 1982). The ERCO/Energy Resources Corp. tested composite sediment samples taken from the Aerovox vicinity for settling rates in a six-foot column when suspended in seawater. They reported that 97% of the particles fell at least two feet in one hour, for an average velocity of w = 0.17 mm/s. Substituting this value into Eq. 3.3, we obtain an average sediment size estimate: D = 10μm. Since this is very nearly equal to the average sediment size from Table 3.2, we conclude that Eq. 3.3 is a good estimate for settling rates of Acushnet River particles. We will use Eq. 3.3 in our deposition model.

3.5 Acushnet River Hydrography

River and tidal flow data for the Acushnet River are summarized in (Cortell, 1982). Tidal currents were measured at four stations across the river at latitude 41° 39.7', or 3000 ft (915 m) south of Aerovox. The data averaged over the four stations are as follows:

Average ebb velocity:	0.265 ft/s (8 cm/s)
Average flood velocity:	0.260 ft/s (7.9 cm/s)
Maximum ebb velocity:	0.443 ft/s (13.5 cm/s)
Maximum flood velocity:	0.495 ft/s (15.1 cm/s)

Average tidal range is 3.8 ft (1.13 m) above the Coggeshall Street Bridge.

Figure 3.2 shows that, above the position of these current meters, 41°39.7', the river is of uniform width and is nearly 'closed' as the river narrows about 1000 ft (305 m) above Aerovox. The average river depth at mean low water varies from 2 to 4 ft (0.6 to 1.2 m) in this area, and the cross-sectional area varies from 2000 to 5000 ft^2 (186 m^3 to 465 m^2). It seems reasonable to model this tidal flow as a 'uniform channel closed at one end', as described e.g. on pp. 498-499 of Ippen (1966). Taking x=0 at the closed end (above Aerovox), the tidal velocity may be approximated by:

$$u = 2 \frac{a}{h} (gh)^{1/2} \sin(\sigma t) \sin(kx) \qquad (3.4)$$

where σ is the tidal frequency and k the tidal wavelength. Taking h = 3 ft (0.91 m) and x = 5000 ft (1524 m) at the position of the current meters, we predict that

u_{avg} = 0.31 ft/s (9.4 cm/s)

u_{max} = 0.45 ft/s (13.7 cm/s)

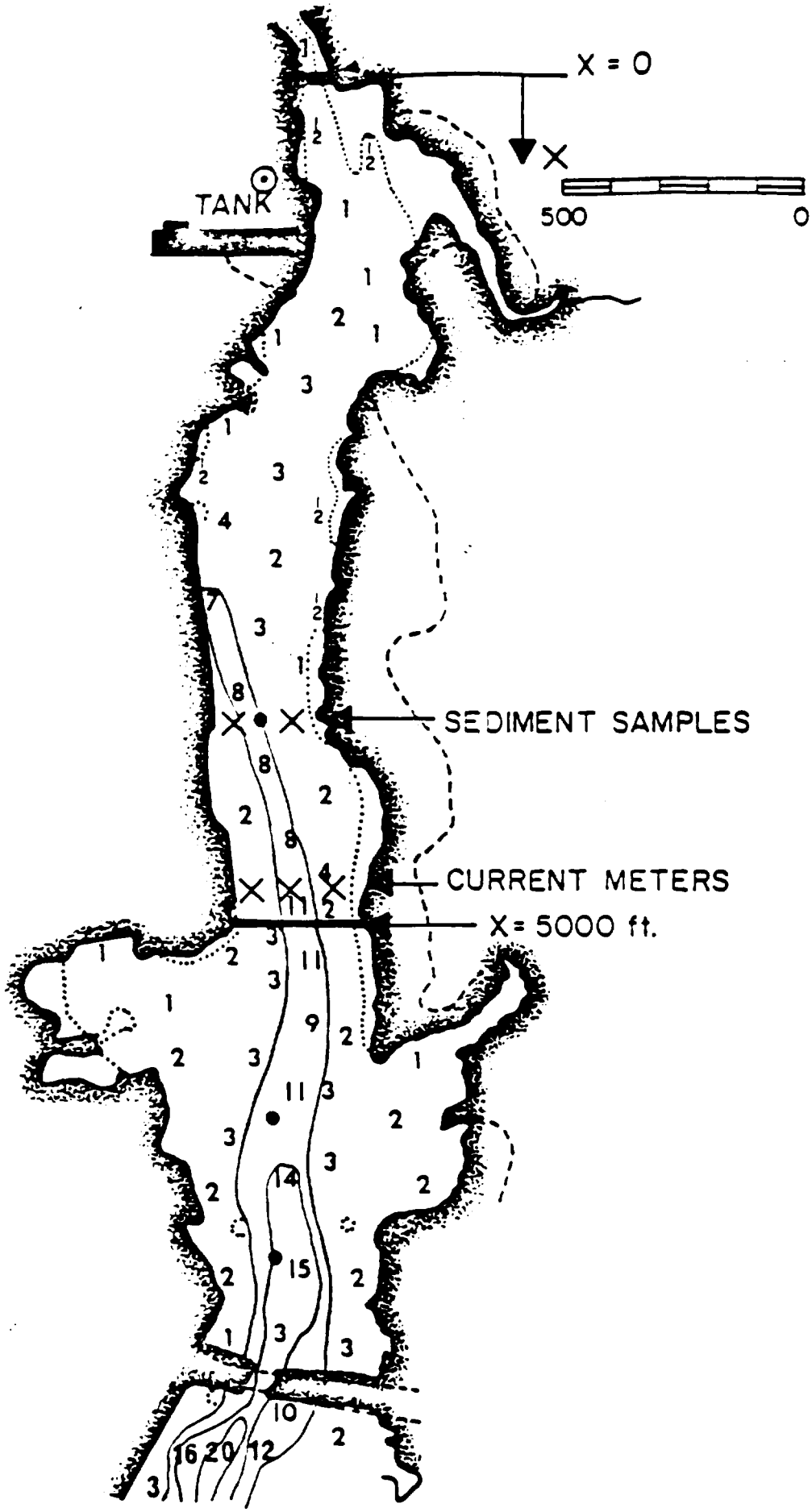

Figure 3.2 Simplified model study area, upper Acushnet River estuary.

This is in reasonable agreement with the limited tidal current data available. We will therefore assume that Eq. 3.4 is valid in the entire area of the river shown in Figure 3.2 and use it in our deposition model.

The river flow in the Acushnet River varies from nearly zero in dry periods to a design 100-year flood rate of 650 ft^3/s (18.4 m^3/s) (Corp of Engineers, 1961). The average river flow is 30 ft^3/s (0.85 m^3/s). The average river velocity at any instant would be

$$u_R = Q_R/A_c \tag{3.5}$$

where A_c is the river cross-sectional area.

3.6 Simple Resuspension and Deposition Model

To predict the fate of sediment particles resuspended into the water column near Aerovox, the following model was implemented on a personal computer. Particles of three ϕ sizes, 6, 8 and 9, were assumed to be resuspended into the water column at x = 1000 ft (305 m) (Aerovox). Their subsequent motion was given by Eqs. 3.4 and 3.5 for longitudinal motion along the river and by Eq. 3.3 for vertical settling:

$$u = \frac{dx}{dt} = Q_R/A_c + \text{const}\cdot\sin(kx)\,\sin\sigma t \tag{3.6a}$$

$$w = \frac{dz}{dt} = \text{const}\ D^{0.937} \tag{3.6b}$$

At time t = 0, particles of any given diameter were assumed to be located at ten equally-spaced levels in the water column: 0.05 h, 0.15 h, 0.25 h, ..., 0.85 h, and 0.95 h. Ten particles, one at each level, were 'released' at x = 1000 ft (305 m), t = 0, during each hour of the twelve-hour tidal cycle, or <u>120 particles total</u>. Their positions x(t) and z(t) were computed by Runge-Kutta

integration of Eqs. 3.6 until the particles either 1) settled back to the bottom; or 2) were swept out of the area south presumably under the Coggeshall Street Bridge.

Although, strictly speaking, the model was derived for the 'channel-flow' region from x=0 to x = 5000 ft (152.4 m) in Figure 3.2, computations were continued up to x = 7000 ft (213.4 m) since it was felt that the particles would tend to stay in the main deep channel as they were carried out on the ebb cycle toward the Coggeshall Street Bridge. Particles which remained in the water column at x = 7000 ft (213.4 m) were assumed to flow 'out of the system', i.e. under the bridge. Only two values of Q_R were studied: 30 ft^3/s (0.85 m^3/s) (annual average) and 650 ft^3/s (18.4 m^3/s) (100-yr flood).

3.7 Computed Results

The results of the six numerical deposition simulations (three particle diameters and two river flow rates) are shown in Figures 3.3-A, B, C, D, E, and F. Each figure shows the fate of the 120 representative particles of that given diameter after release at t = 0, x = 1000 ft (305 m) (the Aerovox plant). Each point "." in the river represents a particle which has settled to the bottom and thus redeposited in the sediment. Each point with an arrow near the bottom of the figure "↓" represents a particle which has been swept out of the flow field, presumably under the Coggeshall Street Bridge.

The Figures 3.3-A,B,C,D,E,F give a picture of the deposition, and the general results may be summarized as follows:

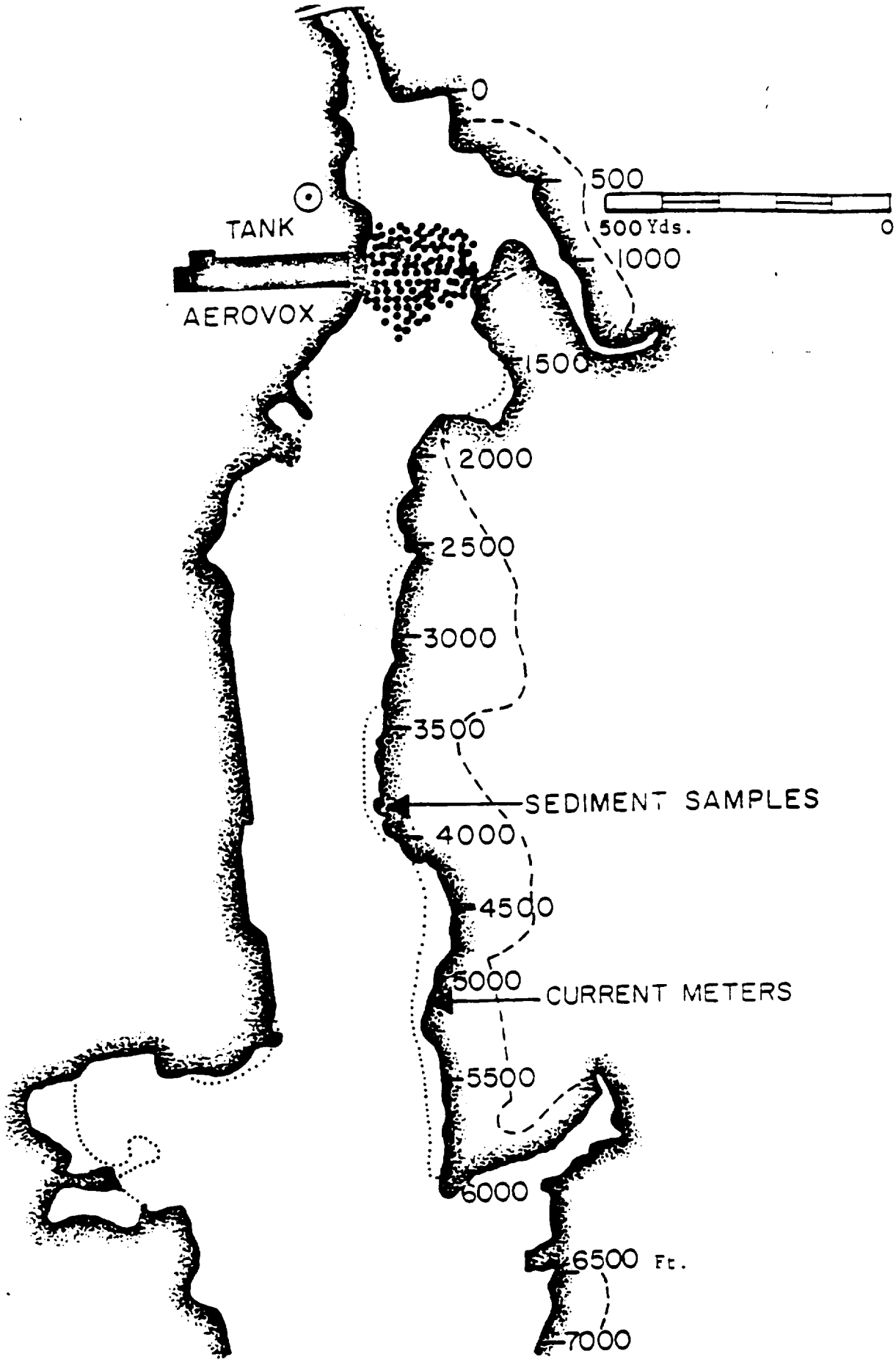

igure 3.3A Model predicted particle deposition sites for a flow rate of 30 ft^3/s (0.85 m^3/s) and a sediment particle size of 15.6 microns (ϕ=6).

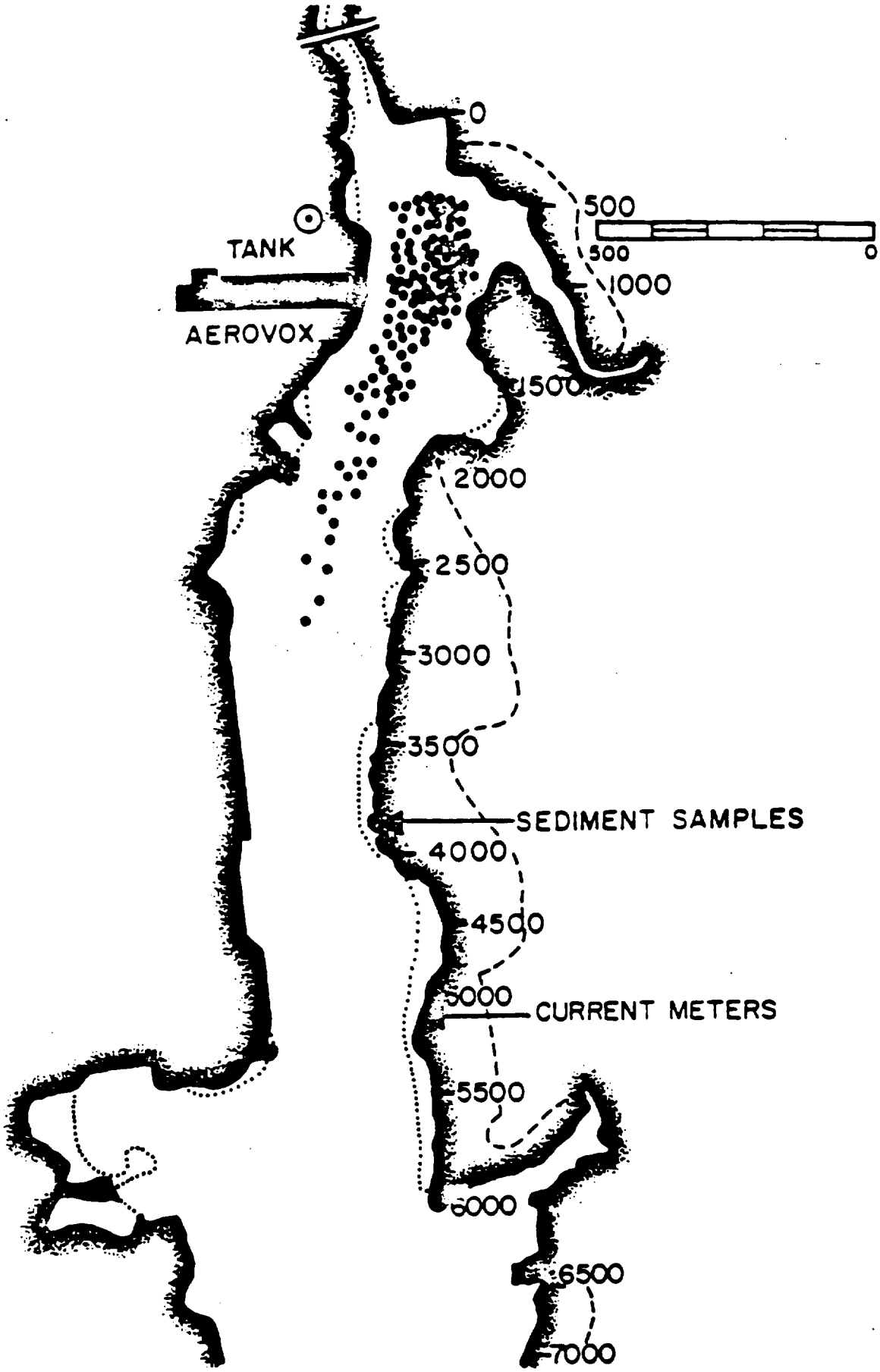

Figure 3.3B Model predicted particle deposition sites for a flow rate of 30 ft^3/s ($0.85m^{33}/s$) and a sediment particle size of 3.906 microns (ϕ=8).

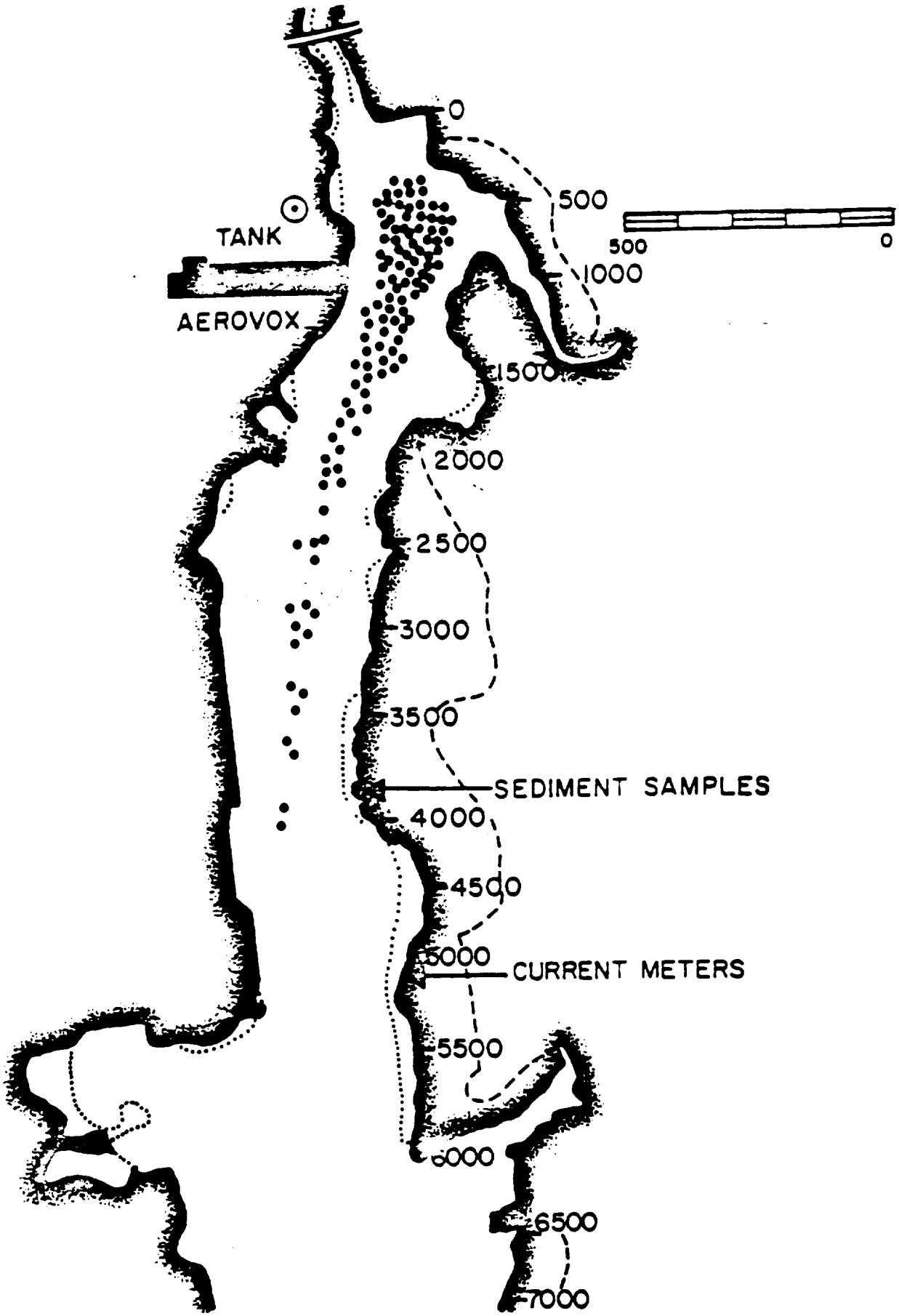

Figure 3.3C Model predicted particle deposition sites for a flow rate of 30 ft^3/s (o.85 m^3/s) and a sediment particle size of 1.95 microns (ϕ=9).

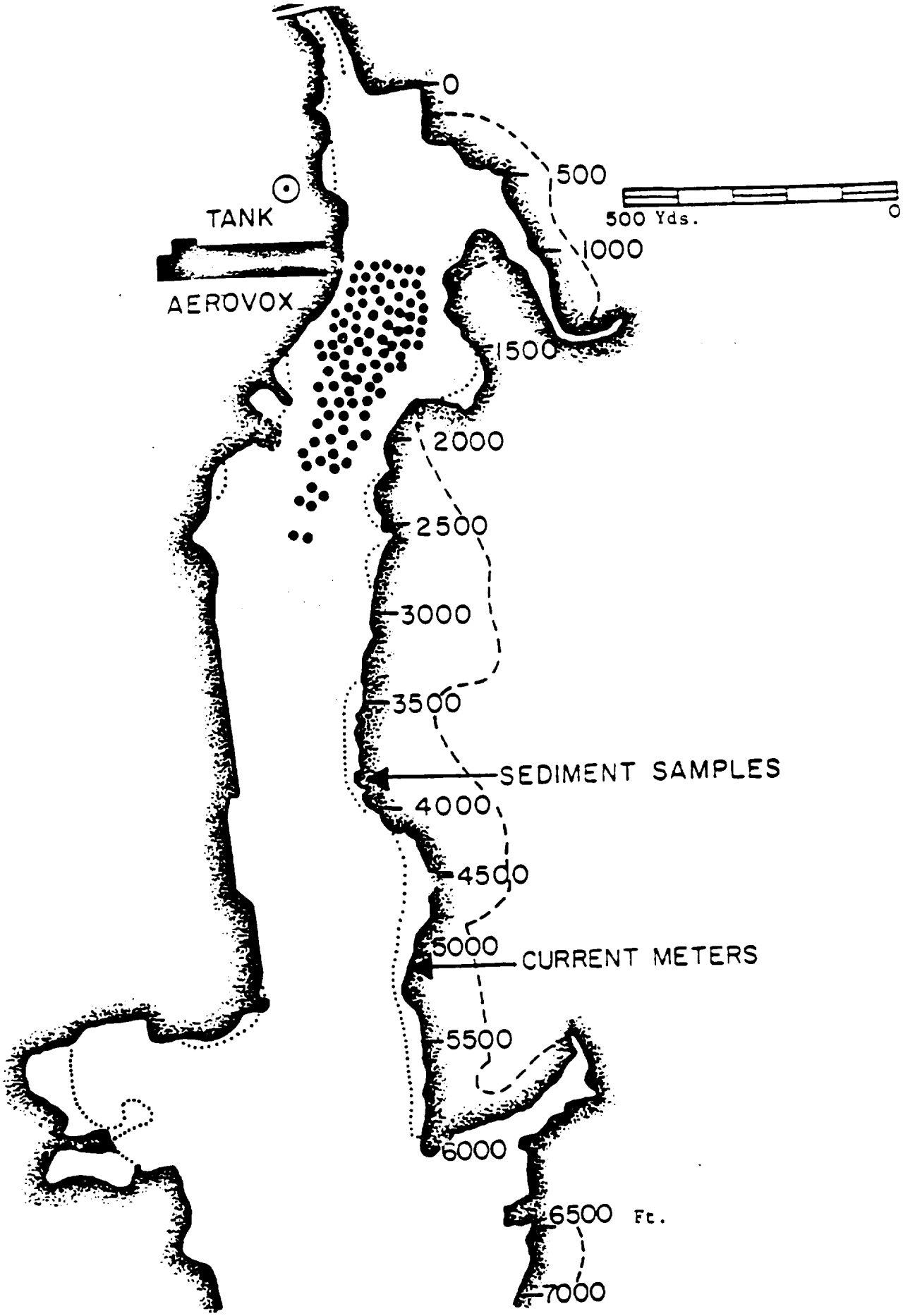

Figure 3.3D Model predicted particle deposition sites for a flow rate of 650 ft^3/s (18.4 m^3/s) and a sediment particle size of 15.6 microns (ϕ=6).

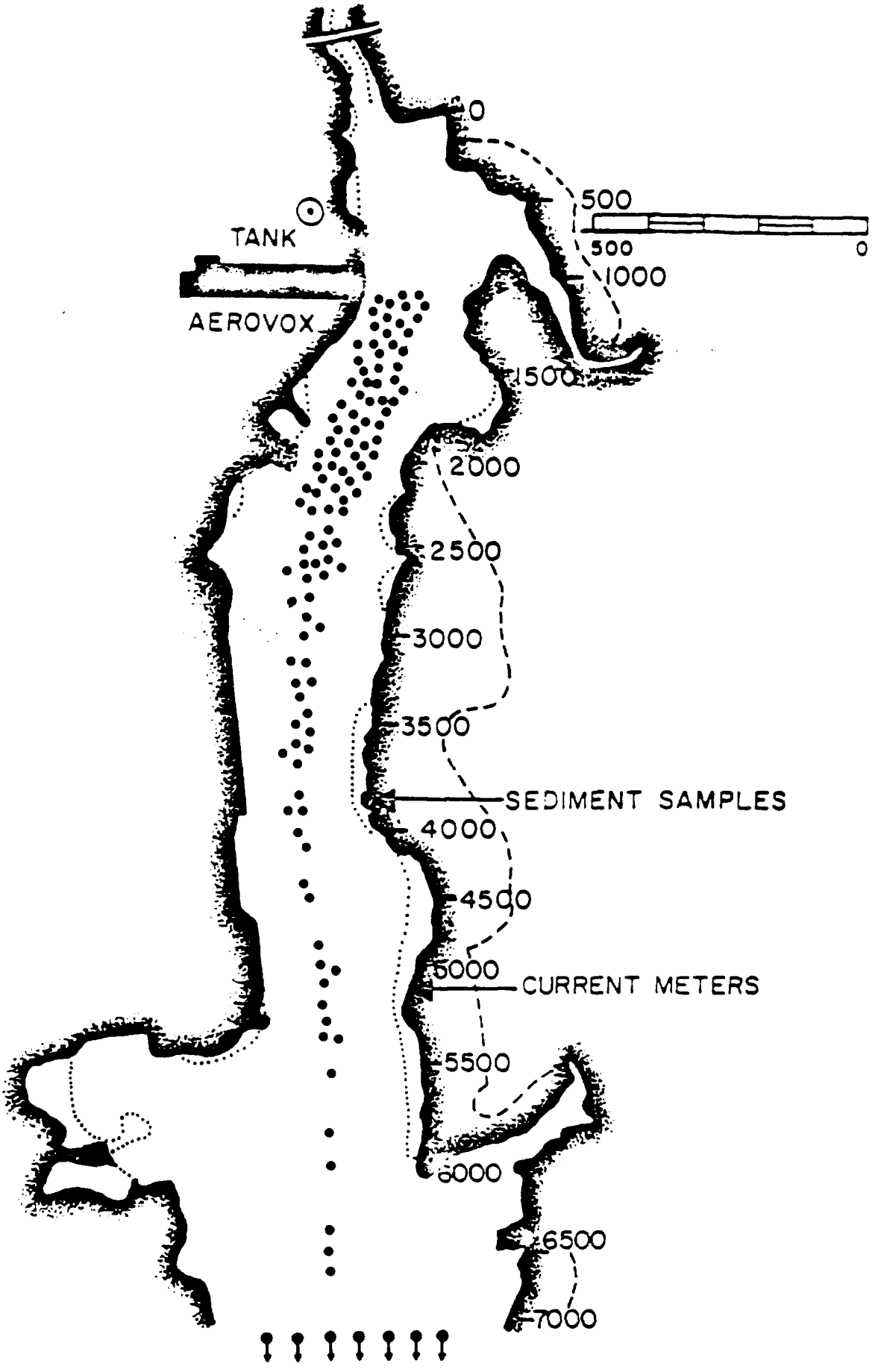

Figure 3.3E Model predicted particle deposition sites for a flow rate of 650 ft^3/s (18.4 m^3/s) and a sediment particle size of 3.906 microns (ϕ=8).

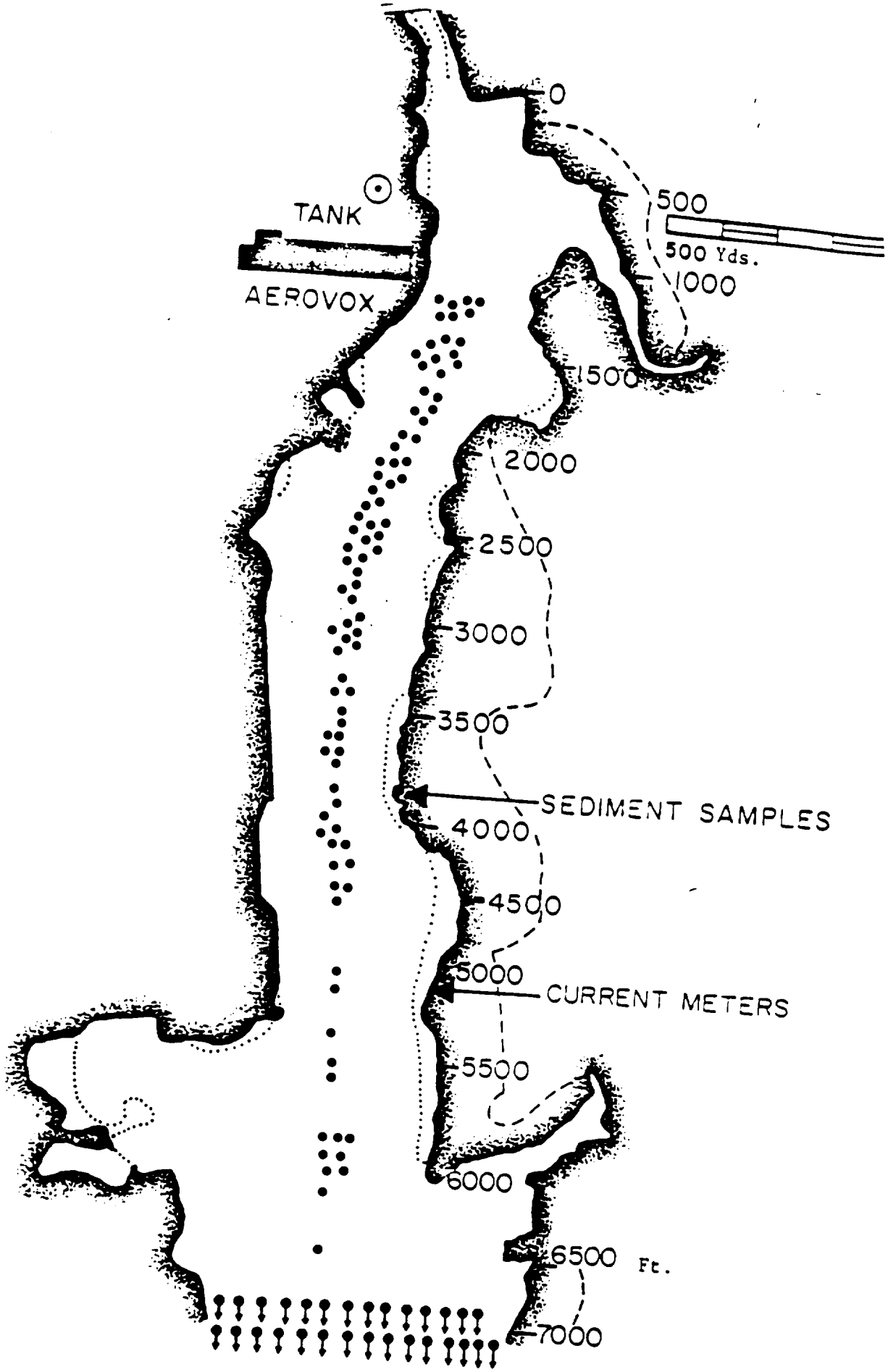

Figure 3.3F Model predicted particle deposition sites for a flow rate of 650 ft^3/s (18.4 m^3/s) and a sediment particle size of 1.95 microns (ϕ=9).

Figure	River Flow Rate, ft^3/s	Particle Diameter, μm	Results
A	30	15.6	Complete deposition - all particles redeposit within 300 ft (91.4 m) of Aerovox.
B	30	3.91	Complete deposition - maximum particle excursion 1900 ft (579 m) south of Aerovox.
C	30	1.95	Complete deposition - maximum particle excursion 3200 ft (975 m) south of Aerovox.
D	650	15.6	Complete deposition - maximum particle excursion 1600 ft (487 m) south of Aerovox.
E	650	3.91	Deposition of 113 particles (94%), while 7 particles (6%) leave the flow field.
F	650	1.95	Deposition of 91 particles (76%), while 29 particles (24%) leave the flow field.

3.8 Summary

A numerical one-dimensional unsteady flow field has been used to predict the deposition of particles in the Acushnet River after resuspension near Aerovox. The most important particle sizes (ϕ = 6, 8, and 9) are released and their paths followed until either redeposition or exit from the flow field. River flows studied are the annual mean flow and the 100-year flood level.

The computed and plotted results show that, during normal river flow rates (30 ft^3/s, 0.85 m^3/s), no particles would leave the flow field but would all redeposit within 3200 feet (975 m) south of Aerovox. At the 100-year flood level of river flow (650 ft^3/s, 18.4 m^3/s), all 15.6 μm particles would redeposit near Aerovox but 6% of the 3.9-micron particles and 24% of the 1.95-micron

particles would leave the flow field and possible be swept south under the Coggeshall Bridge. All particles that redeposit north of the Coggeshall Street Bridge do so within 6 hrs after their release.

4. HYDRODYNAMIC AND POLLUTANT TRANSPORT MODEL

4.1 Governing Equations

Since the water column remains vertically well-mixed over most seasons in the study area (Section 2.5), a two-dimensional vertically averaged hydrodynamics model has been selected to investigate the circulation. The equations of motion and continuity can be found in Leendertsee (1967) or Hess and White (1974). Only a brief overview is presented.

Employing a right-handed cartesian coordinate system where the vertical axis z is measured positive upwards referenced to mean sea level, the vertically averaged x and y momentum equations become

$$\frac{\delta U}{\delta t} + U\frac{\delta U}{\delta x} + V\frac{\delta U}{\delta x} = -g\frac{\delta \eta}{\delta x} + fV + \frac{1}{\rho(h+\eta)}(\tau_{sx} - \tau_{bx}) \qquad (4.1)$$

$$\frac{\delta V}{\delta t} + U\frac{\delta V}{\delta y} + V\frac{\delta V}{\delta y} = -g\frac{\delta \eta}{\delta y} - fU + \frac{1}{\rho(h+\eta)}(\tau_{sy} - \tau_{by}) \qquad (4.2)$$

in which f is the Coriolis parameter; τ_{sx} and τ_{sy} are the surface shear stresses; and τ_{bx} and τ_{by} are the bottom shear stresses in the x and y directions, respectively. It has been assumed that the density, ρ, is constant and that the water column is hydrostatic.

The vertically averaged velocities are defined as

$$U = \frac{1}{(h+\eta)}\int_{-h}^{\eta} u\, dz \qquad (4.3)$$

$$V = \frac{1}{(h+\eta)}\int_{-h}^{\eta} v\, dz \qquad (4.4)$$

in which u and v are the depth dependent velocity components in the x and y directions, respectively; h is the mean sea level depth; and η is the surface elevation measured from mean sea level.

Following a similar procedure the vertically averaged continuity equation becomes

$$\frac{\delta\eta}{\delta t} + \frac{\delta[(h+\eta)\,U]}{\delta x} + \frac{\delta[(h+\eta)\,V]}{\delta y} = 0 \tag{4.5}$$

Specification of bottom stress follows the well-known quadratic relationship:

$$\tau_{bz} = \frac{\rho g U(U^2 + V^2)^{1/2}}{C} \tag{4.6}$$

$$\tau_{by} = \frac{\rho g U(U^2 + V^2)^{1/2}}{C^2} \tag{4.7}$$

in which the Chezy coefficient, C, is weakly dependent on depth h and is inversely dependent on the Manning factor n, which parameterizes bottom roughness as

$$C = \frac{K}{n}\,(h+\eta)^{1/6} \tag{4.8}$$

in which K is a constant and depends on the units employed.

To describe the pollutant transport dynamics in the water column the three dimensional convective dispersion equation is employed in the following form:

$$\frac{\delta C_i}{\delta t} + U\frac{\delta C_i}{\delta x} + V\frac{\delta C_i}{\delta y} + W_{si}\frac{\delta C_i}{\delta z} = \frac{\delta}{\delta x}\left(D_x\frac{\delta C_i}{\delta x}\right) + \frac{\delta}{\delta y}\left(D_y\frac{\delta C_i}{\delta y}\right) + \frac{\delta}{\delta y}\left(D_z\frac{\delta C_i}{\delta z}\right) \tag{4.9}$$

where C_i is the concentration of the ith particle class, U and V are the vertically averaged velocities predicted by the hydrodynamic model, Ws_i is the settling velocity for the ith particle (this is zero for a non-settling pollutant) and D_x, D_y and D_z are the dispersion coefficients in the x, y and z directions, respectively. It has been assumed that the vertical velocity in the water column is small and hence there is no vertical advective transport. This

assumption is consistent with the two dimensional vertically averaged approximation for the flow described earlier.

Specification of the turbulent diffusion coefficients for estuarine applications is a difficult and ongoing problem. Lacking any field observations in the area with which to estimate these parameters, a formulation based on a modified Elder's (1959) approach is proposed for the horizontal dispersion.

$$D_x = 5.93 \frac{h\,U\sqrt{g}}{C} \tag{4.10}$$

$$D_y = 5.93 \frac{h\,V\sqrt{g}}{C} \tag{4.11}$$

where g is gravitational acceleration, C is the Chezy coefficient, h is the local water column depth and U and V are the vertically averaged velocities in the x and y directions, respectively.

In the vertical direction, assuming that for most of the year the water column is well mixed and that the tide mixes the entire column, the vertical dispersion rate is parameterized following Pritchard (1960, 1964) and Pritchard and Kent (1969).

$$D_z = 2.86 \times 10^{-4}\, U_a h \tag{4.12}$$

where U_a (m/s) is the mean velocity defined as $(U^2 + V^2)^{1/2}$, and h (m) is the water column depth. This gives values in the range of 1-5 cm^2/s for the inner New Bedford Harbor area and is typical of many shallow water estuarine systems.

4.2 Computational Approach

The hydrodynamic model equations are solved using the Galerkin weighted residual finite element method with linear interpolation functions and triangular elements. A split time or semi-implicit method (Wang and White, 1976), where the continuity and momentum equations are solved in successive order, is used for the time integration. Detailed development of these equations can be found in Isaji and Spaulding (1981) and Wang and White (1976).

The problem of flow through narrow constrictions with dimensions smaller than one grid length, such as the hurricane barrier passage, is addressed using a simple one dimensional non-linear channel flow model. This technique is described in detail in Isaji et al (1985).

The pollutant transport equation is solved using the Eulerian-Lagrangian particulate based approach given by Spaulding and Pavish (1984) with the exception that dispersion is calculated using a random walk procedure when describing sediment movement. This particulate based approach is particularly convenient for the present problem in that it can readily address, in a computationally efficient way, transport of sediment with a variety of different settling velocities.

For dissolved constituents a standard finite element procedure following Isaji and Spaulding (1981) is used.

5. APPLICATION OF MODEL TO ACUSHNET RIVER AND NEW BEDFORD HARBOR

5.1 Hydrodynamics

5.1.1 Grid System and Bathymetry

The hydrodynamic model was applied to the study area north of the hurricane barrier. The area includes all of New Bedford Harbor. The region extends northward to the approximate head of the tide in the Acushnet River which is north of the Aerovox plant site at approximately the Wood Street Bridge.

The study area was approximated by the triangular mesh finite grid system shown in Figure 5.1. The finite element mesh was chosen to allow variable resolution throughout the study area and specifically to provide higher resolution in areas where bathymetric gradients or topographic changes, and hence changes in currents and sea surface elevations, are significant. In general the finest resolution was employed in the narrow passages of the upper harbor, in the passages around islands and in the vicinity of the shipping channel (lower harbor).

For each node the mean low water (MLW) depth was determined from the NOAA/NOS (National Ocean Survey) navigation charts (13229 and 13230). In general the depths decrease in the northward direction from approximately 10 m to less than 1/3 meter in the upper harbor. The major variance from this basic pattern is the dredged shipping channel which extends from the hurricane barrier in the lower harbor north to Popes Islands. The channel, whose dredged depth is approximately 9.1 m, includes one primary section: the New Bedford Reaches. North of Popes Island, a channel follows the center of the estuary and shoals rapidly north of Coggeshall Street Bridge to approximately 1/3 m in the vicinity of the Aerovox Plant.

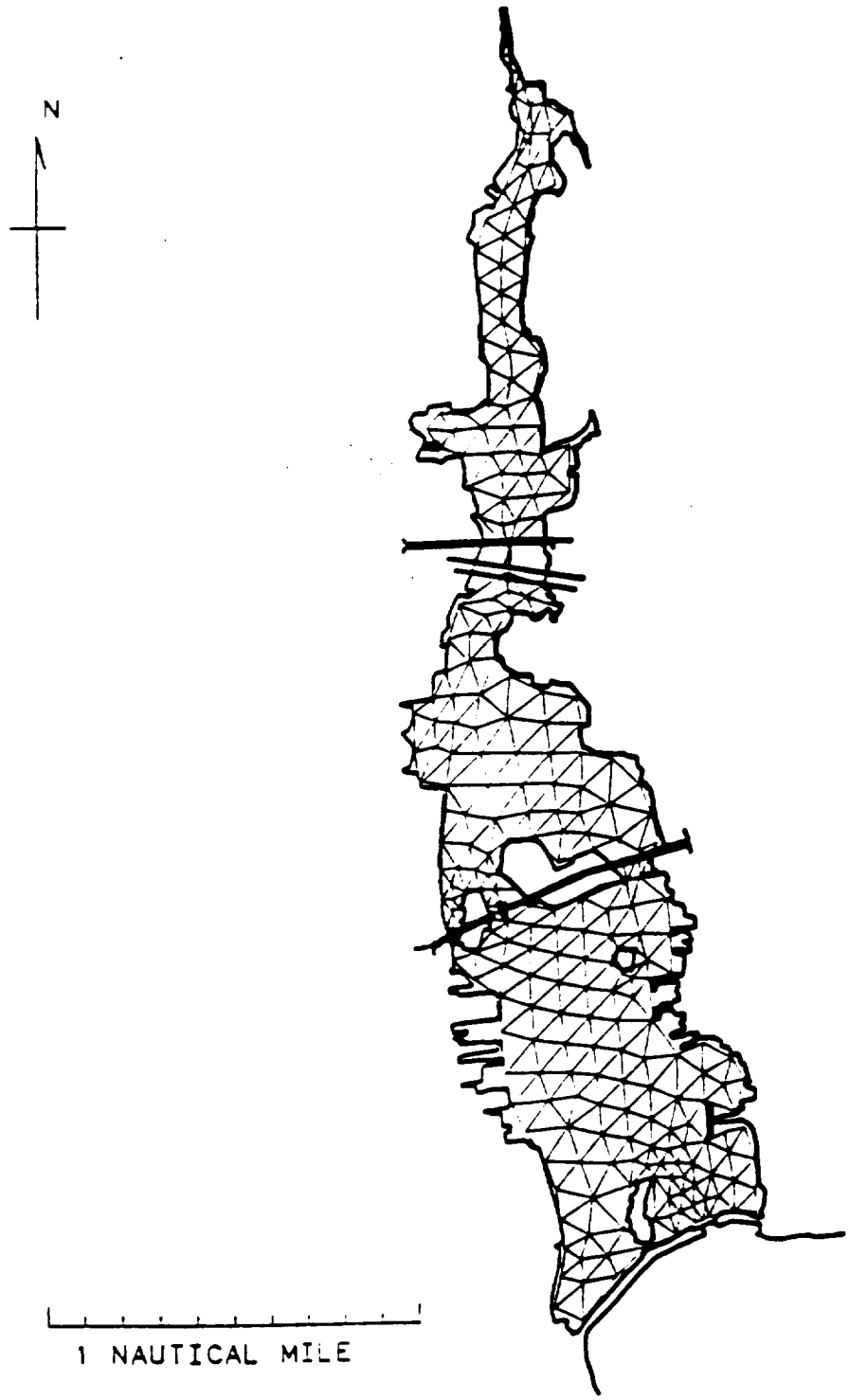

Figure 5.1 Model triangular finite element grid system.

One feature that is too small to be represented by the finite element grid but which has a significant impact on the circulation dynamics is the narrow passage through the I-195 and Coggeshall Street Bridge causeways. It is not computationally practical to reduce the finite element grid size to represent this feature. As an alternate approach this passage is approximated by a one dimensional channel connecting the adjacent areas. The procedure used to perform this calculation is described in Isaji et al (1985).

5.1.2 Tidal Simulation

The most prevalent currents in the study area are produced by tidal forcing with the M2 tide (period of 12.42 hr.) accounting for approximately eighty five percent of the tidal energy. To describe these currents the hydrodynamic model was forced with an M2 tide at the entrance to the hurricane barrier. Height and phase relationships for this open boundary were derived from Spaulding and Beauchamp's (1983) and Spaulding and Gordon's (1982) tidal model of the entire southern New England coastal area, including: Long Island Sound, Block Island Sound, Rhode Island Sound, and Buzzards Bay and the NOS data for New Bedford harbor. Using a horizontal resolution of 1 nautical mile, the two models gave excellent predictions of the tide throughout the area and provide an excellent source of information to describe the open boundary condition. The tide range selected was 1.13 m.

The tidal model was run for several test simulations to determine the most appropriate bottom friction coefficient. Simulation results show that a Manning factor of 0.025 gave the best fit to the available data. The model is generally insensitive to the exact value in the inner harbor since the region has standing tidal wave dynamics (Officer, 1976). Figures 5.2 and 5.3 show the model predicted maximum flood and maximum ebb currents, respectively.

The general pattern of model predictions is in good agreement with the

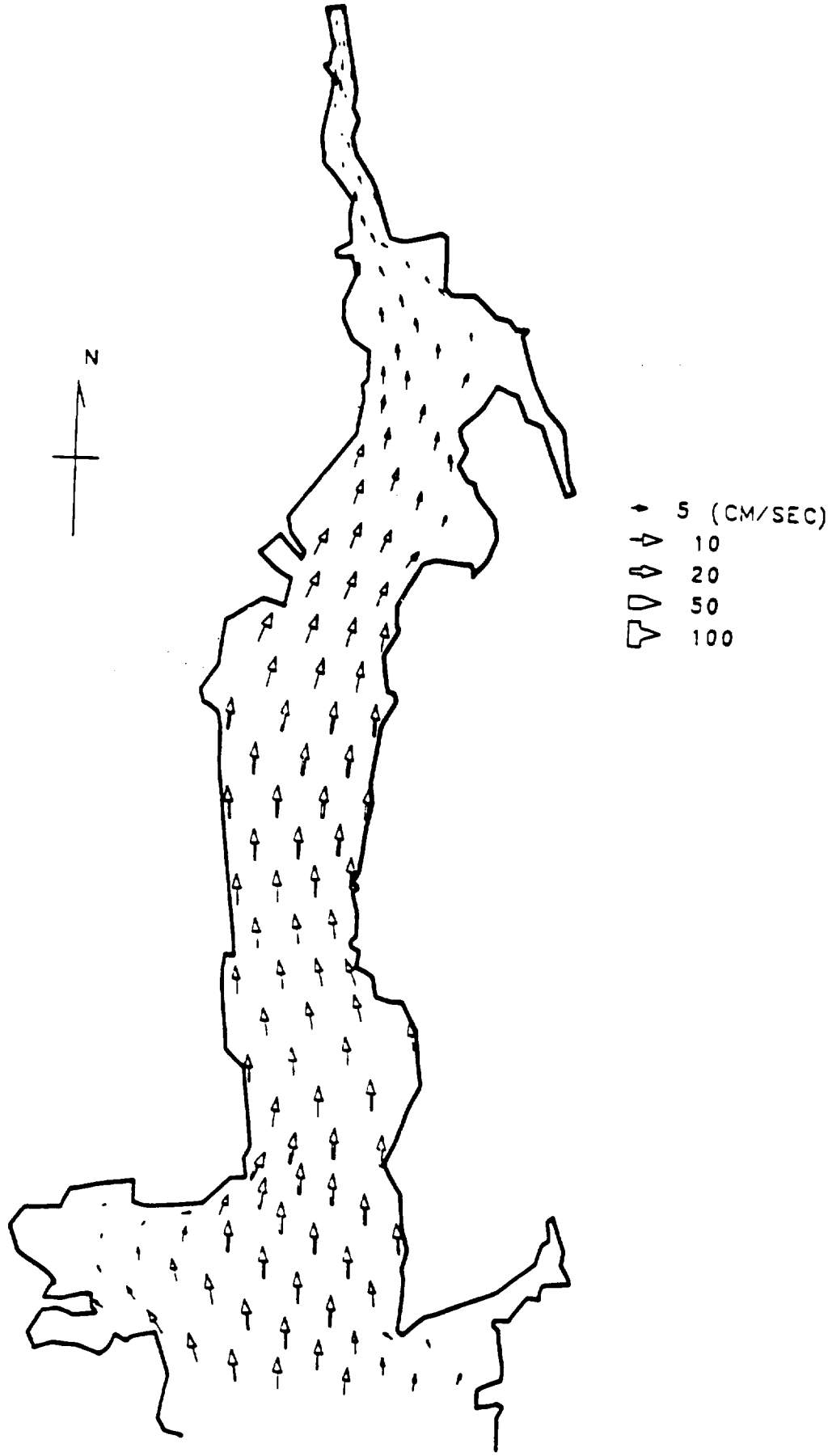

Figure 5.2 Model predicted tidal currents at maximum flood currents approximately 3 hours after high water at the hurricane barrier.

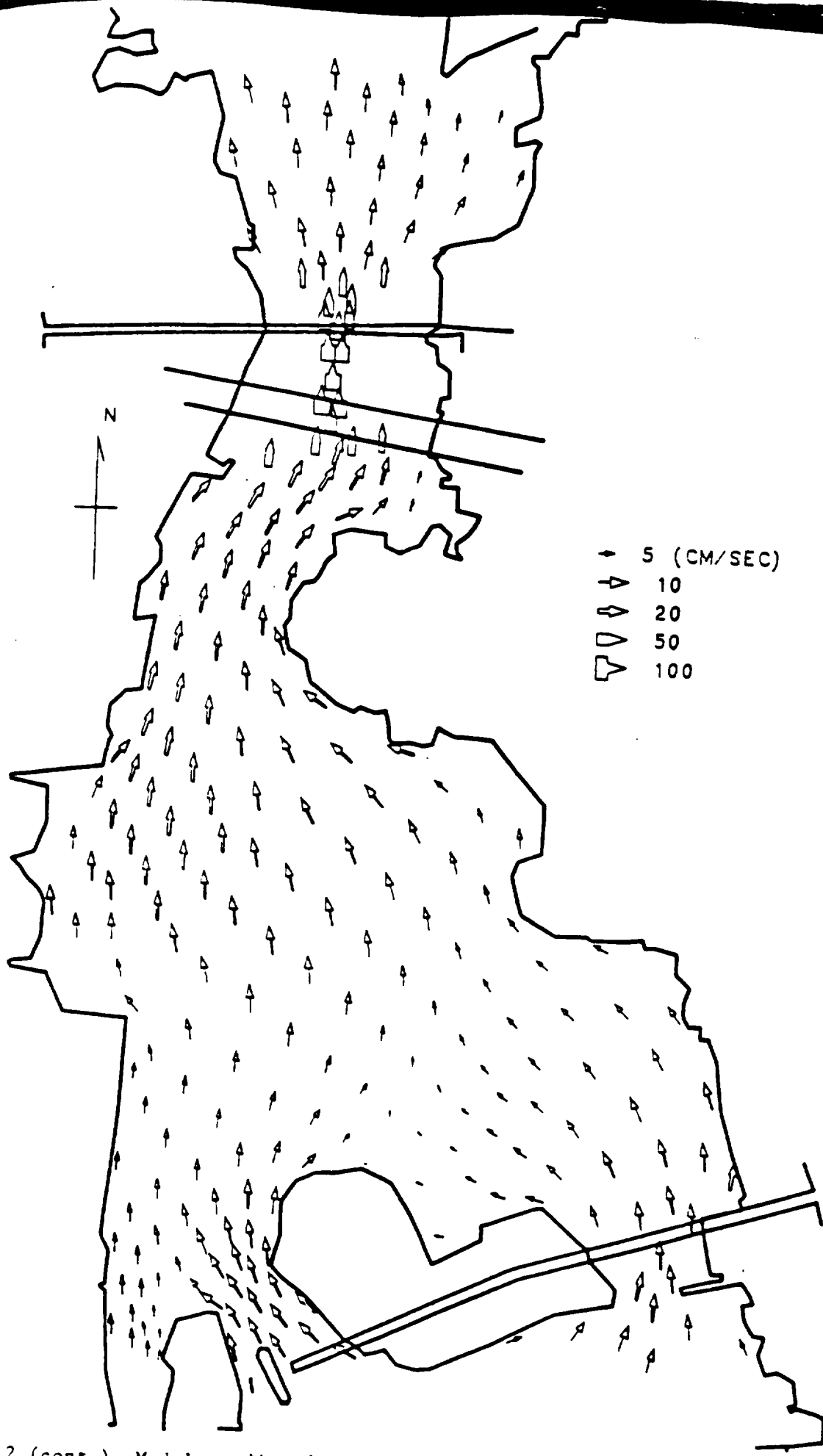

Figure 5.2 (cont.) Model predicted tidal currents at maximum flood currents approximately 3 hours after high water at the hurricane barrier.

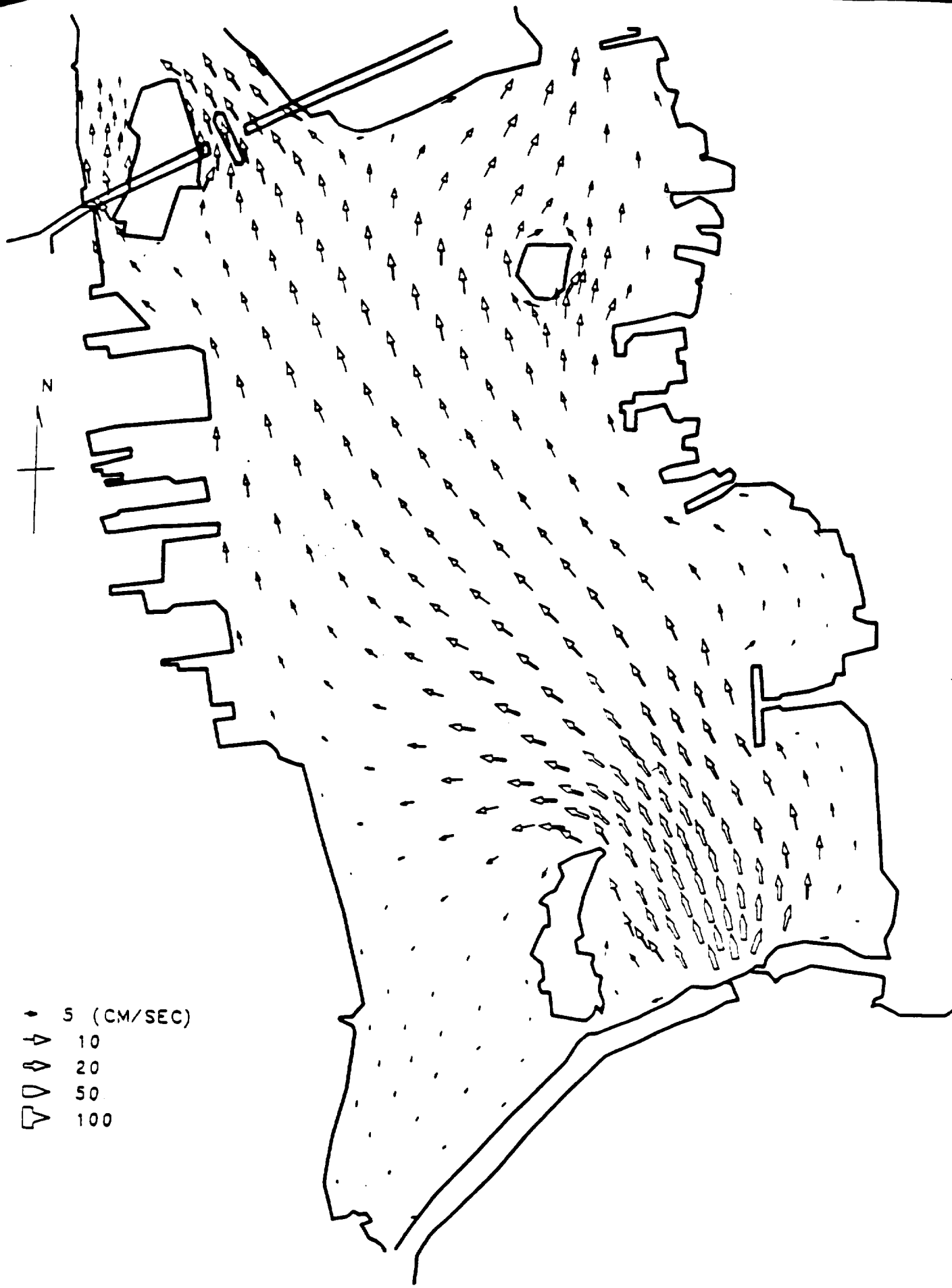

Figure 5.2 (cont.) Model predicted tidal currents at maximum flood currents approximately 3 hours after high water at the hurricane barrier.

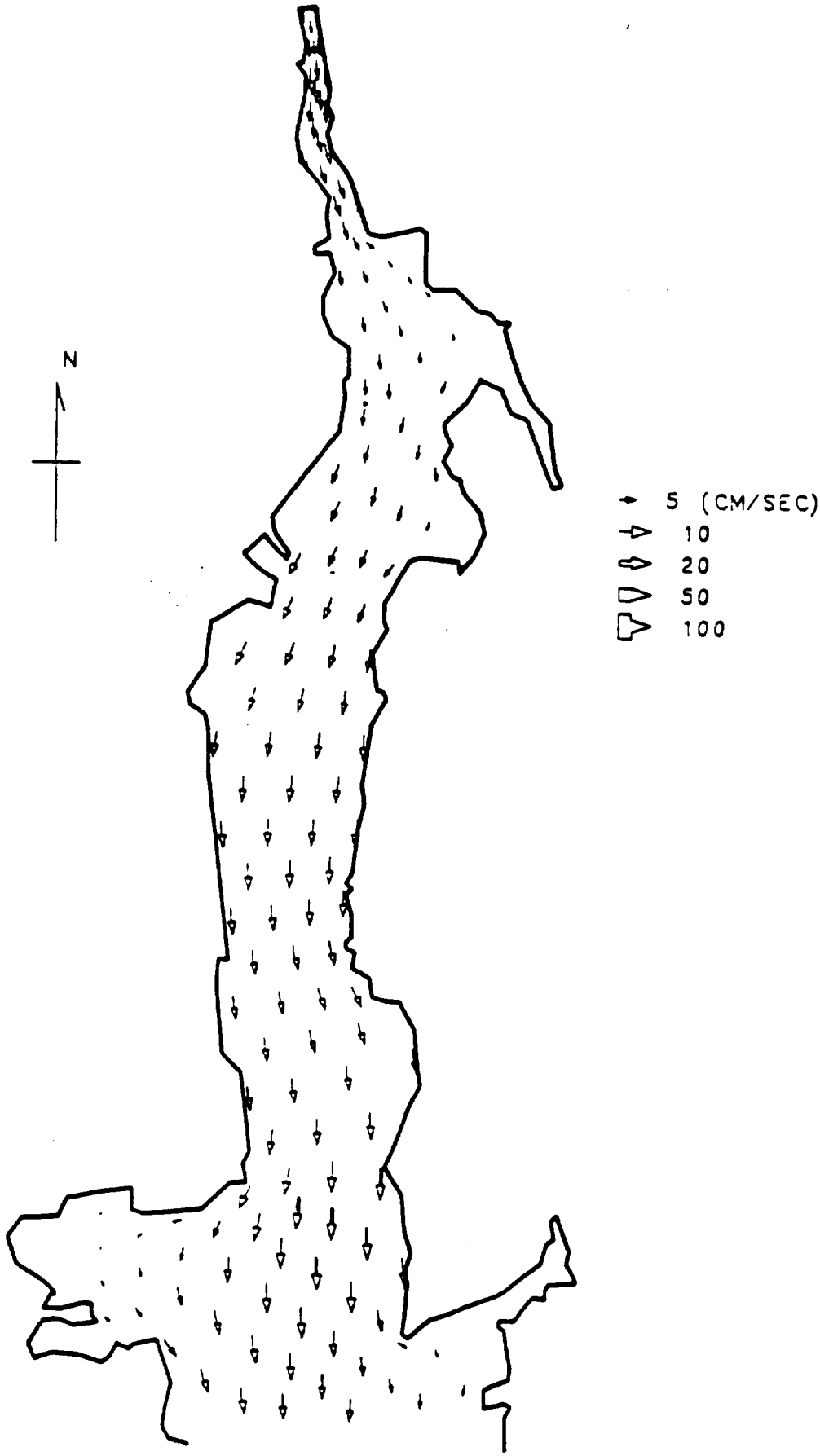

Figure 5.3 Model predicted tidal currents at maximum ebb currents approximately 9 hours after high water at the hurricane barrier.

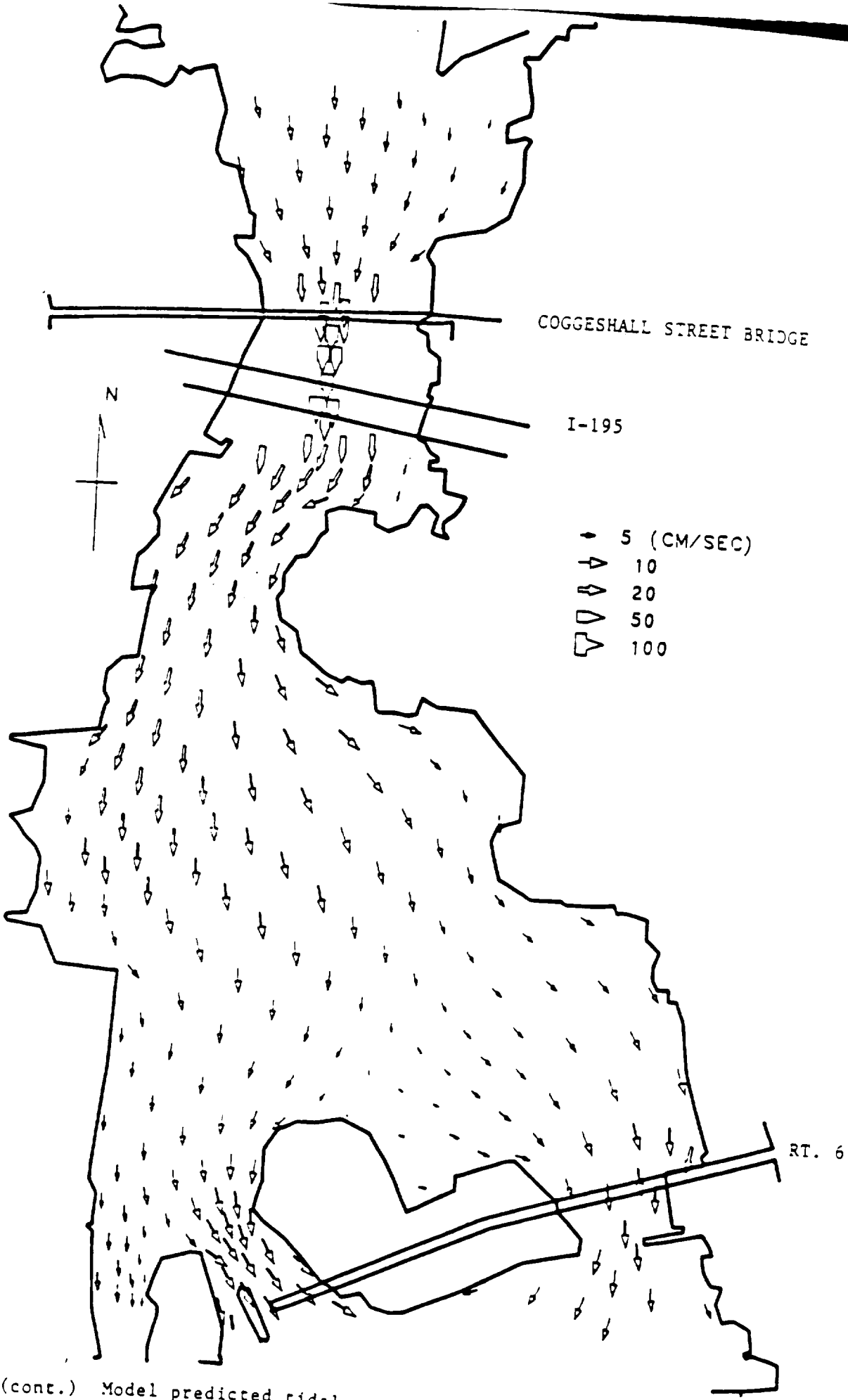

Figure 5.3 (cont.) Model predicted tidal currents at maximum ebb currents approximately 9 hours after high water at the hurricane barrier.

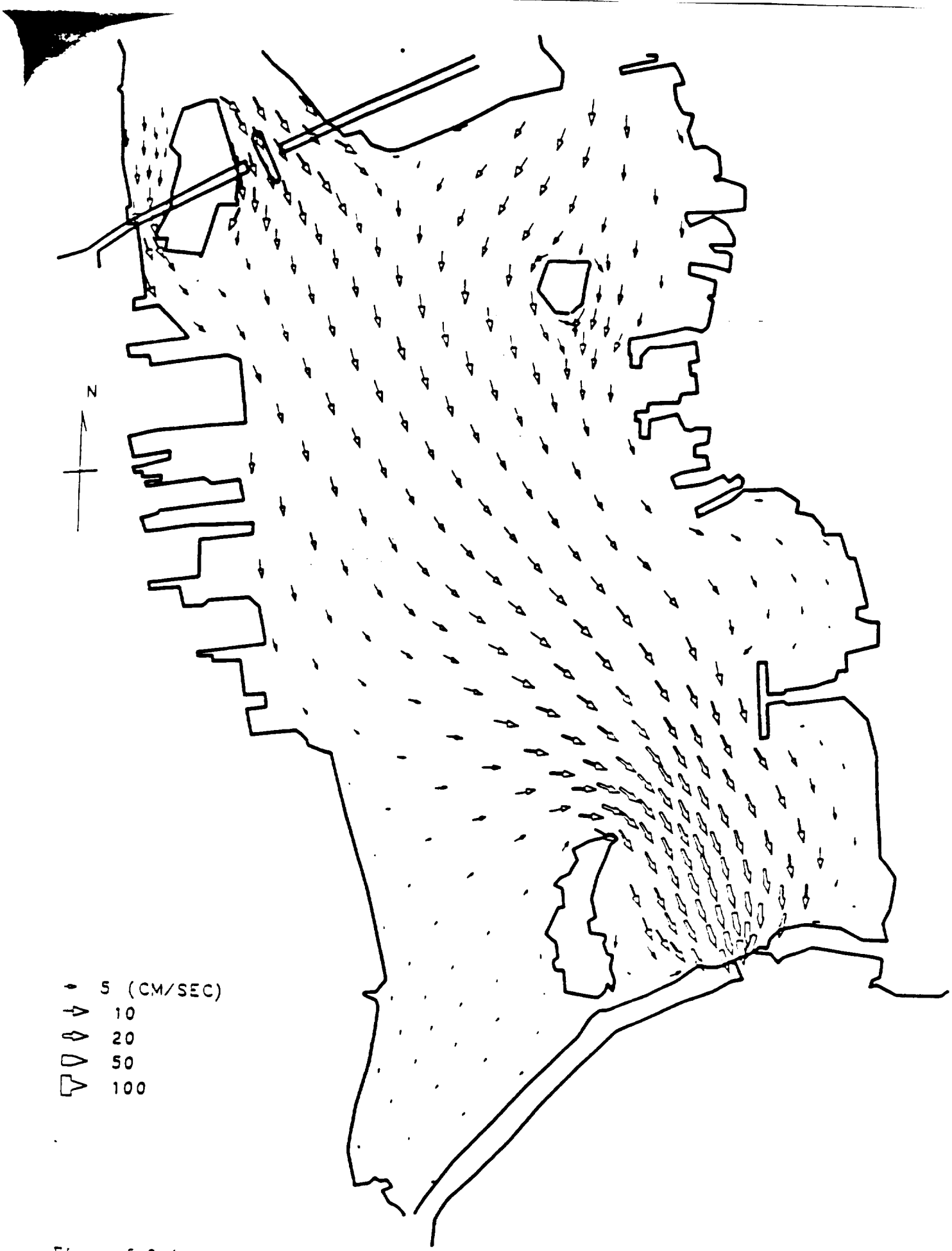

Figure 5.3 (cont.) Model predicted tidal currents at maximum ebb currents approximately 9 hours after high water at the hurricane barrier.

available data, both show tidal currents:

(a) 5-20 cm/s throughout most of the harbor
(b) stronger in the narrow constrictions
Coggeshall Street Bridge maximums 60-100 cm/s
I-195 Bridge maximums 60-100 cm/s
(c) less than 6 cm/s in the upper estuary near the Aerovox facility

Table 5.1 summarizes the detailed comparisons. Currents and surface elevations are approximately 90° out of phase with the current leading the surface elevation. This prediction is in good agreement with the available observations (EPA, 1983; present study, Appendix A, Figure 2.7).

Figure 5.5 shows a time series plot of the surface elevation and currents at the Coggeshall Street Bridge causeway for one tidal cycle. The standing wave character of the tide is clearly evident with the maximum flood and ebb currents occurring at nearly half tide and slack water occurring almost at high and low water.

As one proceeds from the Coggeshall Street Bridge to the upper estuary, the magnitude of the tidal currents decrease from 10 cm/s just north of the bridge to 6 cm/s at the Aerovox plant. This is clearly seen in Figure 5.6 which shows the along channel tidal current speed and heights as a function of distance and time for this area. This behavior is again due to the standing wave character of the tide. As one proceeds further north the river flow dominates and the currents head downstream independent of tidal stage.

A simulation has been made of the river induced flows and is shown in Figure 5.4 for the mean annual flow case (0.85 m^3/s). As seen the currents induced are a strong function of location (cross sectional area of the channel) but are generally very small (< 1 cm/s). Estimates of the river flows for other cases (i.e. 100 year flood event) can be made by simply scaling this map by the ratio of storm to mean river flow rate.

Table 5.1 Comparison of model predicted maximum ebb/flood tidal currents to observed values for selected sites in the Acushnet River estuary.

Maximum Tidal Currents (cm/s)

Location	Model* Predicted Flood	Model* Predicted Ebb	Observed Flood	Observed Ebb	Reference	Dates of Observations
I-195 Bridge Causeway	94	92	85	60**	Present Study	20 June 1986
Coggeshall St. Bridge	94	92	87.7	99	Cortell (1982)	11 December, 1981
			46	62	EPA (1983)	11&12 January, 1983
Coffin Avenue Transect	10.2	9.9	15.1	13.5	Cortell (1982)	12 November, 1981
Opposite Aerovox Facility	5.8	6.5	<5.0	<5.0	Present Study	20 June 1986

* Model predicted duration: 6.09 hours flood and 6.33 hours ebb.
** Low ebb value appears to be due to diurnal inequality for the measurement date (Figure 2.7).

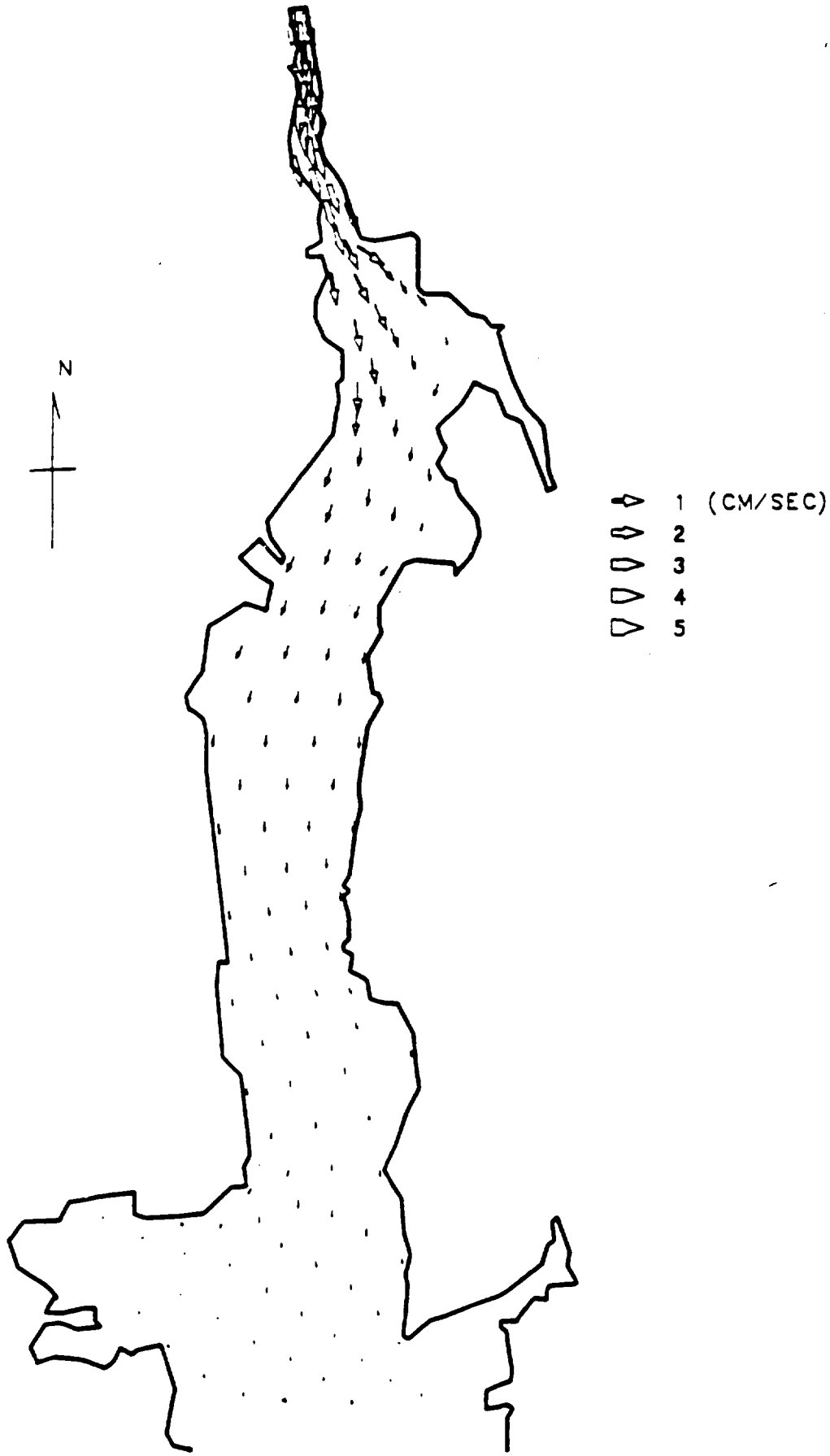

Figure 5.4 River induced flow for the mean annual flow rate (0.85 m^3/s).

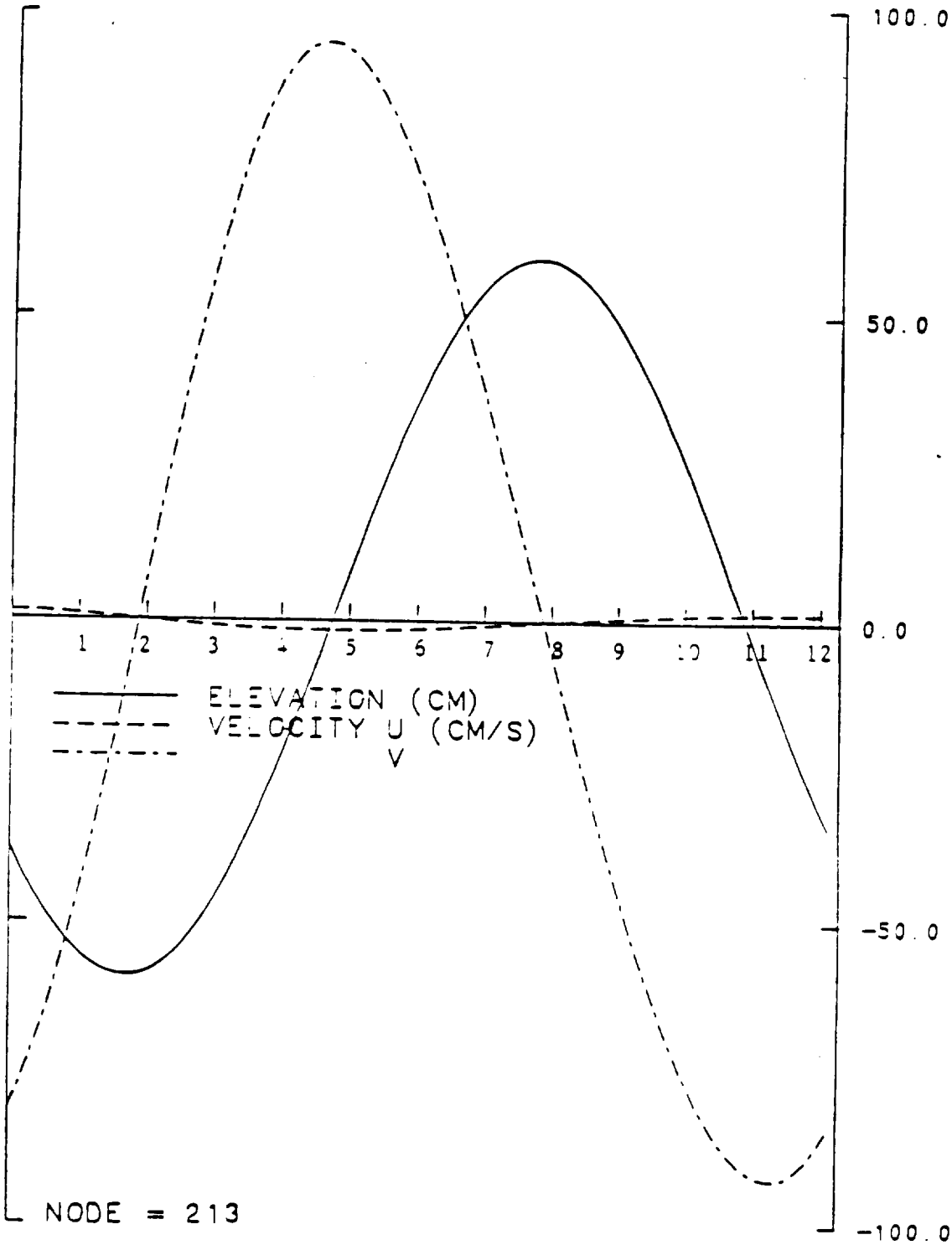

Figure 5.5 Time series plot of surface elevation and tidal currents through the Coggeshall Street Bridge causeway.

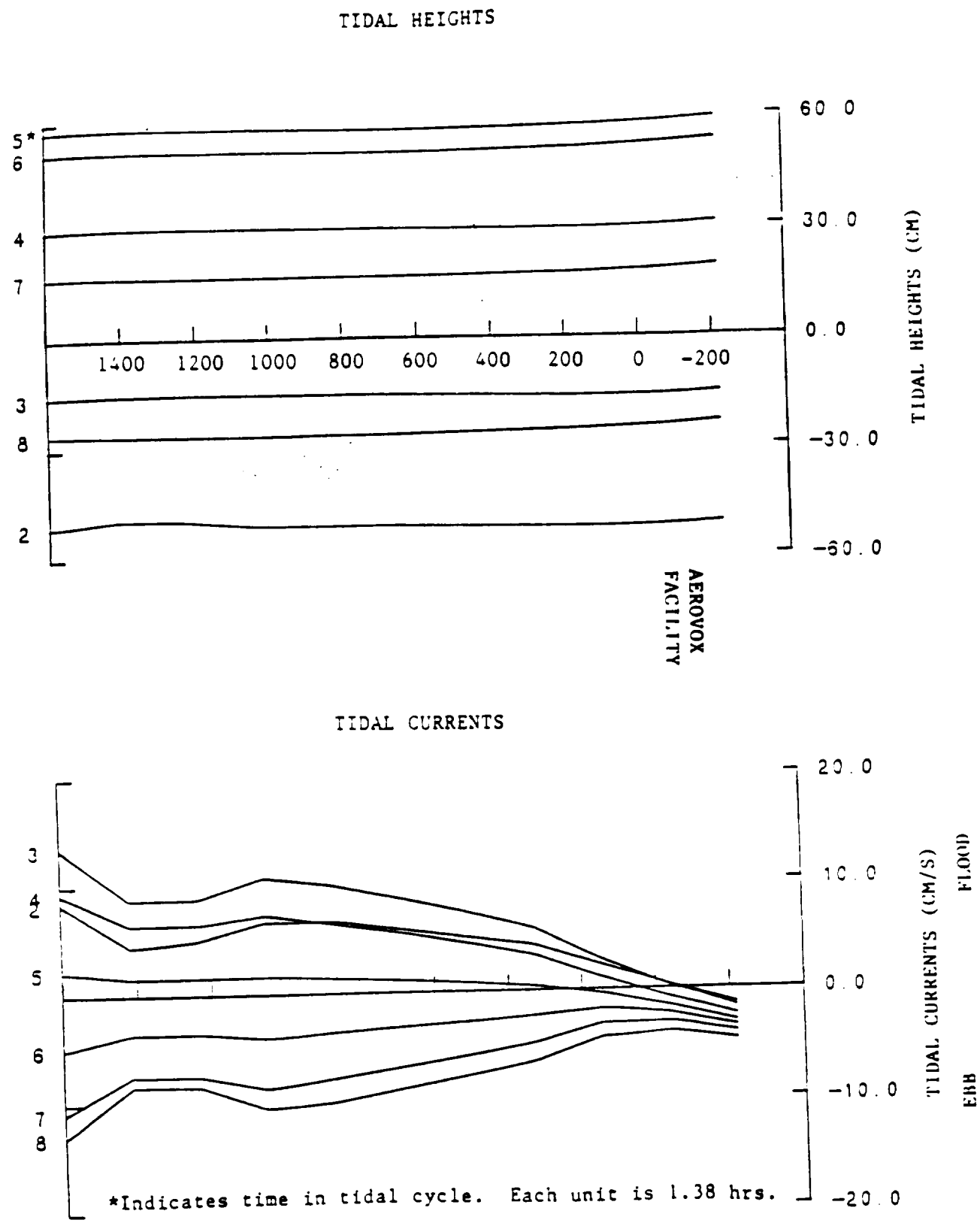

Figure 5.6 Longitudinally averaged tidal height and currents as a function of distance along the upper Acushnet River estuary. The reference is at the head of the estuary. Plots are shown at selected times over a complete tidal cycle.

5.2 Sediment Transport Simulation

To predict the fate of sediment particles resuspended into the water column, the following simulations were performed. Particles of three ϕ sizes, 6, 8, and 9 were assumed to be resuspended in the water column at the Aerovox site. Particles were assumed to be uniformly distributed over the vertical and 10 particles were released every hour over the tidal cycle for a total of 120 particles.

Simulations were performed until particles either deposited on the sea bed or until they had exited the study area (through the hurricane barrier). Simulations were performed with both the mean annual and 100 year storm river flow events. The simulations were exactly the same as for the simple analytic model described in Section 3.

The results of the deposition simulations are shown in Figures 5.7 A, B, C, D, E, and F representing three particle sizes and two river flow rates. Each figure shows the location of the deposition site of the particles by a point ".". Only the area north of Coggeshall Street Bridge for Figures 5.7A, B,C, and D is shown since all deposition for these particles was within this area.

For the mean annual river flow all particles are deposited north of the Coggeshall Street Bridge, with the larger diameter particles showing the smallest excursion from the release site. When subjected to the 100 year storm flood flow the 15.6 micron particles are retained north of the Coggeshall Street Bridge while 4% of the 3.9 micron particles and 20% of the 1.95 micron particles travel south of the bridge. For the finest particle size all sediment is redeposited before reaching the Rte. 6 bridge and Popes Island.

These observations suggest that below some critical river flow rate all particles are retained north of the Coggeshall Street Bridge. Calculations

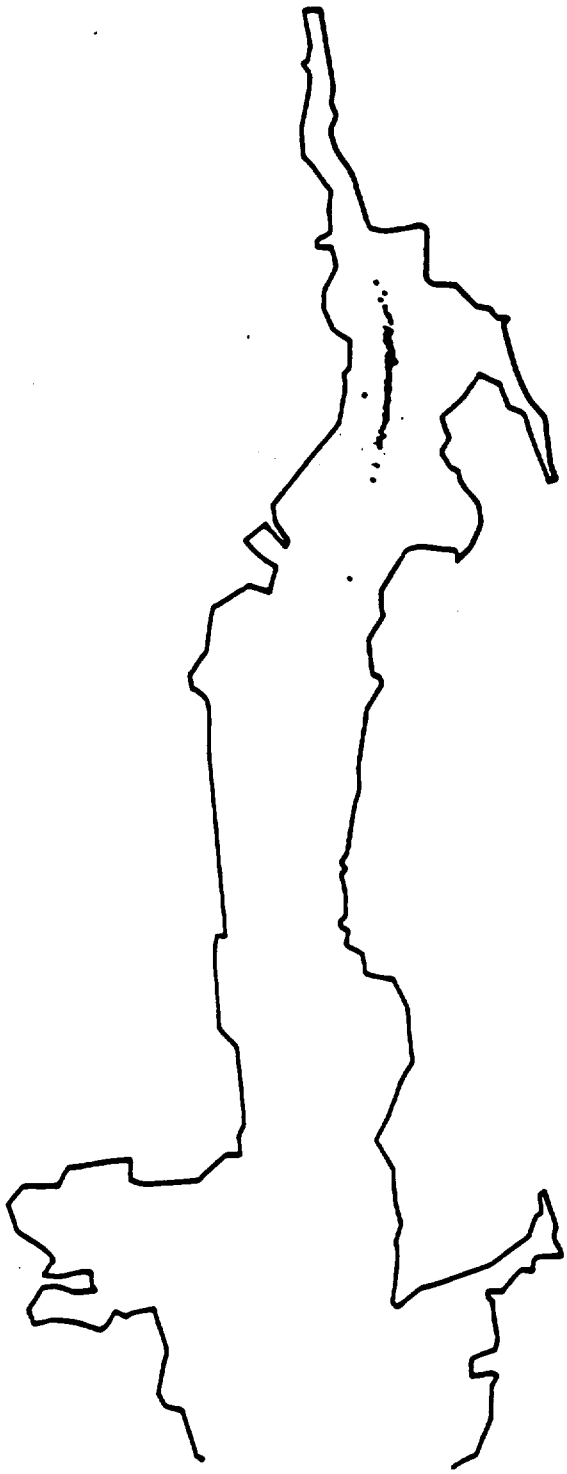

Figure 5.7A Finite element model predicted particle deposition sites for a flow rate of 30 ft^3/s (0.85 m^3/s) and a sediment particle size of 15.6 microns (ϕ=6).

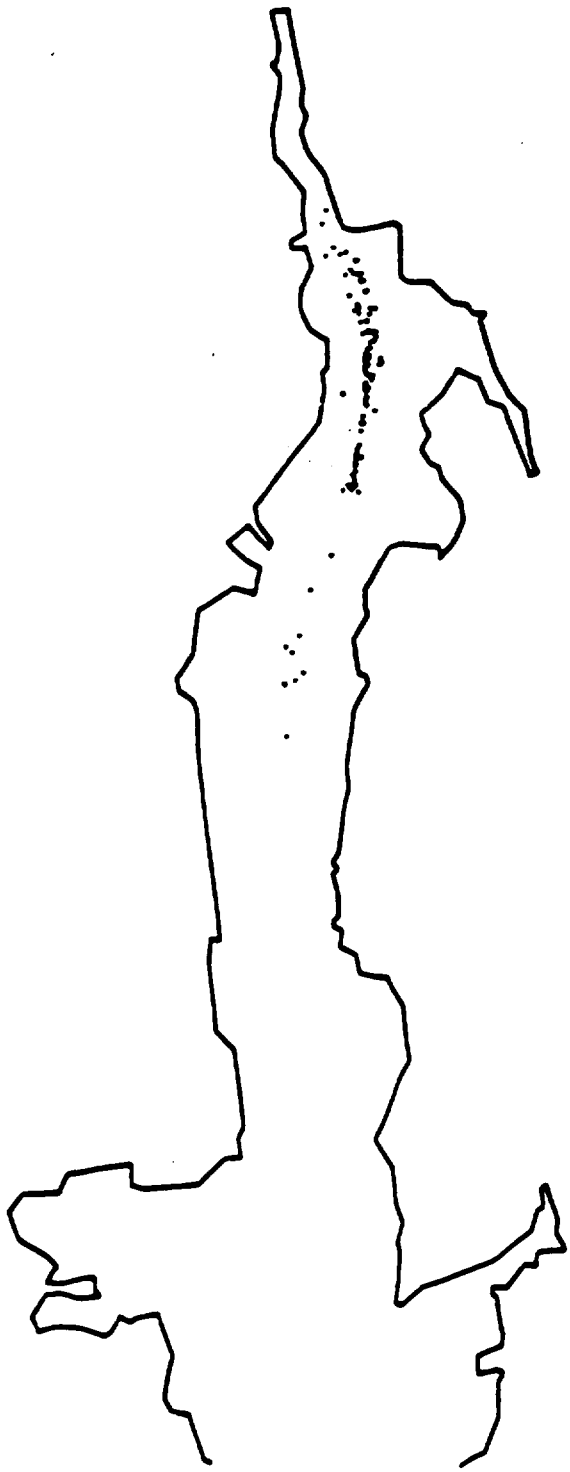

Figure 5.7B Finite element model predicted particle deposition sites for a flow rate of 30 ft^3/s (0.85 m^3/s) and a sediment particle size of 3.906 microns (ϕ =8).

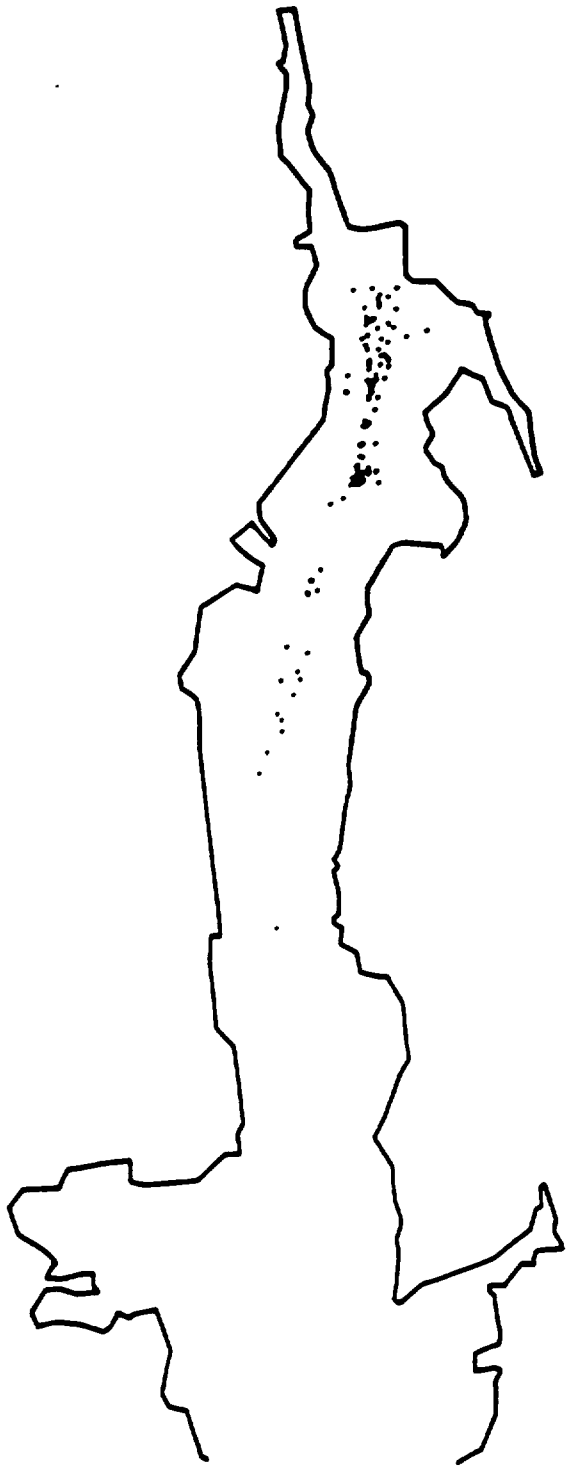

Figure 5.7C Finite element model predicted particle deposition sites for a flow rate of 30 ft^3/s (0.85 m^3/s) and a sediment particle size of 1.95 microns (ϕ=9).

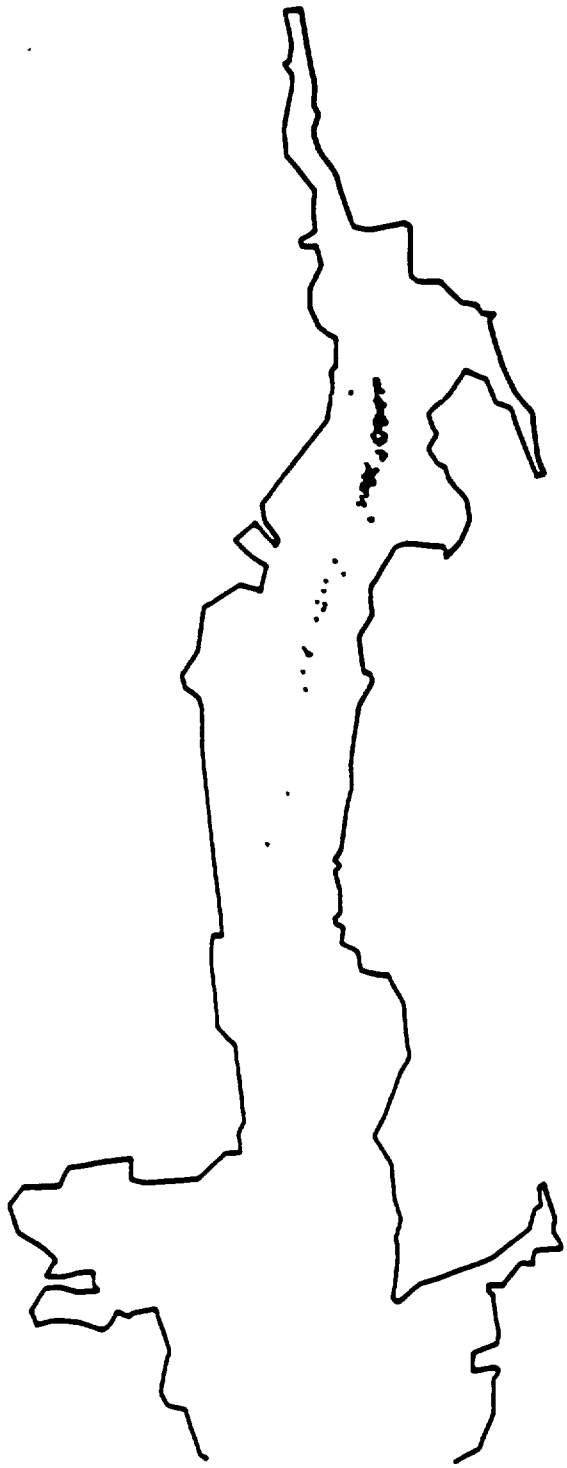

Figure 5.7D Finite element model predicted particle deposition sites for a flow rate of 650 ft^3/s (18.4 m^3/s) and a sediment particle size of 15.6 microns (ϕ=6).

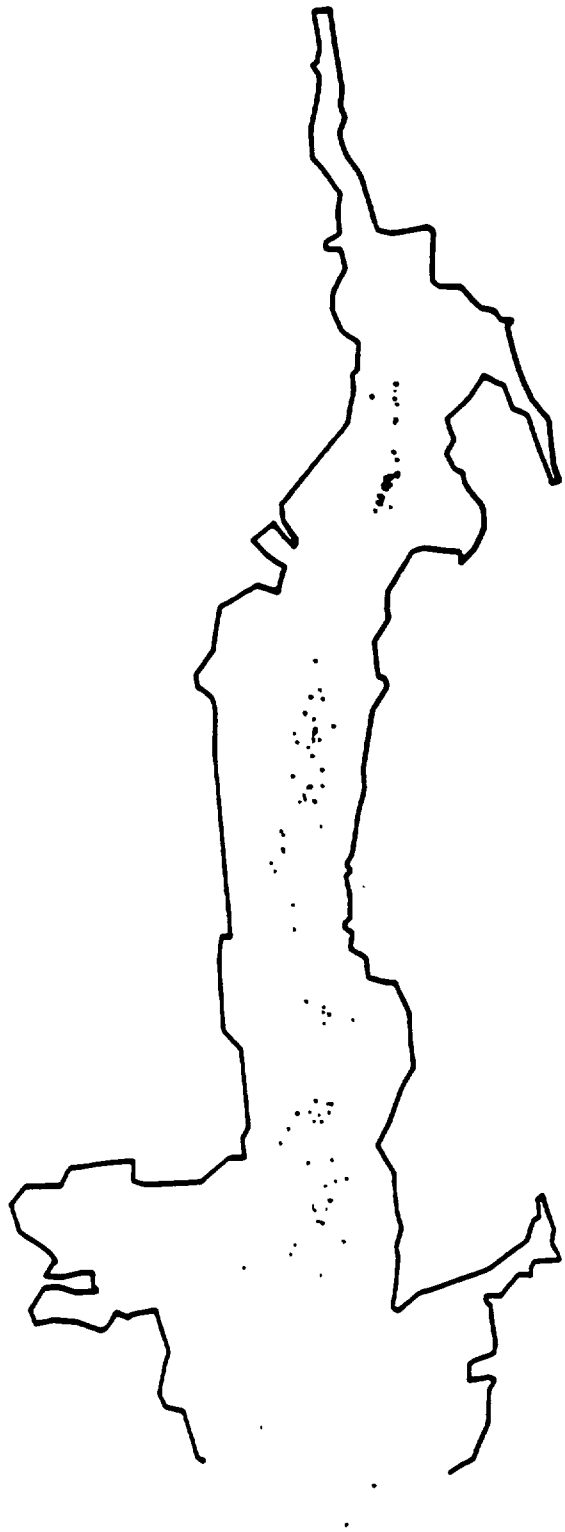

Figure 5.7E Finite element model predicted particle deposition sites for a flow rate of 650 ft^3/s (18.4 m^3/s) and a sediment particle size of 3.906 microns (ϕ=8).

Figure 5.7E (cont.) Finite element model predicted particle deposition sites for a flow rate of 650 ft^3/s (18.4 m^3/s) and a sediment particle size of 3.906 microns (D=8).

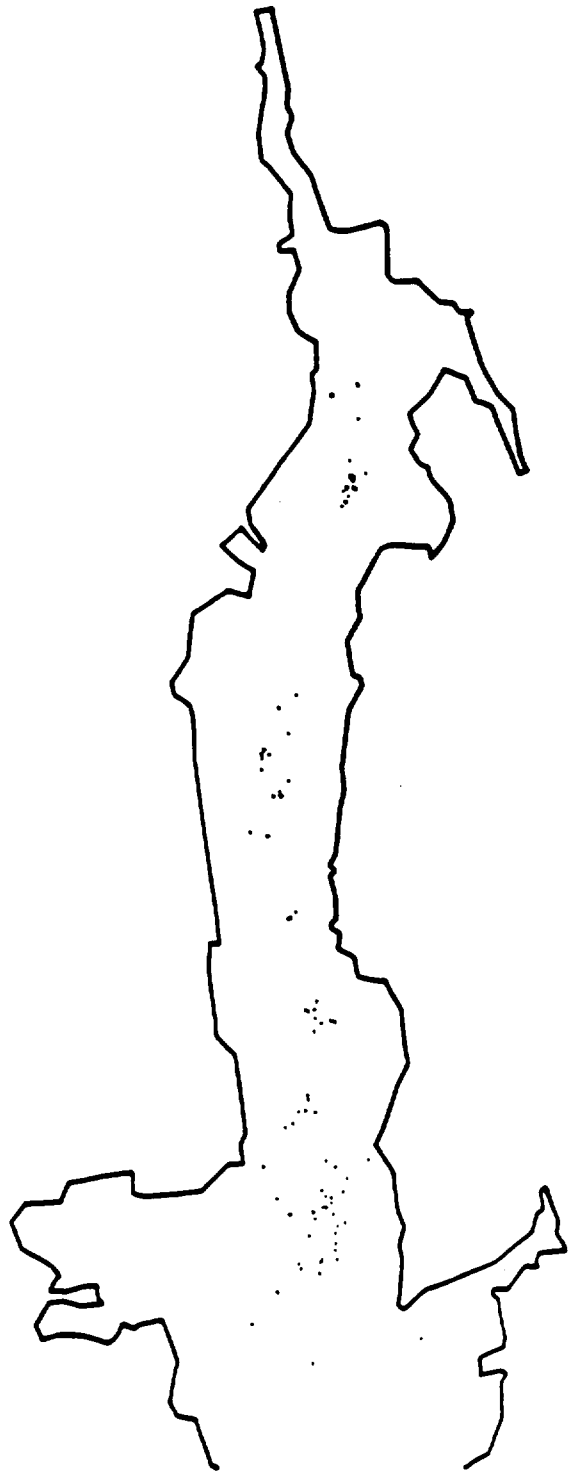

Figure 5.7F Finite element model predicted particle deposition sites for a flow rate of 650 ft^3/s (18.4 m^3/s) and a sediment particle size of 1.95 microns (c=9).

Figure 5.7F (cont.) Finite element model predicted particle deposition sites for a flow rate of 650 ft^3/s (18.4 m^3/s) and a sediment particle size of 1.95 microns (c=9).

were made incrementally increasing the river flow rate and determining the percent of particles (ϕ=9) passing south of the bridge. All particles of smaller phi sizes (6 and 8) are deposited faster than the ϕ=9 particles. Both the simplified (Section 3) and finite element (Section 5) models were used to make these calculations.

Table 5.2 shows the results of these simulations. The simplified model predicts the critical flow rate at 7.08 m^3/s while the finite element model gives a value of 9.6 m^3/s. The general agreement between the two methods is quite good. The finite element model predictions are probably more accurate in that they account for the geometric variations of the cross section and hence river induced flows. Because of the large increase in cross sectional area and decrease in velocity just north of Coggeshall Street Bridge the analytic model is expected to predict higher losses than the finite element calculations. This is consistent with the predictions in Table 5.2.

If we next relate the threshold flow rate to the storm recurrence intervals, (Table 2.2) assuming an average flood flow rate over the storm interval, we see that the simplified and finite element models give frequencies of once every 10 and 25 years, respectively. It is therefore expected that once every 10 to 25 years the smallest grain sediment particles (ϕ=9) will be transported south of the Coggeshall Street Bridge. This estimate must however be viewed with caution due to uncertainties in the river flow estimates during storm flood conditions.

Table 5.2. Percent of ϕ=9 size particles passing south of Coggeshall Street Bridge as a function of river flow rate.

Acushnet River Flow Rate $(ft^3/s)/(m^3/s)$	Estimate ** Flood Recurrence Interval (years)	Percent of ϕ=9 sized particles passing south of Coggeshall Bridge	
		Simplified Model	Finite Element Model
650 (18.4)	100	24.17	20%
500 (14.1)	-	15.0	*
400 (11.3)	50	9.17	*
340 (9.6)	25	-	0
300 (8.5)	10	4.17	0
250 (7.08)	-	0.8	0
200 (5.66)	-	0	0
30 (0.85)	-	0	0

* Greater than zero but exact value not computed.

** Values are determined by multiplying the ratio of the 100 year average flood flow (18.4 m^3/s) to the peak 100 yr flood flow (38.2 m^3/s) times the peak value for the desired storm from Table 2.2.

5.3 Water Column Concentration Simulations

Battelle, New England, Duxbury, Massachusetts collected water column concentrations during three cruises (Cruise #1, Sept-Oct 1984; Cruise #2, November 1984; Cruise #3, June-July, 1985) from the upper Acushnet River estuary down to the lower harbor (Battelle, 1985). Samples were also collected at selected stations in Buzzards Bay. Figure 5.8 shows the station locations in the New Bedford harbor area.

The data collected during the field program are shown in Figures 5.9, 5.10 and 5.11 which present PCB concentrations (ng/l or parts per trillion) versus distance (km) along the estuary for each of the three cruises. The longitudinal distances are measured along a constant longitude line and hence do not exactly follow the center line of the estuary. Key geographic points are noted in the bottom of each figure while the station numbers (Figure 5.8) are given at the top of the figure in a box. The vertical location and timing (relative to the tide) for each sample are noted to the right of the data point. The sub-figure letters A, B, and C indicate filtrate, particulate, and total PCB concentration levels, respectively. The total concentrations are the sum of the filtrate and particulate values. If one value was missing no total was calculated. All available data are shown even though some values did not meet contract specifications. Figures 5.12 A, B, and C are summary plots for all cruises showing filtrate, particulate, and total concentrations, respectively.

Most figures show decreasing concentrations as one proceeds from the upper estuary, (Aerovox Plant) through to the Rte. 6 Bridge. Concentrations then increase slightly again through the hurricane barrier and then decrease further south in the outer harbor. The gradient is a little greater than one order of magnitude between the Aerovox site and the Rte. 6 Bridge. The

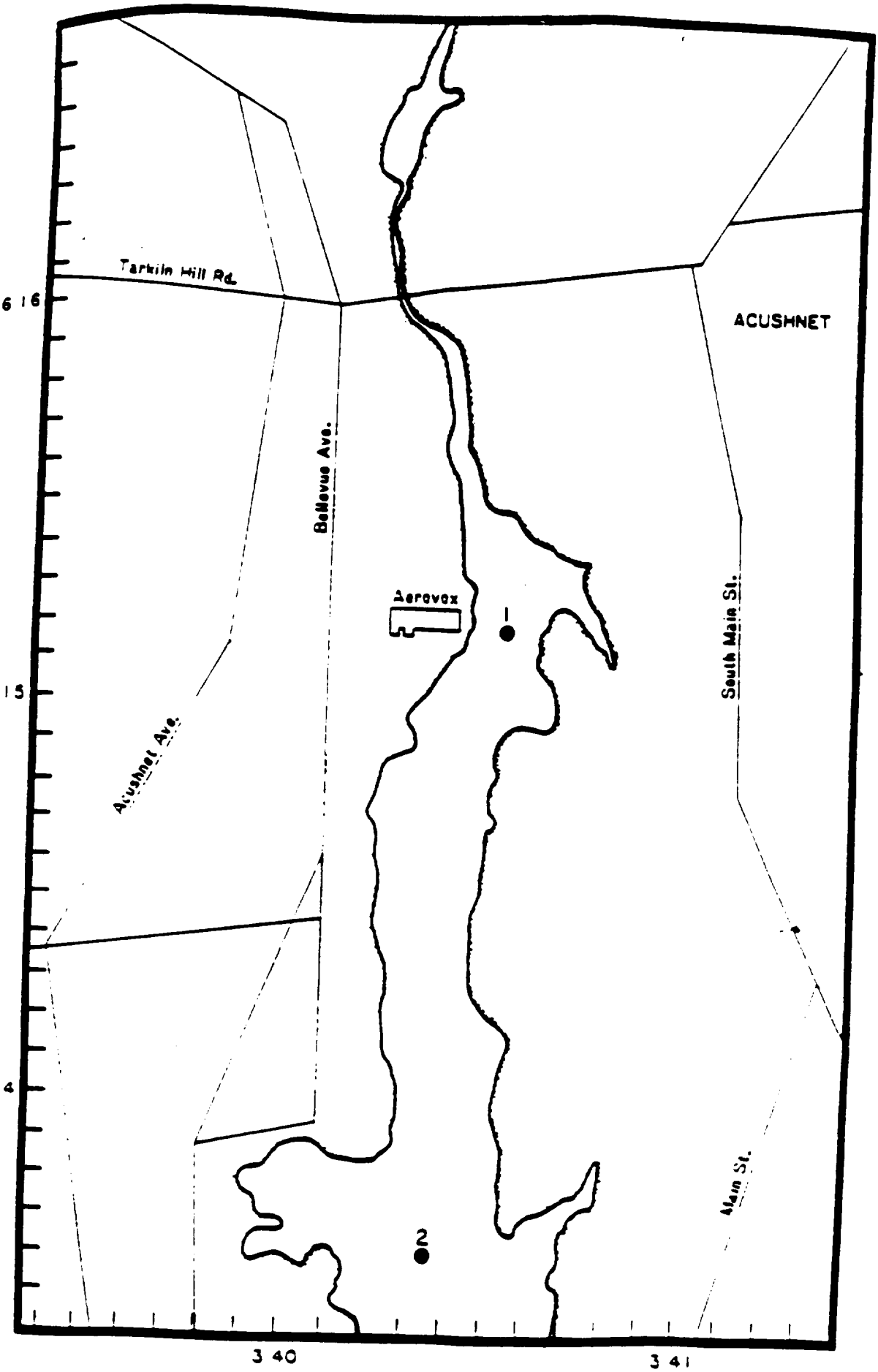

Figure 5.8 Location of Battelle PCB Water Column Sampling Stations.

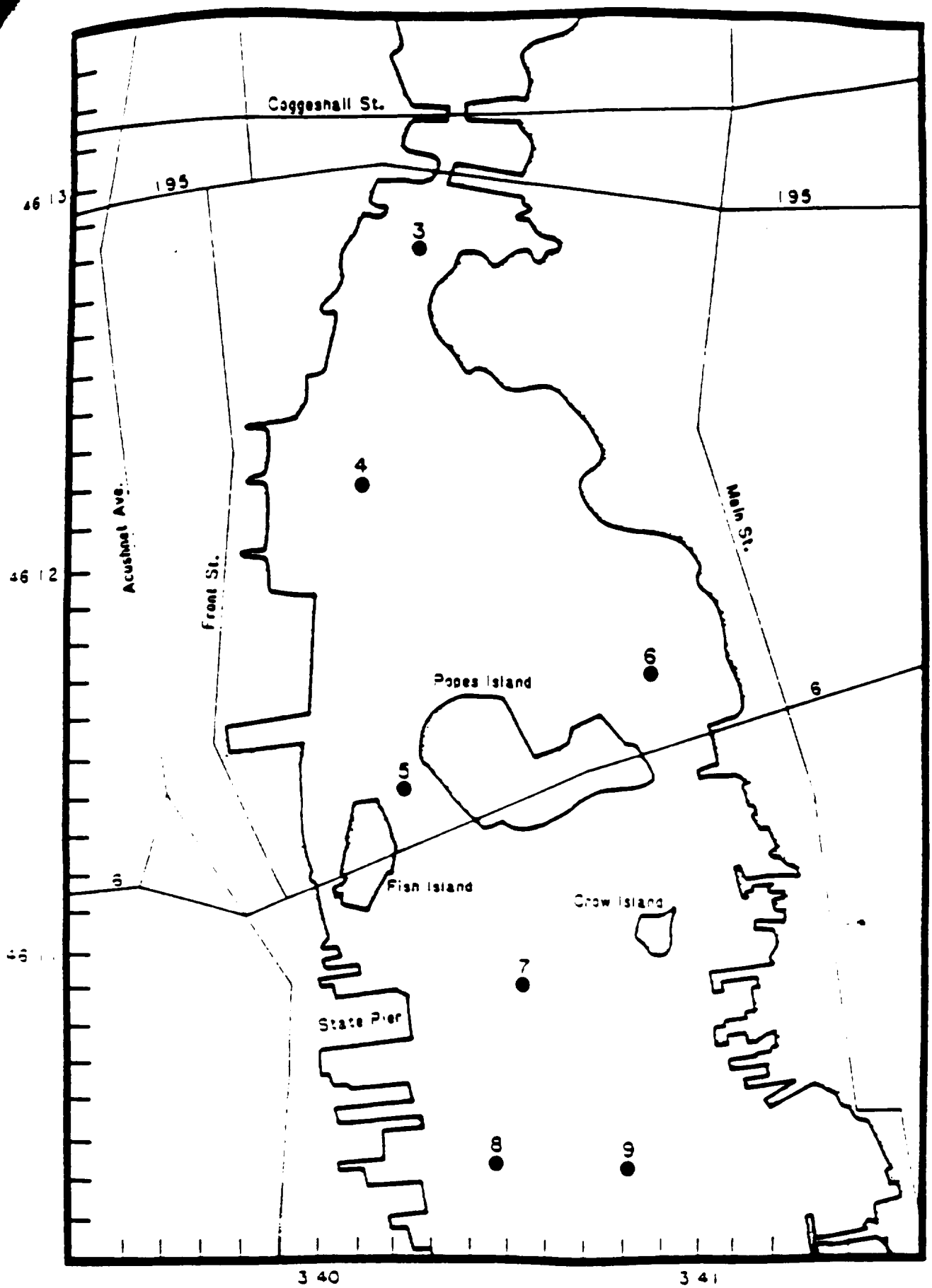

Figure 5.8 (cont.) Location of Battelle PCB Water Column Sampling Stations.

6. OIL SPILL TRANSPORT MODEL

It has been suggested that an alternate path for PCB's to enter the environment is by the suspension of oil containing PCB's that are currently trapped in the sediments of the upper Acushnet River estuary (EPA, 1983). In laboratory experiments of the worst case leaching tests on highly contaminated sediment samples the EPA investigators observed that oil was released forming a film on the surface of the experimental vessels. This observation coincides with what was observed while collecting these sediment samples (EPA, 1983). When the core sampler was pushed into the contaminated sediments, oil was released indicating that the oil incorporated in the sediments was released upon disturbance. Another source of oil containing PCB's might include runoff from parking lots, buildings, and contaminated areas surrounding the Aerovox facility. In Narragansett Bay, the largest contributor of petroleum hydrocarbons to the bay is through land runoff (Hoffman et al, 1982, 1984; Hoffman and Quinn, 1984). In any case, the movement of PCB contaminated oil may be a potential mechanism for transporting PCBs throughout the estuary. To address this transport of oil, which is observed to behave as a surface slick, we have applied the well known ASA oil spill model to the upper Acushnet River estuary (north of Coggeshall Street Bridge). The model is based on a comprehensive three dimensional oil spill fates simulator originally developed for the Department of Energy and the Bureau of Land Management for oil spill - fishery impact assessment (Cornillon et al 1979a, b; Reed 1980; Anderson and Spaulding, 1981; Spaulding et al 1982a, b; 1985). Only the surface trajectory portion of the model is implemented in the present study.

The circulation dynamics of the area are described by the hydrodynamic model and assume a mean river flow rate of 0.85 m^3/s. Wind data is obtained

from observations at Green Airport in Warwick, Rhode Island and includes a 30 year record (1948 to 1977). The wind data is available at 1 hour intervals over the entire period. The Green Airport data were used since it was the closest observation station to have a long uninterrupted wind time series available. The distance from the Green Airport to New Bedford is approximately 45 km. Given this separation distance, the high frequency wind fluctuations of New Bedford are probably not accurately represented by the Green Airport data however the lower frequency characteristic weather pattern cycles of 2-5 days are preserved (Mooers, 1978; Mooers et al, 1976;. This data set hence should be adequate to describe the principal features of the local wind field.

The oil spill trajectory model was run for each of four seasons (Nov.-Jan. - winter; Feb.-April - Spring; May-July - Summer; Aug.-Oct. - fall). For each simulation, the start time was selected at random during the wind record (for a given season) and in the tidal cycle. Using this procedure the variability in trajectories associated with the variability in wind and current conditions is preserved. Using this procedure, a total of 1000 trajectories were simulated for each season starting at a release point near the Aerovox facility.

Figures 6.1 to 6.4 show sample trajectory plots for each of the four seasons. Since the wind direction is normally from the west (NW-W in winter, W, spring and fall and SW in summer) approximately twice as many of the trajectories show surface oil transport to the east with shoreline impact along the Fairhaven side of the estuary versus to the west with impact on the New Bedford shore. The influence of the tide causes the trajectories to deviate either to the north or south depending on the stage of the tide. The seasonal influence of the wind is small but noticeable with summer winds causing shore impacts further to the north and winter and fall winds further to the south.

NEW BEDFORD UPPER HARBOR

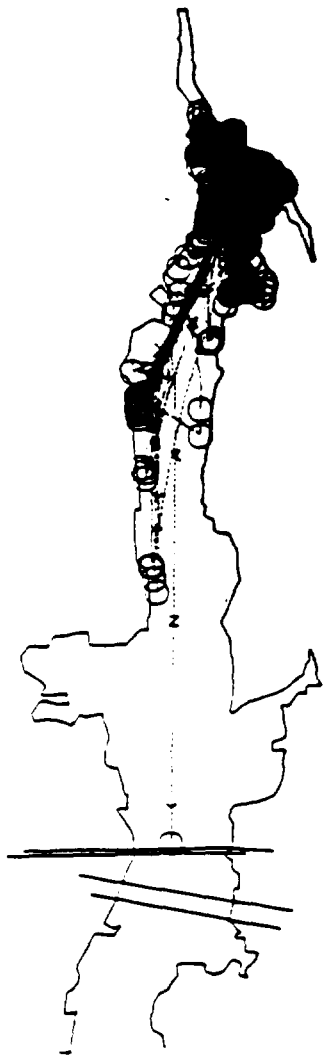

Figure 6.1 Spill trajectories for the winter.

NEW BEDFORD UPPER HARBOR

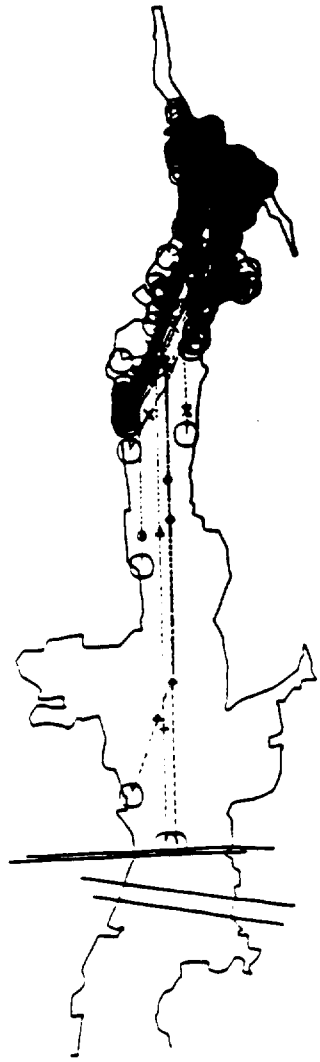

Figure 6.2 Spill trajectories for the spring.

NEW BEDFORD UPPER HARBOR

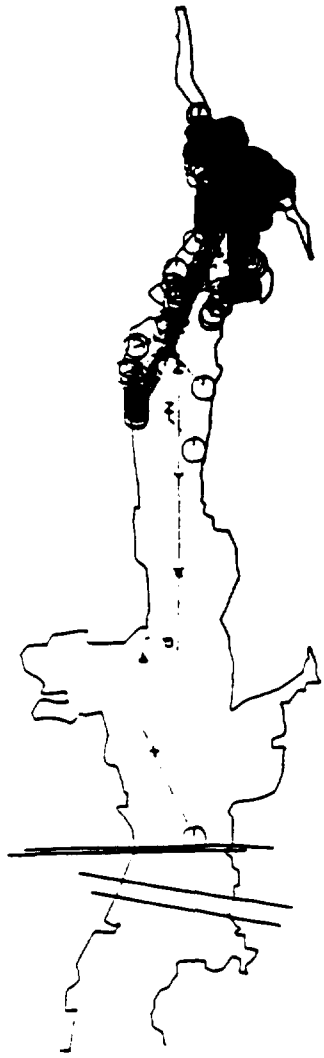

Figure 6.3 Spill trajectories for the summer.

NEW BEDFORD UPPER HARBOR

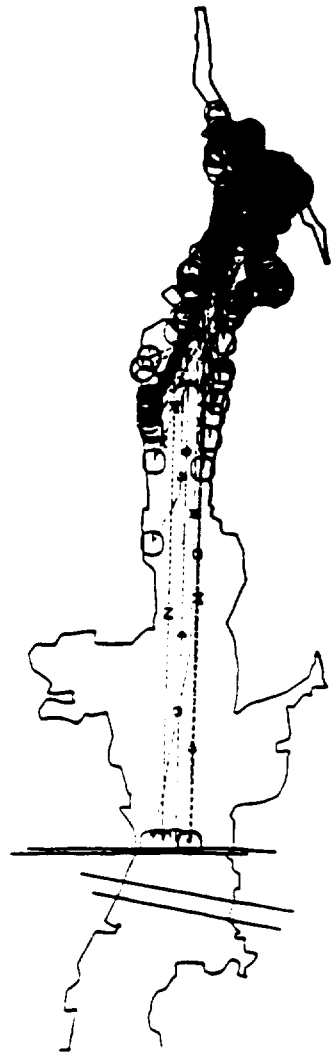

Figure 6.4 Spill trajectories for the fall.

of the trajectories released, few are observed to impact the New Bedford shore (western) (13.5% winter; 20.1% spring; 17.8% summer; and 17.6% fall). These lower percentages are caused by the predominance of westerly winds. Because of the predominance of wind induced transport of surface oil in an easterly direction and the north/south orientation of the estuary only 9 of the 4000 trajectories reached the Coggeshall Street Bridge.

It has been assumed in these simulations that once a trajectory reaches the shoreline, the oil represented by the trajectory remains there. Refloating the oil, say on the next high tide, so that oil remains available for further transport shows more shoreline impacted although the general regions of impact remain the same (i.e. western shore of Fairhaven).

Calculations of the mean, maximum and minimum, and standard deviation of time for a trajectory to reach shore are shown in Table 6.1 for each season. The mean time to reach shore is relatively short at 30-35 minutes and is directly related to the narrowness of the estuary in the vicinity of the spill site and the easterly directed wind. The seasonal variations are generally small. The standard deviations are about constant at 27-33 minutes as is the minimum time for impact of 2-4 minutes. The maximum time to reach shore is longest in the summer due to the light winds and shortest in the winter and spring when the winds are more energetic.

Table 6.2 shows the minimum, maximum, mean and standard deviation of the spill trajectory lengths for each seasonal spill. Also included are the percent distribution of trajectory lengths by direction. The tabulated data serve to provide qualitative support to the trajectory plots given in Figures 6.1 to 6.4.

Based on the calculations performed, surface oil slicks released in the vicinity of the Aerovox facility are essentially trapped in the upper Acushnet

Table 6.1. Mean, Standard Deviation Minimum, and Maximum of time for a spill trajectory to reach shore, release point near Aerovox facility.

	TIME TO REACH SHORE (MIN)			
SEASON	Mean	Standard Deviation	Maximum	Minimum
Winter	28.4	33.0	311	2.
Spring	26.7	30.2	275	2.
Summer	27.8	30.1	408	4.
Fall	33.5	35.7	332	3.

WINTER

Launch Point	Trajectory Lengths [km] Minimum	Maximum	Mean	Std Dev	Trajectory Angle [deg] Mean	Std Dev
1	0.0539	2.0231	0.1686	0.1453	85.9	100.6

LP# 1

TRAJECTORY LENGTH [m]	0-25	->50	->100	->150	->200	->250	->300	->350	->400	->450	->500	500+
TRAJECTORY DIRECTION N	0.0	0.0	0.0	0.0	9.5	3.5	5.1	0.4	0.0	0.0	0.0	0.0
NE	0.0	0.0	0.0	0.9	16.6	0.1	0.0	0.0	0.0	0.0	0.0	0.0
E	0.0	0.0	11.2	10.7	0.0	0.0	0.0	0.0	0.0	0.0	0.0	0.0
SE	0.0	0.0	12.2	6.1	0.1	0.0	0.4	0.0	0.0	0.0	0.0	0.0
S	0.0	0.0	0.0	0.0	0.0	5.0	3.3	0.0	0.0	0.3	0.0	1.1
SW	0.0	0.0	1.3	0.3	0.1	0.1	0.1	0.1	0.1	0.0	0.0	2.2
W	0.0	0.0	4.8	0.0	0.0	0.0	0.0	0.0	0.0	0.0	0.0	0.0
NW	0.0	0.0	2.3	1.0	0.1	1.0	0.0	0.0	0.0	0.0	0.0	0.0

Direction sums:

N	NE	E	SE	S	SW	W	NW
18.5	17.6	21.9	18.8	9.7	4.3	4.8	4.4

SPRING

Launch Point	Trajectory Lengths [km] Minimum	Maximum	Mean	Std Dev	Trajectory Angle [deg] Mean	Std Dev
1	0.0539	2.0227	0.1788	0.1651	97.2	114.8

LP# 1

TRAJECTORY LENGTH [m]	0-25	->50	->100	->150	->200	->250	->300	->350	->400	->450	->500	500+
TRAJECTORY DIRECTION N	0.0	0.0	0.0	0.0	7.5	4.2	7.4	0.4	0.0	0.0	0.0	0.0
NE	0.0	0.0	0.0	0.4	13.5	0.3	0.0	0.0	0.0	0.0	0.0	0.0
E	0.0	0.0	10.9	8.9	0.0	0.0	0.0	0.0	0.0	0.0	0.0	0.0
SE	0.0	0.0	11.2	5.0	0.0	0.1	0.2	0.0	0.0	0.0	0.0	0.0
S	0.0	0.0	0.0	0.0	0.0	4.6	3.3	0.5	0.2	0.3	0.0	1.0
SW	0.0	0.0	2.8	0.0	0.1	0.0	0.5	0.4	0.4	0.0	0.0	3.4
W	0.0	0.0	4.7	0.0	0.0	0.0	0.0	0.0	0.0	0.0	0.0	0.0
NW	0.0	0.0	4.7	1.4	0.2	1.5	0.0	0.0	0.0	0.0	0.0	0.0

Direction sums:

N	NE	E	SE	S	SW	W	NW
19.5	14.2	19.8	16.5	9.9	7.6	4.7	7.8

Table 6.2 Maximum, minimum, mean and standard deviation of trajectory lengths for each season of the year. Also included are the directional distribution of trajectory lengths in percent.

FALL

Launch Point	Trajectory Lengths [km] Minimum	Maximum	Mean	Std Dev	Trajectory Angle [deg] Mean	Std Dev
1	0.0539	2.0311	0.1826	0.1711	49.1	133.7

LP# 1

TRAJECTORY DIRECTION	0-25	->50	->100	->150	->200	->250	->300	->350	->400	->450	->500	500+
N	0.0	0.0	0.0	0.0	13.2	5.7	9.1	0.2	0.0	0.0	0.0	0.0
NE	0.0	0.0	0.0	0.4	18.6	0.0	0.0	0.0	0.0	0.0	0.0	0.0
E	0.0	0.0	7.2	7.2	0.3	0.0	0.0	0.0	0.0	0.0	0.0	0.0
SE	0.0	0.0	7.9	4.2	0.2	0.3	0.2	0.0	0.0	0.0	0.0	0.0
S	0.0	0.0	0.0	0.0	0.0	3.7	2.1	0.3	0.0	0.1	0.0	1.5
SW	0.0	0.0	2.8	0.3	0.4	0.1	1.1	0.3	0.4	0.1	0.0	1.6
W	0.0	0.0	5.4	0.0	0.0	0.0	0.0	0.0	0.0	0.0	0.0	0.0
NW	0.0	0.0	3.4	0.7	0.1	0.9	0.0	0.0	0.0	0.0	0.0	0.0

Direction sums:

N	NE	E	SE	S	SW	W	NW
28.2	19.0	14.7	12.8	7.7	7.1	5.4	5.1

SUMMER

Launch Point	Trajectory Lengths [km] Minimum	Maximum	Mean	Std Dev	Trajectory Angle [deg] Mean	Std Dev
1	0.0539	2.0088	0.1771	0.1127	25.1	156.5

LP# 1

TRAJECTORY DIRECTION	0-25	->50	->100	->150	->200	->250	->300	->350	->400	->450	->500	500+
N	0.0	0.0	0.0	0.0	14.0	6.0	13.3	0.3	0.0	0.0	0.0	0.0
NE	0.0	0.0	0.0	0.7	21.4	0.1	0.0	0.0	0.0	0.0	0.0	0.0
E	0.0	0.0	6.7	6.0	0.1	0.0	0.0	0.0	0.0	0.0	0.0	0.0
SE	0.0	0.0	6.7	1.9	0.4	0.0	0.0	0.0	0.0	0.0	0.0	0.0
S	0.0	0.0	0.0	0.0	0.0	1.9	2.1	0.3	0.0	0.0	0.0	0.3
SW	0.0	0.0	2.9	0.1	0.0	0.1	0.7	0.3	0.1	0.2	0.0	1.8
W	0.0	0.0	4.1	0.0	0.0	0.0	0.0	0.0	0.0	0.0	0.0	0.0
NW	0.0	0.0	3.9	2.0	0.1	1.5	0.0	0.0	0.0	0.0	0.0	0.0

Direction sums:

N	NE	E	SE	S	SW	W	NW
33.6	22.2	12.8	9.0	4.6	6.2	4.1	7.5

Table 6.2 (cont.) Maximum, minimum, mean and standard deviation of trajectory lengths for each season of the year. Also included are the directional distribution of trajectory lengths in percent.

River estuary by the narrow width of the area and the predominate easterly directed winds. Probabilities of oil slicks leaving this area under the model assumptions are extremely small.

7. SUMMARY

Bottom sediments in the subtidal flats in the upper Acushnet River estuary have an erosion threshold velocity of approximately 28 cm/s. The erosion threshold is nicely represented by the standard Shields diagram. Tidal currents in the area are generally small (< 5 cm/s) and the normal annual mean river flows generate currents generally less than 1 cm/s. The wave induced currents are usually very small as well due to the north-south orientation of the estuary, the predominantly westerly winds and the resulting limited fetch. Under normal conditions, bottom sediments are not resuspended.

For the 100 year storm flood event the river induced flows rise to 10-15 cm/s, but they are still insufficient to result in resuspension of bottom sediments. If the flood is accompanied by strong wind forcing, such as in the design project hurricane, wind induced waves of 1 m amplitude and 3 sec period are possible if the wind blows directly along the channel axis. These waves result in bottom currents on the order of 75 cm/s and are capable of eroding the bottom sediments. In fact, if the wind speed exceeds 16 m/s and the wind direction is from the south along the estuary axis bottom sediments near the Aerovox facility may be resuspended. The frequency of occurrence of this event is estimated to be once every 1.25 years with an average duration of 1 hour. While sediments can be resuspended under these conditions, the limited duration of the wind event limits the amount of material that can be eroded.

Assuming that sediments (which may be contaminated with PCBs) are suspended in the water column, simulations of their deposition locations were made as a function of grain size and river flow rate. Most of the sediments in the area are characterized by a mixture of silt and clay with 54% of the

size fractions between ϕ=6 and 9 (15.6 to 1.905 microns). For the mean annual river flow and a continuous release occurring over one tidal cycle all particles are deposited north of Coggeshall Street Bridge and most within 1000 m of the release site. The smallest particles have the largest excursion distances. If the river flow rates increase to the 100 year storm flood level (18.4 m^3/s) the larger particles (ϕ=6) still deposit north of the Coggeshall Street Bridge but 4-5% of ϕ=8 particle and 20-24% of ϕ=9 particles travel south of the bridge. The smallest particles reach the Rte. 6 bridge and Popes Island area before being deposited. If the river flow rate remains below 7-9 m^3/s, which is approximately equivalent to the average flow for the 10-25 year storm event, then all particles remain north of the Coggeshall Street Bridge.

In order for sediment material to travel south of the bridge, not only do the river flow rates have to exceed the above threshold, but wind generated waves must also be sufficient to resuspend the sediment. Data is unfortunately not available to calculate the probability of this combined event. The probability must however be lower than the lowest probability of the individual events, hence 10-25 years. This suggests that only during major storm events will ϕ=9 sediment particles be transported south of the Coggeshall Street Bridge.

Assuming a continous release of a conservative pollutant in the vicinity of the Aerovox facility the pollutant transport model predicts reduction by a factor of 200 in total PCB water column concentration between the release point and the hurricane barrier. The observed total PCB concentration gradients show a general decrease with distance from the head of the estuary to the Rte. 6 Bridge and then a slight increase starting south of Popes Island, out through the hurricane barrier and then decrease again in the outer harbor. The present model predictions and those of an earlier modeling study

by ASA (1983) for both the inner and outer harbor show good agreement between predictions and observations for the estuary north of the Rte. 6 bridge. Both simulations however show concentration predictions below those observed south of this point. In all model simulations the PCBs were assumed as a conservative substance (without deposition or resuspension). This observation and prior calculations by ASA (1983) suggest the observed concentration increases at the lower end of the harbor may be due to a second source of PCBs associated with the Cornell Dubilier facility.

PCB contaminated oil slicks may be generated in the upper estuary by disturbance of the bottom sediments. To address the transport of this oil an oil spill model has been employed to predict the trajectory of hypothetical releases at a site near the Aerovox facility where PCB concentrations in the sediment are high. Trajectories (1000) were run for each season of the year with random start times within the season. The results are relatively independent of season and show oiling of both shores in the immediate vicinity of the release (1000 m down stream). The Fairhaven shore receives the largest impact because of the general westerly winds and the north - south orientation of the estuary. Some spill trajectories approach the Coggeshall Street Bridge but very few pass south of the bridge. Approximately 5-6 days are required for the combined river and tidally induced flows to transport oil from the release site southward to the bridge assuming no wind forcing.

In summary, the simulations performed here suggest that the upper Acushnet River estuary, north of the Coggeshall Street Bridge acts to retain both suspended sediment and oil spill releases. Only under unusual storm events does material escape this area and even in those situations only a minimum amount is expected to be transported to the lower harbor.

Appendix A

Current measurements were made on 20 June 1986 at the I-195 Bridge causeway using a Endeco impeller current meter (Model 110). The measurements were made at three locations across the transect. In the center of the bridge span [water depth, 6.4 m] and 12 m east and west of the center measurement station. The water depths versus distance across the transect at approximately mean high water are as follows. The tidal range is approximately 1.13 m.

Distance [Referenced to Western Shore] (New Bedford) (m)	Depths (m)
0	0
3.9	1.3
7.8 West	3.7
11.7	3.7
15.6	6.4
19.5 Center	6.4
23.4	6.4
27.3	6.4
31.2 East	5.8
35.1	4.6
39.	2.4
42.9	0

The depth profiles in the north-south direction along the bridge centerline display a slight slope with depths of 7.3 m, 100 m south of the bridge to a depth of 5.8 m, 100 m north of the bridge.

The data are presented below. All times are given in parentheses after the station location and are in Eastern Daylight Time (EDT). The vertical reference is the sea surface and all depth values are in meters. The currents are given in cm/s.

Tidal currents were also measured at the hurricane barrier on 20 June

1986. All measurements were made at the approximate center of the barrier. Making current measurements was extremely difficult because of the strong currents in the region and since mooring of the boat, from which current measurements were made, was impossible due to the shipping traffic. The measurements should hence be viewed with caution. Depth measurements made across the barrier opening at high slack water showed an almost flat bottom at 13 m below MSL. Water depths were approximately 1.5 m shallower 100 m north or south of the barrier throat. Tidal heights at the hurricane barrier were obtained from the U.S. Army Corp of Engineers tide gauge at the barrier.

Figure 2.7 (Section 2) shows the cross sectionally averaged tidal currents at the I-195 causeway and the hurricane barrier, and the tidal height (hurricane barrier) versus time for 20 June 1986. The data are given for one complete tidal cycle.

I-195 Bridge Current Observations

Center (0845)		East (0900)		West (0900)	
Depth (m)	Speed (cm/s)	Depth (m)	Speed (cm/s)	Depth (m)	Speed (cm/s)
~0	60				
1	55	1	60	1	40
2	45-55	2	60	2	35
3	57/52/50	3	60	3	30
3	40	4	55		
EBB		EBB		EBB	

Center (1120)		East (1125)		West (1115)	
Depth (m)	Speed (cm/s)	Depth (m)	Speed (cm/s)	Depth (m)	Speed (cm/s)
1	35	1	20	1	25
2	32	2	20	2	25
		2	20		
4	25	4	20		
EBB		EBB		EBB	

Center (1445)		East (1450)		West (1440)	
Depth (m)	Speed (cm/s)	Depth (m)	Speed (cm/s)	Depth (m)	Speed (cm/s)
1	30	1	25	1	25
2	30	2	25	2	30
3	30	3	25	3	30
4	30			4	30
5	30			4.5	30
FLOOD		FLOOD		FLOOD	

Center (1610)		East (1605)		West (1620)	
Depth (m)	Speed (cm/s)	Depth (m)	Speed (cm/s)	Depth (m)	Speed (cm/s)
1	50	1	55	1	50
2	60	2	60	2	50
3	55	3	50	3	50
4	55			4	35
4.5	55				
FLOOD		FLOOD		FLOOD	

Center (1700) Depth (m)	Speed (cm/s)	East (1710) Depth (m)	Speed (cm/s)	West (1655) Depth (m)	Speed (cm/s)
1	85	1	60	1	70
2	80	2	80	2	75
3	85	3	80	3	75
4	90	4	75	4	60
5	85	4.5	75		
FLOOD		FLOOD		FLOOD	

Center (1800) Depth (m)	Speed (cm/s)	East (1805) Depth (m)	Speed (cm/s)	West (1755) Depth (m)	Speed (cm/s)
1	70	1	80	1	65
2	70	2	75	2	65
3	72	3	72	3	65
4	70	4	70	4	55
5	65	5	60		
FLOOD		FLOOD		FLOOD	

Hurricane Barrier - Current Observations

0640 (high slack) Depth (m)	Speed (cm/s)	0830 Depth (m)	Speed (cm/s)
All < 10 cm/s, ebb		1	60
		4	50
		8	50
		10	60
		12	50
EBB		EBB	

0955 Depth (m)	Speed (cm/s)	1205 (low slack) Depth (m)	Speed (cm/s)
1	75	1	15
2	75	2	15
3	60	3	<10
4	75		
6	65		
10	40		
EBB		FLOOD	

1425

Depth (m)	Speed (cm/s)
1	50
3	40
5	35
7	30
9	40
11	20

FLOOD

1523-1600

Depth (m)	Speed (cm/s)
1	85
3	90
5	80
7	85

FLOOD

1630

Depth (m)	Speed (cm/s)
1	65
3	75
5	70
7	80

FLOOD